Supplementary Information for

Synthesis and reactivity of o-carboranyl-I(OTf)$_2$ and -I(X)(OTf) reagents: Triflation of C$_1$ chlorocarbons, arene iodo-o-carboranylation, and unsaturation of *n*-alkanes

Marcus Sceney, Harini A. Sivakumar, David J.D. Wilson, and Jason L. Dutton*

Department of Biochemistry and Chemistry, La Trobe Institute for Molecular Science, La Trobe University, Melbourne, Victoria, Australia, 3086

j.dutton@latrobe.edu.au

Table of Contents

NMR Quick Reference Tables

Table S 1. NMR (^{1}H, ^{13}C{^{1}H}, ^{19}F) data for triflate esters in $CDCl_3$ and CD_2Cl_2.

TfO-CX$_n$H$_{3-n}$ (X = Cl, H, D)	δ_H		$\delta_{\underline{C}X}$ (mult, J_{Hz})		$\delta_{C\underline{F}}$		$\delta_{\underline{C}F}$ (mult, J_{Hz})	
	$CDCl_3$	CD_2Cl_2	$CDCl_3$	CD_2Cl_2	$CDCl_3$	CD_2Cl_2	$CDCl_3$	CD_2Cl_2
TfO-CCl_3	-	-	109.0[a]	109.4	−73.18[a]	−73.46	118.1 (q, 321)[a]	118.3 (q, 322)
TfO-$CDCl_2$	-	-	94.5 (t, 32)	*	−73.71	−74.07	118.3 (q, 321)	*
TfO-$CHCl_2$	7.59	7.65	94.7	95.3	−73.73	−74.08	118.3 (q, 321)	*
TfO-CD_2Cl	-	-	*	77.7 (p, 28)	−74.42[b]	−74.89	*	118.6 (q, 320)
TfO-CH_2Cl	*	5.97	*	78.1	*	−74.86	*	118.6 (q, 320)

Shifts (δ) are given in ppm. [a]Solvent 10-20 v% CCl_4. [b]Solvent 10-20 v% CD_2Cl_2. Multiplicity: t = triplet, q = quartet, p = quintet. *Not obtained.

Table S 2. NMR (^{1}H, ^{13}C{^{1}H}, ^{11}B, ^{19}F) data for relevant **1**I(III) compounds in $CDCl_3$ or [a]CD_2Cl_2.

1I(X)(Y)$_n$	o-Carborane nuclei			Ligand (L) nuclei		
	$\delta_{\underline{C}H}$	$\delta_{C\ 1,2,3}$ (mult, J_{Hz})	$\delta_{\underline{B}Cl\ a,b,c}$	$^{L}\delta_{I\underline{F}}$	$^{L}\delta_{C\underline{F}}$	$^{L}\delta_{\underline{C}F}$ (mult, J_{Hz})
1I	2.25	**−1.30**, 58.8, 26.5	**6.44**, 4.00, 0.20	-	-	-
1IF_2	2.39	[a]**51.3** (t, 20), [a]62.3, [a]25.9	**8.32**, 4.45, −0.22	−132.92	-	-
1I(Cl)(OTf)	2.37	**41.0**, 61.7, 25.7	**9.08**, 4.82, 0.38	-	−76.15	118.3 (q, 321)
1I(F)(OTf)	2.42	**52.3** (d, 30), 61.4, 25.9	**9.20**, 4.94, 0.16	−147.35	−75.69	118.6 (q, 319)
[**1**I(F)(OTf)$_2$]$^-$	2.34	*	*	−162.92	−76.47, −77.85	*
1I(OTf)$_2$	2.46	**54.0**, 62.0, 26.0	**9.64**, 5.24, 0.45	-	−74.34	118.3 (q, 321)
[**1**I(OTf)$_3$]$^-$	2.39	**52.5**, 62.2, 25.6	*	-	−74.26, −77.84	118.7 (p, 320)
[4-(**1**I)PhBr]$^+$	2.40	**32.8**, 59.8, 25.4	**8.66**, 4.35, 0.74	-	-	-

Shifts (δ) are given in ppm. BH environments (often poorly resolved) are omitted. Multiplicity: d = doublet, t = triplet, q = quartet, p = quintet. *Not obtained. Bold environments are those most affected by I(I)→(III) oxidation (Δδ).

Experimental

General

NMR spectra were obtained using a 400 or 500 MHz instrument, where the latter was equipped with a cryoprobe. ^{1}H, $^{13}C\{^{1}H\}$ and $^{29}Si\{^{1}H\}$ NMR are referenced to tetramethylsilane and $^{1}H/^{13}C\{^{1}H\}$ are calibrated using solvent residuals, while $^{29}Si\{^{1}H\}$ spectra are not internally calibrated. All shifts are reported in units of ppm. ^{19}F NMR spectra are referenced to $CFCl_3$, with hexafluorobenzene (C_6F_6) included in the solvent of applicable samples for calibration (C_6F_6: δ −161.64 ppm in $CDCl_3$, −162.61 in CD_2Cl_2, −164.38 in CD_3CN, and −162.45 in DMSO-d_6).[1] ^{11}B NMR are referenced to $BF_3{\cdot}OEt_2$ and are not internally calibrated. 1-methyl-o-carborane was obtained commercially from Zhengzhou Yuanli Biological Technology Co., Ltd. Air sensitive reactions were performed in a glovebox under an atmosphere of dry N_2. Solids used in air/moisture sensitive reactions were first dried under high vacuum with heat where possible, and solvents were cold distilled under reduced pressure from calcium hydride and stored over 3 Å molecular sieves.

Synthetic Methods

TfO-CCl_3 solution in CCl_4

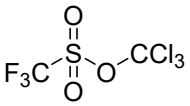

By the method of Chapman et al.:[2] moist AgOTf (once dry: 202 mg, 0.79 mmol) was subjected to heat (~150-200 °C) under high vacuum until grainy and dry in appearance (~15 min), then was placed under CCl_4 (0.5 mL, 5.17 mmol) in a flask attached to a condenser with a $CaSO_4$-packed drying tube, before refluxing for 17 h. A 4-drop sample of the supernatant was taken and diluted to 0.6 mL in CD_2Cl_2 for comparison with products of the reaction between $Cl_4MeOCb\text{-}I(OTf)_2$ and CCl_4 in CD_2Cl_2 by ^{19}F and ^{13}C NMR spectroscopy. For ^{13}C NMR, an additional 4 drops were added to achieve a detectable concentration. A separate sample was diluted in $CDCl_3$ for comparison to literature and found to be in close agreement with values reported by Chapman[2] (^{13}C) and Petrov[3] (^{19}F).

NMR spectra: Figure S1, Figure S2, Figure S3, Figure S4.

TfO-CCl_3 (generated via AgOTf) **^{19}F NMR** ($CDCl_3$ + ~10 v% CCl_4, 470 MHz):[3] δ −73.18 (s). **^{13}C{^{1}H} NMR** ($CDCl_3$ + ~20 v% CCl_4, 126 MHz):[2] δ 118.1 (q, $J_{C\text{-}F}$ = 321 Hz; *C*F_3), 109.0 (s, *C*Cl_3).**^{19}F NMR** (CD_2Cl_2 + ~10 v% CCl_4, 470 MHz): δ −73.49 (s). **^{13}C{^{1}H} NMR** (CD_2Cl_2 + ~20 v% CCl_4, 126 MHz): δ 118.5 (q, $J_{C\text{-}F}$ = 322 Hz; *C*F_3), 109.5 (s, *C*Cl_3).

TfO-CCl_3 (generated via Cl_4MeoCb-I(OTf)$_2$) **^{19}F NMR** (CD_2Cl_2, 470 MHz): δ −73.46 (s). **^{13}C{^{1}H} NMR** (CD_2Cl_2, 126 MHz): δ 118.3 (q, $J_{C\text{-}F}$ = 322 Hz; *C*F_3), 109.4 (*C*Cl_3).

$Si(OTf)_4$

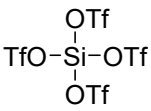

By the method of Hermannsdorfer and Driess;[4] under an atmosphere of dry N_2 in darkness, a mixture of AgOTf (1009 mg, 3.93 mmol) and SiI_4 (505 mg, 0.94 mmol) were stirred under CH_2Cl_2 (4 mL) for 72 hr. Following this, yellow solids (AgI) were pelleted by centrifugation while protected from light, and the supernatant decanted and concentrated *in vacuo*. A colourless to faintly brown oil was obtained (511 mg, 87%) which crystallizes below 0 °C to form white solids with some brown inclusions. These can be separated manually if desired, but the material was found to be sufficiently pure for further reactions in our case. Stored at −30 °C under N_2.

NMR spectra: Figure S5, Figure S6, Figure S7.

$Si(OTf)_4$[4] **^{19}F NMR** ($CDCl_3$, 470 MHz): δ −73.48 (s). **^{13}C{^{1}H} NMR** ($CDCl_3$, 126 MHz): δ 118.2 (q, $J_{C\text{-}F}$ = 320 Hz). **^{29}Si{^{1}H} NMR** ($CDCl_3$, 99 MHz): δ −121.10 (s).

Cl_4MeoCb

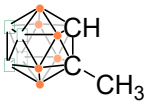

• = BH
□ = BCl

Procedure A (slow, higher yield): A mixture of 1-methyl-o-carborane (572 mg, 3.62 mmol) and finely ground trichloroisocyanuric acid (TCCA) (3.6 g, 15.5 mmol) in 98%

H_2SO_4 (12 mL) was stirred at 55°C for 1 hour* before raising the temperature to 65°C for a further 47 hours. The cooled mixture was decanted into chilled water (150 mL) and solids were collected and washed with water (350 mL), then dissolved in acetone and concentrated until saturated (~25 mL). Trituration with water (75 mL) produced white solids which were collected and dried at 150°C under high vacuum to obtain Cl_4MeoCb with a ~10% Cl_3MeoCb impurity (963 mg, 90%).

Procedure B (fast, lower yield): A mixture of 1-methyl-o-carborane (330 mg, 2.1 mmol) and finely ground TCCA (1078 mg, 4.6 mmol) in 98% H_2SO_4 (6 mL) was stirred at 55°C for 1 hr,* then the temperature was raised to 110 °C over a period of 20 minutes. During this time a fine white precipitate formed. After a further 2.5 hr, the mixture was transferred into 40 mL chilled water. Crude white solids were collected and triturated from acetone (15 mL) by addition of water (75 mL), then were recrystallized in two batches from 20-30% EtOAc:Hexane (reflux → −20 °C) to receive colourless needles (total 442 mg, 72%) composed of Cl_4MeoCb with a ~10% Cl_3MeoCb impurity.

*This step allows initial chlorination to occur before temperatures are reached at which unreacted MeoCb would evaporate.

Cl_4MeoCb[5] **^{1}H NMR** ($CDCl_3$, 500 MHz): δ 3.50 (s, 1H; C*H*), 3.24-1.85 (m, 6H; B*H*), 2.14 (s, 3H; CH_3). **^{11}B NMR** ($CDCl_3$, 160 MHz): δ 6.22 (s; *B*Cl), 2.99 (s; *B*Cl), −0.64 (s; *B*Cl), −13.70 (d, $J_{B\text{-}H}$ = 171 Hz; *B*H), −15.83 (d, $J_{B\text{-}H}$ = 172 Hz; *B*H), −19.68 (d, $J_{B\text{-}H}$ = 183 Hz; *B*H). **^{13}C{^{1}H} NMR** ($CDCl_3$, 126 MHz): δ 54.3 (m; *C*-CH_3), 45.0 (m; *C*H), 24.2 (m; *C*H_3).

Cl_4MeoCbI (improved procedure)

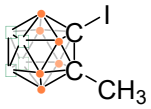

Adapted from the method of Streubel;[6] under an atmosphere of dry N_2, n-butyllithium in hexane (1.6 M, 3.1 mL, 5.0 mmol) was added to a chilled (-30 °C) solution of Cl_4MeoCb (1.4 g, 4.7 mmol) in diethyl ether (50 mL) and the mixture stirred at room temperature for 1 hr. The mixture was then re-chilled (-30 °C) before addition of I_2 (1.3 g, 5.1 mmol) and was stirred at

room temperature for a further 1 hr. Water (25 mL) was added, followed by saturated sodium thiosulfate solution until colourless (~2 drops, strongly stirred). Products were extracted into diethyl ether and concentrated to receive crude off-white to yellow solids (2.15 g, 107%).* These were redissolved in dichloromethane (55 mL) to which oxone (17 g, 55 mmol) was added, causing immediate development of I_2 from residual LiI (deep purple). Water (3 mL, 167 mmol), and trifluoroacetic acid (5 mL, 65 mmol) were added and the mixture strongly stirred for a further 1 hour, after which time it had fully decolourized. Supernatant was collected by filtration and washed with water, dried on $MgSO_4$, and concentrated. Resulting off-white solids were washed with petroleum spirits (BP 40-60°C) (3 × 5 mL) and dried under vacuum to receive white Cl_4MeoCbI (1.4 g, 70%).

*Solids obtained this way contain residual lithium iodide which is resistant to removal by washing with water. The impurity becomes apparent in later oxidation where excess XeF_2 is necessary to first consume the more reactive I^-, transiently generating visible I_2. The following step is an optional pre-oxidation intended to convert LiI to less coordinating iodates such as IO_3H and prevent waste of XeF_2.

Cl_4MeoCbI[5] **^{1}H NMR** ($CDCl_3$, 500 MHz): δ 3.88-1.98 (br, 6H; B*H*), 2.25 (s, 3H; C*H*$_3$). **^{11}B NMR** ($CDCl_3$, 160 MHz): δ 6.44 (s; *B*Cl), 4.00 (s; *B*Cl), 0.20 (s; *B*Cl), −10.09 (d, $J_{B\text{-}H}$ = 176 Hz; *B*H), −12.86 (d, $J_{B\text{-}H}$ = 176 Hz; *B*H), −14.60 (d, $J_{B\text{-}H}$ = 201 Hz; *B*H). **^{13}C{^{1}H} NMR** ($CDCl_3$, 126 MHz): δ 58.8 (m; *C*-CH$_3$), 26.5 (m; *C*H$_3$), −1.3 (m; *C*-I). **^{1}H NMR** (CD_2Cl_2, 500 MHz): δ 4.20-1.80 (br, 6H; B*H*), 2.24 (s, 3H; C*H*$_3$). **^{11}B NMR** (CD_2Cl_2, 160 MHz): δ 6.23 (s; *B*Cl), 3.79 (s; *B*Cl), 0.10 (s; *B*Cl), −10.06 (d, $J_{B\text{-}H}$ = 177 Hz; *B*H), −13.49 (m; *B*H). **^{13}C{^{1}H} NMR** (CD_2Cl_2, 126 MHz): δ 59.9 (m; *C*-CH$_3$), 26.7 (m; *C*H$_3$), −0.8 (m; *C*-I).

Cl_4MeoCb-IF_2 (improved procedure)

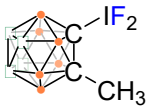

To a polypropylene centrifuge tube containing Cl_4MeoCbI (415 mg, 0.984 mmol) in CH_2Cl_2 (6 mL) was added XeF_2 (190 mg, 1.12 mmol) under an N_2 atmosphere. The

mixture was briefly agitated to dissolve the XeF_2, then allowed to stand for 2 hours at room temperature before transfer to a −30 °C freezer where it was left overnight. While

cold, the supernatant was decanted and crystals washed with chilled CH_2Cl_2 (−30 °C, 2 × 2 mL). Once dry, 369 mg (80%) colourless blocky crystals were collected.

The material slowly reacts with glass to produce SiF_4 but appears stable for extended periods when stored in a polypropylene vessel under inert atmosphere at −30 °C.

NMR spectra (CD_2Cl_2): Figure S8, Figure S9, Figure S10, Figure S11.

Cl_4MeoCb-IF_2[5] **^{1}H NMR** ($CDCl_3$, 500 MHz): δ 2.39 (s, 3H; C*H*$_3$). **^{19}F NMR** ($CDCl_3$, 470 MHz): δ −132.92 (s, 2F). **^{11}B NMR** ($CDCl_3$, 160 MHz): δ 8.32 (s, ; *B*Cl), 4.45 (s; *B*Cl), −0.22 (s; *B*Cl), −12.05 (d, $J_{B\text{-}H}$ = 173 Hz; *B*H), −13.27 (d, $J_{B\text{-}H}$ = 173 Hz; *B*H), −18.43 (d, $J_{B\text{-}H}$ = 187 Hz; *B*H).**^{1}H NMR** (CD_2Cl_2, 500 MHz): δ 4.00-2.00 (br, 6H; B*H*), 2.38 (s, 3H; C*H*$_3$). **^{19}F NMR** (CD_2Cl_2, 470 MHz): δ −133.83 (s). **^{11}B NMR** (CD_2Cl_2, 160 MHz): δ 8.05 (s, ; *B*Cl), 4.16 (s; *B*Cl), −0.36 (s; *B*Cl), −12.55 (m; *B*H), −18.14 (d, $J_{B\text{-}H}$ = 193.5 Hz; *B*H). **^{13}C{^{1}H} NMR** (CD_2Cl_2, 126 MHz): δ 62.3 (m; *C*CH_3), 51.3 (tm, $J_{C\text{-}I\text{-}F}$ = 20.4 Hz; *C*IF_2), 25.9 (m; *C*H_3).

Cl_4MeoCb-I(F)(OTf)

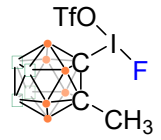

Under an atmosphere of dry N_2, a solution of $Si(OTf)_4$ (11.4 mg, 0.018 mmol) in CD_2Cl_2 (0.5 mL) was added dropwise with agitation over a period of 10 minutes to a glass vial containing partially dissolved Cl_4MeoCb-IF_2 (30.9 mg, 0.067 mmol) under a separate volume of CD_2Cl_2 (0.5 mL). When addition was complete, all solids had dissolved to produce a faintly yellow solution which was analysed by NMR spectroscopy and found to contain predominantly Cl_4MeoCb-I(F)(OTf). The sample was then transferred with CH_2Cl_2 to a vial under dry N_2 and solvent was removed *in vacuo*. The resulting white, microcrystalline solids were left under high vacuum for a further 1.5 h, yielding an apparently dry mass of 47 mg (119%).

A sample redissolved in $CDCl_3$ and analysed by NMR spectroscopy revealed the source of extra mass as residual CH_2Cl_2, of which 0.5 eq was present, and therefore an undetected additional quantity of CD_2Cl_2 as well. We suspect the solvent to be coordinated and hence not readily removed *in vacuo*.

NMR spectra: Figure S12 to Figure S19.

Cl_4MeoCb-I(F)(OTf) **^{1}H NMR** ($CDCl_3$, 500 MHz): δ 2.42 (s, 3H; C*H*$_3$). **^{19}F NMR** ($CDCl_3$, 470 MHz, *): δ −75.69 (s, 3F; C*F*$_3$), −147.35 (s, 1F; I*F*). **^{11}B NMR** ($CDCl_3$, 160 MHz): δ 9.20 (s; *B*Cl), 4.94 (s; *B*Cl), 0.16 (s; *B*Cl), −12.46 (m, 4B; *B*H), −18.56 (d, $J_{B\text{-}H}$ = 173 Hz; *B*H). **^{13}C{^{1}H} NMR** ($CDCl_3$, 126 MHz): δ 118.6 (q, $J_{C\text{-}F}$ = 319 Hz; *C*F$_3$), 61.4 (*C*-CH$_3$), 52.3 (dm, $J_{C\text{-}I\text{-}F}$ = 30 Hz; *C*-I), 25.9 (*C*H$_3$).**^{1}H NMR** (CD_2Cl_2, 500 MHz): δ 2.40 (s, 3H; C*H*$_3$). **^{19}F NMR** (CD_2Cl_2, 470 MHz, *): δ −76.29 (s, 3F; C*F*$_3$), −151.94 (s, 1F; I*F*). **^{11}B NMR** (CD_2Cl_2, 160 MHz): δ 8.90 (s; *B*Cl), 4.63 (s; *B*Cl), 0.03 (s; *B*Cl), −12.33 (m, 4B; *B*H), −18.31 (d, $J_{B\text{-}H}$ = 170 Hz; *B*H). **^{13}C{^{1}H} NMR** (CD_2Cl_2, 126 MHz): δ 118.8 (q, $J_{C\text{-}F}$ = 319 Hz; *C*F$_3$), 62.5 (m; *C*-CH$_3$), 52.7 (dm, $J_{C\text{-}I\text{-}F}$ = 25 Hz; *C*-I), 26.1 (m; *C*H$_3$).

* The relaxation time of the I-bound fluorine nucleus was found to be faster than that of C-bound (triflate) nuclei. Therefore, to obtain correctly integrating ^{19}F NMR signals the delay between scans (D1) was lengthened to 3 seconds from our usual default of 1.

Cl_4MeoCb-I(OTf)$_2$

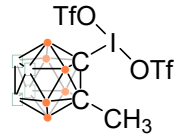

Under an atmosphere of dry N_2, a solution of $Si(OTf)_4$ (15 mg, 0.024 mmol) in CH_2Cl_2 (0.75 mL) was decanted atop solid Cl_4MeoCb-IF_2 (20 mg, 0.044 mmol) in a **glass** vial.

The vial was loosely capped and periodically agitated for 10-15 minutes, during which time bubbles of SiF_4 were observed as the solids gradually dissolved. Once homogenous, the solution was concentrated* *in vacuo* to obtain amorphous, slightly iridescent, colourless solids which were allowed to dry under vacuum for a further 45 min (30.6 mg, 98%). These were found to contain 10 mol% Cl_4MeoCbI by ^{1}H NMR. Solid Cl_4MeoCb-I(OTf)$_2$ appears stable at −30°C in glass for at least 24 hr, however, for most further studies it was generated *in situ* and used immediately to avoid degradation by reaction with the solvent during workup.

*The concentrate expanded to several times its initial volume into a structure of large, solidified bubbles as the last traces of solvent evaporated, so ample distance between the sample and vacuum line is recommended.

NMR spectra: Figure S20, Figure S21, Figure S22, Figure S23, Figure S53.

Cl_4MeoCb-I(OTf)$_2$[5] **^{1}H NMR** ($CDCl_3$**, 500 MHz): δ 2.46 (s, C*H*$_3$). **^{19}F NMR** ($CDCl_3$, 470 MHz): δ −74.34 (s, 6F; C*F*$_3$). **^{11}B NMR** ($CDCl_3$, 160 MHz): δ 9.64 (s; *B*Cl), 5.24 (s; *B*Cl), 0.45 (s; *B*Cl), −12.47 (m; *B*H), −18.33 (m; *B*H). **^{13}C{^{1}H} NMR** ($CDCl_3$, 126 MHz): δ 118.3 (q, $J_{C\text{-}F}$ = 321 Hz; *C*F$_3$), 62.0 (m; *C*-CH$_3$), 54.0 (m; *C*-I), 26.0 (m; *C*H$_3$). **^{1}H NMR** (CD_2Cl_2, 500 MHz): δ 2.45 (s, 3H; C*H*$_3$). **^{19}F NMR** (CD_2Cl_2, 470 MHz): δ −74.61 (s, 6F; C*F*$_3$). **^{11}B NMR** (CD_2Cl_2, 160 MHz): δ 9.38 (s; *B*Cl), 4.95 (s; *B*Cl), 0.34 (s; *B*Cl), −12.52 (m, 4B; *B*H), −18.26 (m, 2H; *B*H). **^{13}C{^{1}H} NMR** (CD_2Cl_2, 126 MHz): δ 118.2 (q, $J_{C\text{-}F}$ = 320 Hz; *C*F$_3$), 63.0 (m; *C*-CH$_3$), 55.1 (m; *C*-I), 26.3 (m; *C*H$_3$).

**NMR in $CDCl_3$ not recommended due to reaction with the solvent.

SiF_4[4] **^{19}F NMR** ($CDCl_3$, 470 MHz): δ −161.4 (s). **^{19}F NMR** (CD_2Cl_2, 470 MHz): δ −161.8 (s).

[4-(Cl_4MeoCbI)PhBr][OTf]

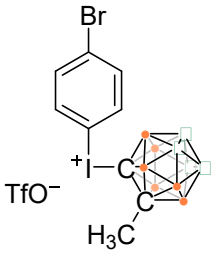

A solution of Cl_4MeoCb-I(OTf)$_2$ (0.090 mmol) in CH_2Cl_2 (1 mL) was prepared by the reported method and cooled to −30°C, then added dropwise over a period of 30 minutes to a −30°C solution of BrPh (20 µL, 0.19 mmol) in CH_2Cl_2 (0.5 mL) with agitation under dry N_2 (glass vial). Both solutions were maintained at low temperature during addition. Once mixed, the red-brown solution was allowed to stand at −30°C for 24 hours before removal to open air and transfer with CH_2Cl_2 (2 mL) to a polypropylene centrifuge tube. The iodonium salt was precipitated by addition of petroleum spirits (BP 40-60°C) (7 mL). Supernatant was discarded after centrifugation of the solids, which were washed with a further 2 mL

petroleum spirits, then 2 mL DCM:petroleum spirits (1:1). The resulting white powder was dried under high vacuum with mild heat (~50 °C) for a final mass of 55 mg (84%).

After workup the product is nearly insoluble in chloroform and dichloromethane, but addition of ~2-5 v% HOTf leads to full dissolution.

NMR spectra (isolated product): Figure S24 to Figure S27.

NMR spectra (*o*-isomer in crude reaction concentrate): Figure S28, Figure S29.

Mass spectrum: Figure S94.

[4-(Cl_4MeOCbI)PhBr][OTf] **^{1}H NMR** ($CDCl_3$ + 5 v% HOTf, 500 MHz): δ 7.97 (d, *J* = 8.8 Hz, 2H), 7.91 (d, *J* = 8.8 Hz, 2H), 2.40 (s, 3H). **^{19}F NMR** ($CDCl_3$ + 5 v% HOTf, 470 MHz): δ −76.91 (s, OTf^-,*). **^{11}B NMR** ($CDCl_3$ + 5 v% HOTf, 160 MHz): δ 8.66 (s; *B*Cl), 4.35 (s; *B*Cl), 0.74 (s; *B*Cl), −10.20—21.6 (m; *B*H). **^{13}C{^{1}H} NMR** ($CDCl_3$ + 5 v% HOTf, 126 MHz): δ 138.5 (aryl *C*H), 137.7 (aryl *C*H), 133.9 (aryl *C*), 118.6 (q, $J_{C\text{-}F}$ = 317 Hz; CF_3), 112.7 (aryl *C*), 59.8 (m), 32.8 (m), 25.4 (m, CH_3). **^{1}H NMR** (CH_2Cl_2 reaction mixture, 500 MHz): δ 7.98 (d, *J* = 8.9 Hz, 2H), 7.91 (d, *J* = 8.9 Hz, 2H), 2.39 (s, 3H). **^{1}H NMR** (CD_3CN, 500 MHz): δ 8.17 (d, *J* = 8.8 Hz, 2H), 7.92 (d, *J* = 8.8 Hz, 2H), 2.38 (s, 3H). **ESI-MS** (m/z) $[M]^+$ = 577.83.

[2-(Cl_4MeOCbI)PhBr][OTf] (crude reaction concentrate) **^{1}H NMR** ($CDCl_3$, 500 MHz): δ 8.22 (d, *J* = 8.2 Hz, 1H), 8.12 (d, *J* = 8.2 Hz, 1H), 7.88 (t, *J* = 7.9 Hz, 1H), 7.69 (t, *J* = 7.9 Hz, 1H). **^{19}F NMR** ($CDCl_3$, 470 MHz): δ −77.05 (s, OTf^-,*).

*Converged with HOTf signal.

Exploratory Reactions

Cl_4MeoCb-I(OTf)$_2$ with C_1 halocarbons to form triflate esters

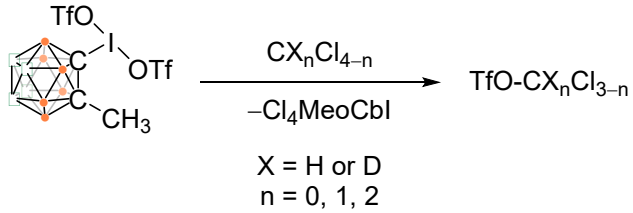

Cl_4MeoCb-I(OTf)$_2$ with neat chloroform and dichloromethane: Cl_4MeoCb-I(OTf)$_2$ was generated *in situ* by the above synthetic method at scales of 0.03-0.05 mmol in each of the following solvents: $CDCl_3$, $CHCl_3$, CD_2Cl_2, CH_2Cl_2 (0.5-0.6 mL). Reactions were transferred to parafilm-sealed borosilicate glass NMR tubes following complete solvation of Cl_4MeoCb-IF_2 and cessation of bubbling. Some reactions were performed entirely within PTFE NMR tube inserts as glass controls. All reactions were tracked until completion at ~5-25 h for chloroform and ~170-240 h for dichloromethane.* Conversion to triflate ester(s) is calculated by comparison of their ^{19}F signals to that of HOTf (the sole major side product) and is 71-96% for $CDCl_3$/$CHCl_3$ and 57-68%.for CD_2Cl_2/CH_2Cl_2.*

*Reaction times and conversions appear to depend on vessel material and potentially whether the halocarbon is deuterated or protonated, however, more data with higher consistency in monitoring and conditions (concentration, temperature) is necessary to draw conclusions for $CHCl_3$, CD_2Cl_2, and CH_2Cl_2. Reasonable comparison of reaction efficiency between vessel materials can be made for $CDCl_3$ and is tabulated in the next section (Table S 3).

TfO-$CHCl_2$ was isolated as a solution in $CHCl_3$ from a reaction of Cl_4MeoCb-I(OTf)$_2$ with neat $CHCl_3$ (glass, 5 h) by washing the mixture with water (0.5 mL) to remove acids, followed by cold distillation of the organic phase under reduced pressure to a receiving NMR tube cooled directly by liquid nitrogen. The compound appears stable for a month or longer in $CHCl_3$, even in the presence of a ^1H NMR-detectible quantity of water.

TfO-CD_2Cl was isolated as a solution in CD_2Cl_2 alongside TfO-$CDCl_2$ (molar ratio 87:13 resp., ^{19}F NMR) by the same method as for TfO-$CHCl_2$ with the exception that the solvent was CD_2Cl_2 and reaction time was 170 h. The two species' pre-workup molar ratio was 93:6 (^{19}F NMR), suggesting TfO-CD_2Cl is not as resistant to hydrolysis as its more highly chlorinated analogues.

NMR spectra (TfO-$CXCl_2$, X = H, D): Figure S30 to Figure S38.

NMR spectra (TfO-CX_2Cl, X = H, D): Figure S39 to Figure S45.

TfO-$CHCl_2$ **^{1}H NMR** ($CHCl_3$ + $CDCl_3$, 400 MHz): δ 7.59 (s). **^{19}F NMR** ($CHCl_3$ + $CDCl_3$, 470 MHz): δ −73.73 (s). **^{13}C{^{1}H} NMR** ($CHCl_3$ + $CDCl_3$, 126 MHz): δ 118.3 (q, $J_{C\text{-}F}$ = 321 Hz; *C*F_3), 94.7 (*C*HCl_2). **^{1}H NMR** (CD_2Cl_2, 500 MHz): δ 7.65 (s). **^{19}F NMR** (CD_2Cl_2, *in situ* gen., 470 MHz): δ −74.08 (s). **^{19}F NMR** (CD_2Cl_2 + ~5 v% $CHCl_3$, isolated, 470 MHz): δ −74.12 (s). **^{13}C{^{1}H} NMR** (CD_2Cl_2 + ~5 v% $CHCl_3$, 126 MHz): 118.6 (q, $J_{C\text{-}F}$ = 321 Hz; *C*F_3), 95.3 (*C*HCl_2).

TfO-$CDCl_2$ **^{19}F NMR** ($CDCl_3$, 470 MHz): δ −73.71 (s). **^{13}C{^{1}H} NMR** ($CDCl_3$, 126 MHz): δ 118.3 (q, $J_{C\text{-}F}$ = 321 Hz; *C*F_3), 94.5 (t, $J_{C\text{-}D}$ = 32 Hz; *C*DCl_2). **^{19}F NMR** (CD_2Cl_2, 470 MHz): δ −74.08 (s).

TfO-CH_2Cl **^{1}H NMR** (CH_2Cl_2 + CD_2Cl_2, 500 MHz): δ 5.97 (s). **^{19}F NMR** (CH_2Cl_2 + CD_2Cl_2, 470 MHz): δ −74.86 (s). **^{13}C{^{1}H} NMR** (CH_2Cl_2 + CD_2Cl_2, 126 MHz): δ 118.6 (q, $J_{C\text{-}F}$ = 320 Hz; *C*F_3), 78.1 (*C*H_2Cl).

TfO-CD_2Cl **^{19}F NMR** (CD_2Cl_2, 470 MHz): δ −74.89 (s). **^{13}C{^{1}H} NMR** (CD_2Cl_2, 126 MHz): δ 118.6 (q, $J_{C\text{-}F}$ = 320 Hz; *C*F_3), 77.7 (quint, $J_{C\text{-}D}$ = 28 Hz; *C*D_2Cl).

Observation of TfO-$CXCl_2$ and $CHCl_3$ generated by reaction of Cl_4MeoCb-I$(OTf)_2$ with CX_2Cl_2 (X = H/D): During a reaction of Cl_4MeoCb-I$(OTf)_2$ with neat CH_2Cl_2, alongside the expected TfO-CH_2Cl, trace generation of $CHCl_3$ was observed in ^{1}H NMR followed by that of its respective triflate ester, TfO-$CHCl_2$. In the final scan, $CHCl_3$ (also detected in $^{13}C\{^1H\}$ NMR) and TfO-$CHCl_2$ appear in greater quantity in a 1:1 ratio as minor products (Figure S39, Figure S40, Figure S42). In the analogous reaction with CD_2Cl_2, TfO-$CDCl_2$ is detectable in ^{19}F NMR (Figure S43 to Figure S45).

Cl_4MeoCb-I(OTf)$_2$ with CCl_4: CCl_4 (8.5 µL, 0.088 mmol) was added to a solution of Cl_4MeoCb-I(OTf)$_2$ (generated *in situ* by the reported method, 0.044 mmol) in CD_2Cl_2 (0.6 mL). The reaction was tracked by NMR (glass tube) until completion at 130 h (full reduction of Cl_4MeoCb-I(OTf)$_2$ to Cl_4MeoCbI), at which time TfO-CCl_3, TfO-CD_2Cl, and TfO-$CDCl_2$ were present in a 71:27:2 respective molar ratio, with 72% of total triflate having formed esters and the remainder present as HOTf (^{19}F NMR). Signals of the major product (TfO-CCl_3) in ^{19}F and $^{13}C\{^1H\}$ NMR closely match those of TfO-CCl_3 generated by a literature method in a similar solvent environment.

NMR spectra: Figure S46, Figure S47.

TfO-CCl_3 (generated via Cl_4MeoCb-I(OTf)$_2$) **^{19}F NMR** (CD_2Cl_2, 470 MHz): δ −73.46 (s). **$^{13}C\{^1H\}$ NMR** (CD_2Cl_2, 126 MHz): δ 118.3 (q, $J_{C\text{-}F}$ = 322 Hz; CF_3), 109.4 (CCl_3).

TfO-CCl_3 (generated via AgOTf) **^{19}F NMR** (CD_2Cl_2 + ~10 v% CCl_4, 470 MHz): δ −73.49 (s). **$^{13}C\{^1H\}$ NMR** (CD_2Cl_2 + ~20 v% CCl_4, 126 MHz): δ 118.5 (q, $J_{C\text{-}F}$ = 322 Hz; CF_3), 109.5 (s, CCl_3).

Cl_4MeoCb-I(OTf)$_2$ with $CDCl_3$ in glass vs PTFE; Observation of Cl_4MeoCb-I(Cl)(OTf)

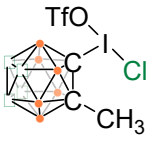

Cl_4MeoCb-I(OTf)$_2$ generated *in situ* by the reported method in $CDCl_3$ was tracked by NMR to obtain the following data on conversion to TfO-$CDCl_2$ and observations of the proposed intermediate Cl_4MeoCb-I(Cl)(OTf).

Table S 3. Comparison of the reaction between Cl_4MeoCb-I(OTf)$_2$ and $CDCl_3$ (solvent) in different vessel materials (multiple runs). [a]Initial loading of Cl_4MeoCb-I(OTf)$_2$. [b]For full reduction to Cl_4MeoCbI. [c]By comparison of ^{19}F NMR signal intensity of TfO-$CDCl_2$ *vs* HOTf.

Vessel	µM[a]	Time[b]	Conv. to TfO-$CDCl_2$[c]
Glass	36-55	5-12 h	68-73%
PTFE	50-66	16-25 h	89-96%

NMR spectra (vessel material comparison): Figure S36 compared with Figure S37

NMR spectra (intermediate observation): Figure S48 to Figure S53.

Cl_4MeoCb-I(Cl)(OTf) **^{1}H NMR** ($CDCl_3$, 500 MHz): δ 2.37 (s; C*H_3*), **^{19}F NMR** ($CDCl_3$, 470 MHz): δ −76.15 (s; C*F_3*). **^{11}B NMR** ($CDCl_3$, 160 MHz): δ 9.08 (s; *B*Cl), 4.82 (s; *B*Cl), 0.38 (s; *B*Cl), −9.00 - −22.00 (m; *B*H). **^{13}C{^{1}H} NMR** ($CDCl_3$, 126 MHz): δ 118.3 (q, $J_{C\text{-}F}$ = 321 Hz; *C*F_3), 61.7 (m; *C*-CH_3), 41.0 (m; *C*-I), 25.7 (m; *C*H_3).

Glassware/solvent H_2O quantification with Tf_2O

Under an atmosphere of dry N_2, a concentrated sample of Tf_2O (60 mg) in $CDCl_3$ (0.6 mL) was prepared. The sample was analysed by NMR spectroscopy for comparison of the amount of acid arising from the glass and/or present in the Tf_2O itself to that produced by the reaction of Cl_4MeoCb-I(OTf)$_2$ with $CDCl_3$ under the same conditions.

NMR spectra (Tf_2O): Figure S54, Figure S55.

NMR spectra (Completed $CDCl_3$ + Cl_4MeoCb-I(OTf)$_2$ reaction): Figure S56, Figure S37.

Tf_2O **^{19}F NMR** ($CDCl_3$, 376 MHz): δ 71.45 (s).

Cl_2 detection in the reaction of Cl_4MeoCb-I(OTf)$_2$ with $CDCl_3$ using Ph_3Sb

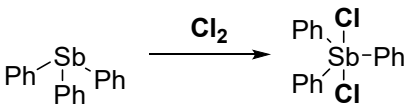

Cl_4MeoCb-I(OTf)$_2$ (0.033 mmol) generated *in situ* by the reported method in $CDCl_3$ (0.6 mL, glass NMR tube, parafilm sealed) was allowed to react overnight, then analysed by NMR to ensure full reduction to I(I) had occurred. At this time, Cl_4MeoCbI, HOTf, and TfO-$CDCl_2$ were the only species detectible, and the solution was faintly yellow. Ph_3Sb (10.4 mg, 0.03 mmol) was added under N_2, which led to complete decolourisation. Further NMR analysis (^{1}H, ^{13}C{^{1}H}) showed Ph_3SbCl_2, Ph_2SbCl, C_6H_6, and residual Ph_3Sb. One other major aromatic product was present with NMR shifts in $CDCl_3$ closely matching those of $Ph_3Sb(OTf)_2$ in CD_2Cl_2 across ^{1}H, ^{13}C{^{1}H}, and ^{19}F spectra.

Alongside comparison to literature, the identity of Ph_3SbCl_2 was confirmed by its synthesis in a separate solution. Ph_3Sb (11 mg) in $CDCl_3$ (0.6 mL) was exposed to Cl_2 gas until the solution remained yellow, then the mixture was analysed by NMR. Near quantitative conversion to Ph_3SbCl_2 was observed with some trace side products.

NMR spectra (reaction): Figure S57 to Figure S60.

NMR spectra (Cl_2SbPh_3 standard): Figure S61, Figure S62.

Ph_2SbCl[7] **^{1}H NMR** ($CDCl_3$, 500 MHz): δ 7.64 (m, *), 7.46-7.37 (m, *). **^{13}C{^{1}H} NMR** ($CDCl_3$, 126 MHz): δ 144.7, 134.5, 130.2, 129.4.

*Signal mostly overlapped.

Ph_3SbCl_2[7] **^{1}H NMR** ($CDCl_3$, 500 MHz): δ 8.23 (m, 6H), 7.56 (m, 9H). **^{13}C{^{1}H} NMR** ($CDCl_3$, 126 MHz): δ 140.1, 134.3, 131.9, 129.8.

$Ph_3Sb(OTf)_2$[8] **^{1}H NMR** ($CDCl_3$, 500 MHz): δ 8.07 (m, 6H) 7.66 (m, 9H). **^{19}F NMR** ($CDCl_3$, 470 MHz): δ −77.87 (s). **^{13}C{^{1}H} NMR** ($CDCl_3$, 126 MHz): δ 134.1, 133.3, 130.6, 119.1 (q, $J_{C\text{-}F}$ = 319 Hz).

Attempted syntheses of Cl_4MeoCb-I(Cl)(OTf)

Cl_4MeoCb-I(OTf)$_2$ + [NBu$_4$]Cl: Cl_4MeoCb-I(OTf)$_2$ was generated in situ at 0.045 mmol scale by the reported procedure in CD_2Cl_2 (0.25 mL), then the mixture was cooled to −30 °C. A separate solution of tetrabutylammonium chloride ([NBu_4]Cl, 12.6 mg, 0.045 mmol) in CD_2Cl_2 (0.4 mL) was chilled to −30 °C, then added dropwise with agitation over 2 minutes. The resulting faintly yellow solution was transferred to an NMR tube and analysed immediately.

At the time of first scan, 42% of the Cl_4MeoCb-I(OTf)$_2$ had already been reduced to I(I), with the remainder composed of a species of similar CH_3 chemical shift to previous observation of Cl_4MeoCb-I(Cl)(OTf) and a small quantity of an unidentified species appearing at 2.33 ppm (^{1}H NMR). ^{19}F NMR

diverged considerably from previous observations with a single covalent triflate chemical shift instead matching Cl_4MeoCb-I(OTf)$_2$. Ionic triflate was also generated in a 1:1 ratio with bound triflate (^{19}F NMR). For a single species to achieve this ratio when approximately half the I(III) is already reduced to I(I) necessitates its ligation by two covalent triflates.

The solution was returned to inert conditions (dry N_2), and the solvent removed in vacuo to receive a colourless oil which was immediately redissolved in $CDCl_3$ for further NMR analysis. Similar results to those in CD_2Cl_2 were obtained, where the I(III) species' ^{1}H chemical shift was almost identical to previous observations of Cl_4MeoCb-I(Cl)(OTf), however, its ^{19}F signal was significantly downfield, closely matching Cl_4MeoCb-I(OTf)$_2$. The mixture was tracked over the course of an unusually lengthy degradation of I(III) to I(I) (62 h). Reduction was not driven by the expected reaction with solvent $CDCl_3$, as this only occurred in trace quantity. Instead, signals in the alkene/alkyl triflate region appeared in ^{1}H NMR, and numerous new triflates in ^{19}F NMR, indicating a potential reaction with $[NBu_4]^+$.

NMR spectra (initial): Figure S63 to Figure S67.

NMR spectra (+ 62 h): Figure S68, Figure S69.

Cl_4MeoCb-I(OTf)$_2$ + [NBu_4][OTf]: Cl_4MeoCb-I(OTf)$_2$ was generated in situ at 0.012 mmol scale by the reported procedure in $CDCl_3$ (0.6 mL) containing [NBu_4][OTf] (5.2 mg, 0.013 mmol). Normally when Cl_4MeoCb-I(OTf)$_2$ is synthesised in $CDCl_3$ a brief but intense colour change to yellow is observed (suspected to be Cl_2), but in the presence of [NBu_4][OTf] no colour developed. ^{1}H and ^{19}F NMR showed near identical signals to those observed in the case of [NBu_4]Cl, which can hence be assigned as [NBu_4][Cl_4MeoCb-I(OTf)$_3$]. Consistent with previous observation of this compound, no initial reaction with the solvent occurred but a trace was detectable after ~4 h.

If substoichiometric Si(OTf)$_4$ is used in this reaction, a second set of signals in ^{1}H and ^{19}F NMR are observed which correspond to [NBu_4][Cl_4MeoCb-I(F)(OTf)$_2$]. This was also previously observed in trace quantity in the reaction of Cl_4MeoCb-I(OTf)$_2$ with [NBu_4]Cl.

NMR spectra: Figure S70 to Figure S73.

[NBu_4][Cl_4MeoCb-I(OTf)$_3$] **^{1}H NMR** (CD_2Cl_2, 500 MHz): δ 3.11 (m; NBu_4^+), 2.36 (s, 3H; CH_3), 1.61 (quint; NBu_4^+), 1.42 (hext; NBu_4^+), 1.01 (t; NBu_4^+). **^{19}F NMR** (CD_2Cl_2, 470 MHz): δ −74.59 (s; $IOSO_2CF_3$), −78.43 (s; $^-OSO_2CF_3$). **^{1}H NMR** ($CDCl_3$, 500 MHz): δ 3.14 (m; NBu_4^+), 2.39-2.35* (s, 3H; CH_3), 1.60 (quint; NBu_4^+), 1.43 (hext; NBu_4^+), 1.02 (t; NBu_4^+). **^{19}F NMR** ($CDCl_3$, 470 MHz): δ −74.18-−74.26* (s; $IOSO_2CF_3$), −77.84 (s; $^-OSO_2CF_3$). **^{13}C{^{1}H} NMR** ($CDCl_3$, 126 MHz): δ 118.7 (quint, $J_{C\text{-}F}$ = 320 Hz; $IOSO_2CF_3$ + $^-OSO_2CF_3$, offset = $J_{C\text{-}F}$), 62.2 (m), 52.5 (m), 25.6 (m).

*Shift variation observed with [NBu_4][OTf] loading (apparent 0.75 *vs* 2 eq). Higher loading leads to upfield shift of CH_3 in ^{1}H, and downfield shift of covalent OTf in ^{19}F.

[NBu_4][Cl_4MeoCb-I(F)(OTf)$_2$] **^{1}H NMR** ($CDCl_3$, 400 MHz): δ 3.14 (m; NBu_4^+), 2.34 (s, 3H; CH_3), 1.61 (quint; NBu_4^+), 1.43 (hext; NBu_4^+), 1.02 (t; NBu_4^+). **^{19}F NMR** ($CDCl_3$, 376 MHz): δ −76.47 (s; $IOSO_2CF_3$), −77.85 (s; $^-OSO_2CF_3$), −162.92 (s; I-*F*).

Cl_4MeoCb-I(OTf)$_2$ + TMSCl: Cl_4MeoCb-I(OTf)$_2$ was generated in situ (0.032 mmol) in CD_2Cl_2 (0.25 mL) by the reported method, then transferred to a PTFE NMR tube insert, to which TMSCl (4 µL, 0.032 mmol) in CD_2Cl_2 (0.25 mL) was added dropwise over 4 minutes with agitation. Immediate NMR analysis showed Cl_4MeoCb-I(OTf)$_2$ and Cl_4MeoCbI signals in a ~1:1 ratio (^{1}H) with a trace of residual Cl_4MeoCb-I(F)(OTf) (from generation of Cl_4MeoCb-I(OTf)$_2$), and full conversion of TMSCl to TMSOTf. Over the following 30 minutes TMSOTf reacted with Cl_4MeoCb-I(F)(OTf) to form the typical set of products associated with this reaction; TMSF, Me_2SiF_2, and MeOTf.[5]

NMR spectra: Figure S74, Figure S75.

NMR spectra (TMSOTf standard in CD_2Cl_2): Figure S76, Figure S77.

TMSOTf **^{1}H NMR** (CD_2Cl_2, 400 MHz): δ 0.50 (s). **^{19}F NMR** (CD_2Cl_2, 376 MHz): −77.48 (s).

Interception of Cl_4MeoCb-I(Cl)(OTf) with BrPh as a chlorination probe

A typical reaction of *in situ* generated Cl_4MeoCb-I(OTf)$_2$ (0.03 mmol) with $CDCl_3$ (0.5 mL) in a PTFE insert was tracked by NMR until Cl_4MeoCb-I(Cl)(OTf) appeared to have reached its maximum concentration (~3 h in this case), then bromobenzene (3 µL, 0.03 mmol) was added under dry N_2. This resulted in immediate development of a red-brown hue.

NMR spectra: Figure S78 to Figure S82.

p-bromochlorobenzene[9] **^{1}H NMR** ($CDCl_3$, 400 MHz): δ 7.42 (d, *J* = 8.7 Hz), 7.21* (lit.). **^{13}C{^{1}H} NMR** ($CDCl_3$, 101 MHz): δ 133.4, 132.9, 130.4, 120.4.

o-bromochlorobenzene[10] **^{1}H NMR** ($CDCl_3$, 400 MHz): δ 7.62 (d, *J* = 7.7 Hz, 1H), 7.45 (d, *J* = 7.7 Hz), 7.21* (lit.), 7.12 (t, *J* = 7.7 Hz, 1H). **^{13}C{^{1}H} NMR** ($CDCl_3$, 101 MHz): δ 134.6, 134.0, 130.6, 128.6, 128.0, 122.4* (lit.).

*Marked signal obscured due to overlap and/or low intensity, so literature value is given.

[4-(Cl_4MeoCbI)PhBr][OTf] with [NBu_4]Cl as a nucleophilic chlorination control

Under dry N_2 a solution of [NBu_4]Cl (4.1 mg, 0.015 mmol) in $CDCl_3$ (0.6 mL) was deposited atop solid [4-(Cl_4MeoCbI)PhBr][OTf] (9.7 mg, 0.013 mmol). The mixture was analysed by NMR spectroscopy after 20 minutes to find that approximately one third of the [4-(Cl_4MeoCbI)PhBr] had dissolved (typically insoluble), and its ^{1}H environments had, on average, shifted slightly upfield relative to their positions in media containing HOTf (used for solubilisation). Aryl ^{1}H environments had diverged +0.04 ppm and −0.2 ppm, and the o-carboranyl CH_3 environment by −0.05 ppm. Aside from this apparent interaction with Cl^-, no aryl chlorination was observed.

NMR spectra: Figure S83, Figure S84.

[4-(Cl_4MeoCbI)PhBr][OTf]·[NBu_4]Cl **^{1}H NMR** ($CDCl_3$, 400 MHz): δ 8.01 (d, *J* = 8.7 Hz, 2H), 7.72 (d, *J* = 8.7 Hz, 2H), 2.34 (s, 3H). **^{19}F NMR** ($CDCl_3$, 376 MHz): δ 78.10 (s).

Attempted syntheses of Cl_4MeoCb-I(Cl)(F) and Cl_4MeoCb-ICl_2

Cl_4MeoCb-IF_2 + TMSCl: Under dry N_2 in a polypropylene Eppendorf tube, Cl_4MeoCb-IF_2 (10.6 mg, 0.023 mmol) and TMSCl (2.6 µL, 0.020 mmol) were combined under $CDCl_3$ (0.6 mL) and stirred for 3 h before transfer to a PTFE NMR tube insert for analysis. Solid Cl_4MeoCb-IF_2 remained mostly undissolved. ^{1}H and ^{19}F NMR showed TMSCl, TMSF, Cl_4MeoCb-IF_2, and a larger quantity of Cl_4MeoCbI in solution simultaneously, with no signals attributable to Cl_4MeoCb-I(Cl)(F).

NMR spectra: Figure S85, Figure S86.

TMSF **^{1}H NMR** ($CDCl_3$, 500 MHz): 0.24 (d, $J_{H\text{-}C\text{-}Si\text{-}F}$ = 7.5 Hz). **^{19}F NMR** ($CDCl_3$, 470 MHz): δ −157.61 (m). **^{13}C{^{1}H} NMR** ($CDCl_3$, 126 MHz): 0.25 (d, $J_{C\text{-}Si\text{-}F}$ = 15 Hz).

Cl_4MeoCb-I$(OTf)_2$ + 2 [NBu_4]Cl: Under dry N_2, [NBu_4]Cl (10.3 mg, 0.037 mmol) was added to a solution of Cl_4MeoCb-I$(OTf)_2$ (0.018 mmol) generated in CD_2Cl_2 (0.6 mL) by the typical method, causing the solution to become faintly yellow. Immediate NMR analysis showed complete reduction of the oxidant by CH_3 shift (^{1}H), and full conversion of I-bound triflates to ionic (^{19}F NMR: δ −74.61 to −78.8 ppm).

Cl_4MeoCb-I$(OTf)_2$ with alkanes

Cyclohexane: Under dry N_2 cyclohexane (6.3 µL, 0.058 mmol) was added to a solution of Cl_4MeoCb-I$(OTf)_2$ (0.058 mmol) generated in CD_2Cl_2 (0.6 mL) by the reported method. The solution developed a deep yellow hue after 1-2 min, darkening to black by 10 min. The mixture was analysed by NMR after 50 minutes.

NMR spectra: Figure S87, Figure S88.

Pentane: Under dry N_2, Cl_4MeoCb-I(OTf)$_2$ (50 mg, 0.074 mmol)* was dissolved in CD_2Cl_2 (0.6 mL) and pentane (10 µL, 0.086 mmol) was added. The solution was stored in a sealed glass NMR tube under inert conditions for 3 days, after which time the solution had turned black.

*Cl_4MeoCb-I(OTf)$_2$ was synthesized in and isolated from CH_2Cl_2 by the reported method, then stored at −30 °C overnight before use. It was found to consist of 85 mol% I(III), with a resulting average molar mass of ~675 gmol^{-1}. This is used to calculate the mmol value reported above. A trace of TfO-CH_2Cl was also detected prior to use.

NMR spectra: Figure S89, Figure S90.

Propane: A solution of Cl_4MeoCb-I(OTf)$_2$ (0.03 mmol) in CD_2Cl_2 (0.6 mL) was prepared by the stated procedure , transferred to a glass NMR tube sealed with a pierceable septum and tightly wrapped with parafilm. A $CaSO_4$-packed drying tube (approx. 30 × 4 cm) that had been heated to 120°C for the prior 24 h was purged with N_2 until cool, then connected to a supply of propane (camping stove supply sourced from Bunnings Warehouse) and purged until the gas began to visibly emerge from the output line. The solution containing Cl_4MeoCb-I(OTf)$_2$ was frozen on LN_2 and the NMR tube headspace purged with propane until a small amount of the gas liquified atop the sample. Then, ensuring the tube remained safely vented, the sample was allowed to warm until the excess propane had boiled out, then was sealed under slight positive pressure. The sample was allowed to react for 25 h before NMR analysis, at which time reduction of Cl_4MeoCb-I(OTf)$_2$ was found to be complete. After 3 days the reaction mixture had turned dark brown.

NMR spectra: Figure S91, Figure S92.

Propane **^{1}H NMR** (CD_2Cl_2, 400 MHz): δ 1.33 (sept, J = 7.3 Hz, 2H), 0.90 (t, J = 7.3 Hz, 6H).

Propene **^{1}H NMR** (CD_2Cl_2, 400 MHz): δ 5.28 (dqd, $J_{1,2}$ = 6.6 Hz, J_3 = 2.6 Hz, 1H), 4.65 (dd, J_1 = 11.9 Hz, J_2 = 2.6 Hz, 1H), 4.58 (dd, J_1 = 11.9 Hz, J_2 = 6.6 Hz, 1H), 1.60 (d, J = 6.6 Hz, 3H).

Ethane, methane (no reaction): Gases were delivered as an apparent 75:13:12 mol (C_2H_6:CH_4:C_3H_8) mixture (from building supply) by the same method as used for propane, and their presence in solution confirmed by ^{1}H NMR. Ethane appeared at an abundance of 1.2 eq, methane at 0.2 eq, and undesired propane at 0.19 eq relative to Cl_4MeoCb-I(OTf)$_2$. Propane was consumed to form previously observed products, but the presence of methyl triflate, ethene, or ethyl triflate(s) could not be confirmed after full reduction of the oxidant, even at up to 50°C (24 h). Higher temperatures and allowance of longer reaction time are counterproductive in this case due to the oxidant's competing reaction with the solvent (CD_2Cl_2), which lead to full reduction within the stated time.

NMR spectrum (initial conditions): Figure S93.

Ethane **^{1}H NMR** (CD_2Cl_2, 500 MHz): δ 0.85 (s).

Methane **^{1}H NMR** (CD_2Cl_2, 500 MHz): δ 0.21 (s).

NMR Spectra

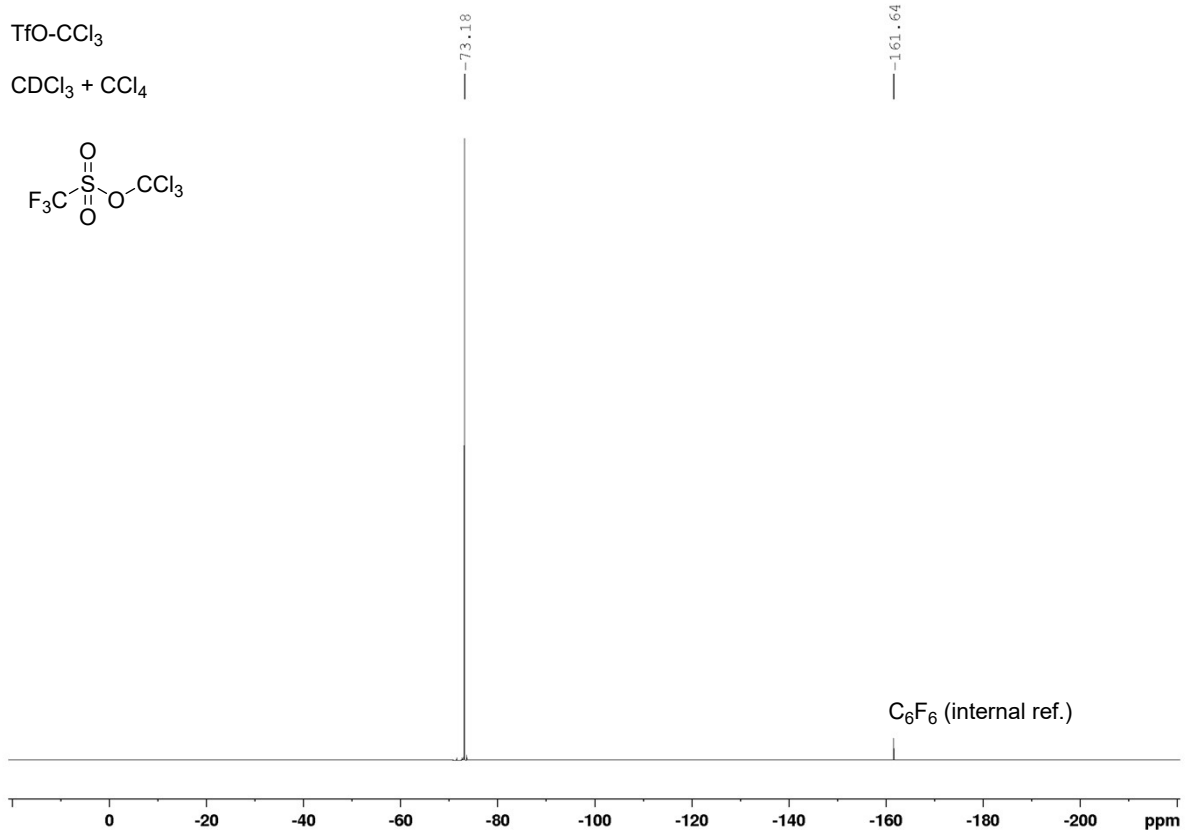

Figure S1. ^{19}F NMR ($CDCl_3$ + ~10 v% CCl_4, 470 MHz): TfO-CCl_3.

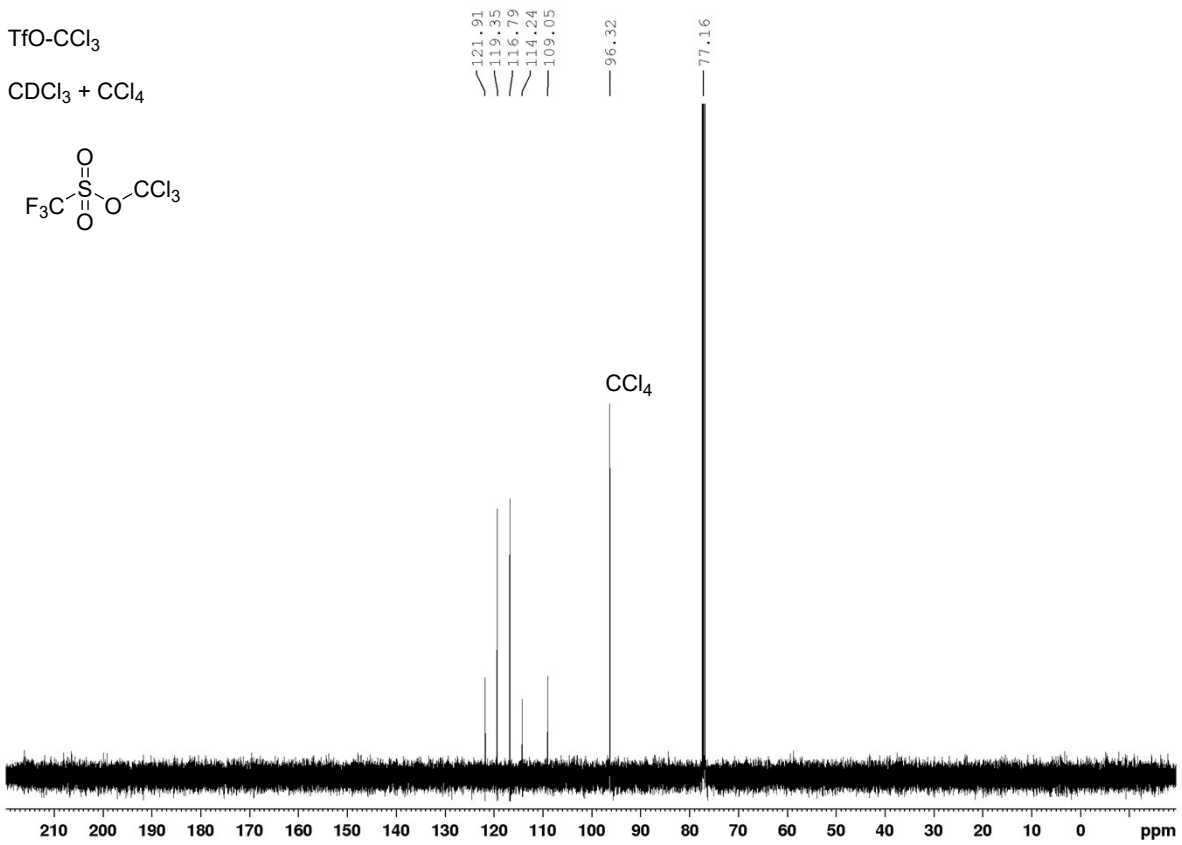

Figure S2. $^{13}C\{^{1}H\}$ NMR ($CDCl_3$ + ~20 v% CCl_4, 126 MHz): TfO-CCl_3.

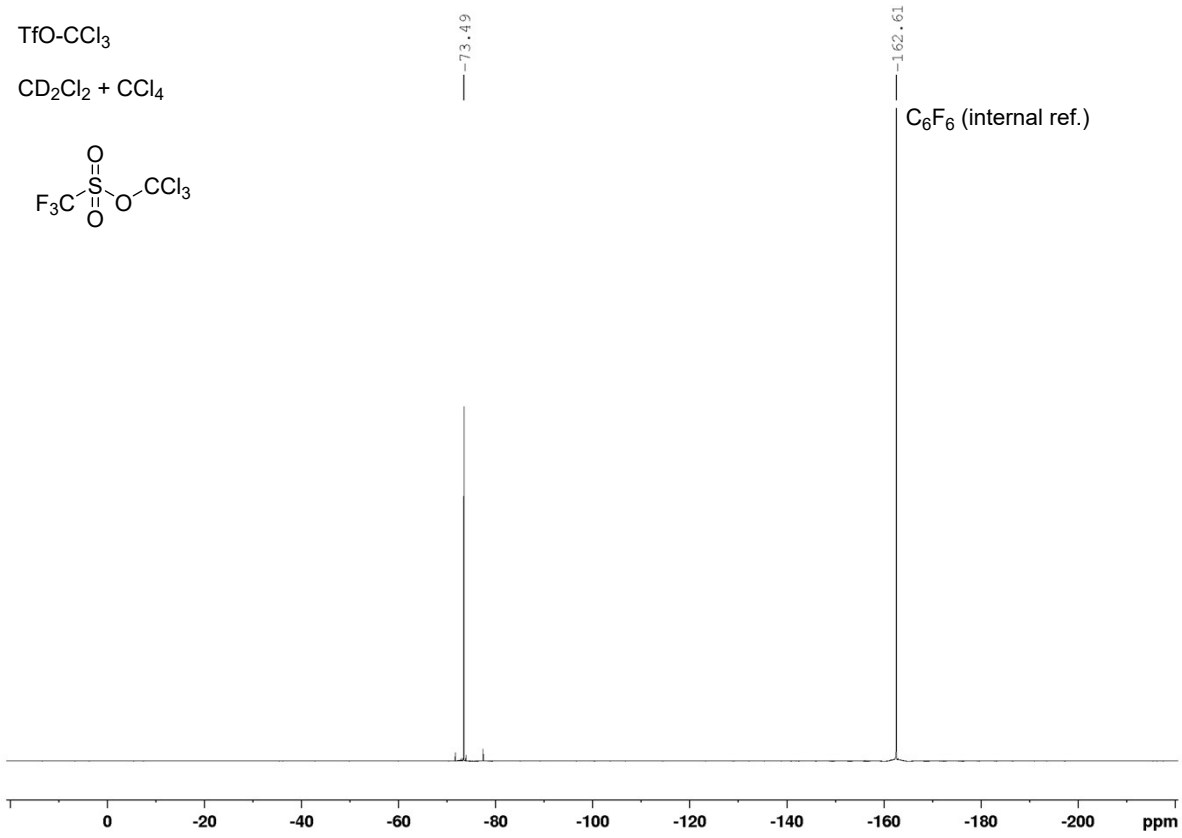

Figure S3. ^{19}F NMR (CD_2Cl_2 + ~10 v% CCl_4, 470 MHz): TfO-CCl_3.

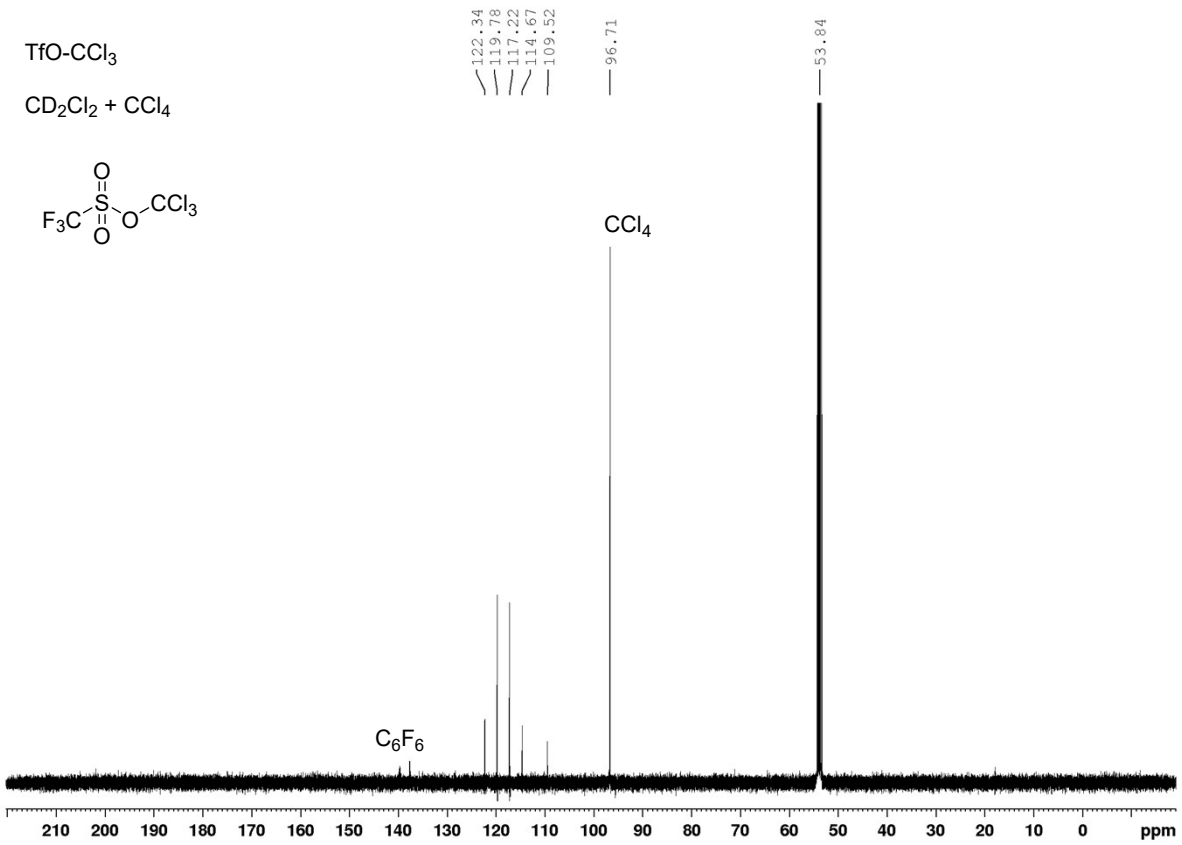

Figure S4. $^{13}C\{^{1}H\}$ NMR (CD_2Cl_2 + ~20 v% CCl_4, 126 MHz): TfO-CCl_3.

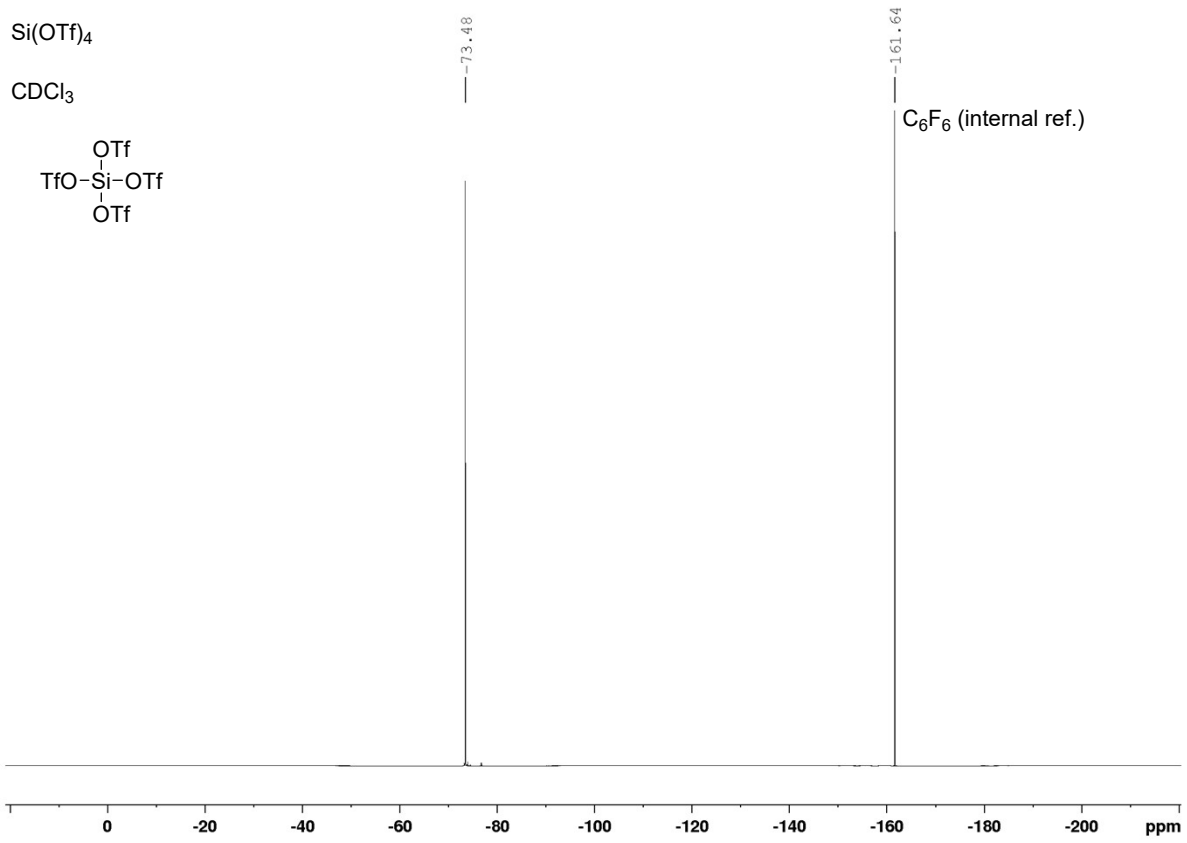

Figure S5. ^{19}F NMR ($CDCl_3$, 470 MHz): $Si(OTf)_4$.

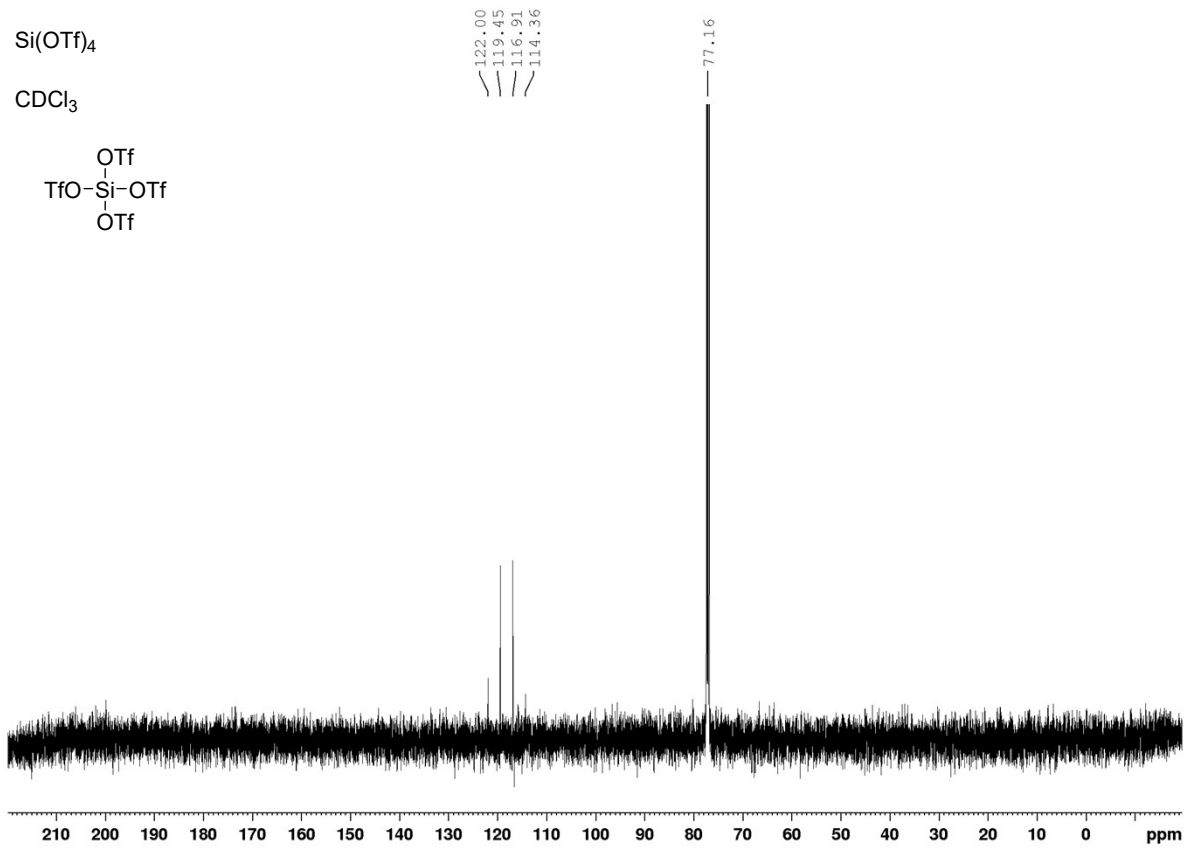

Figure S6. $^{13}C\{^{1}H\}$ NMR ($CDCl_3$, 126 MHz): $Si(OTf)_4$.

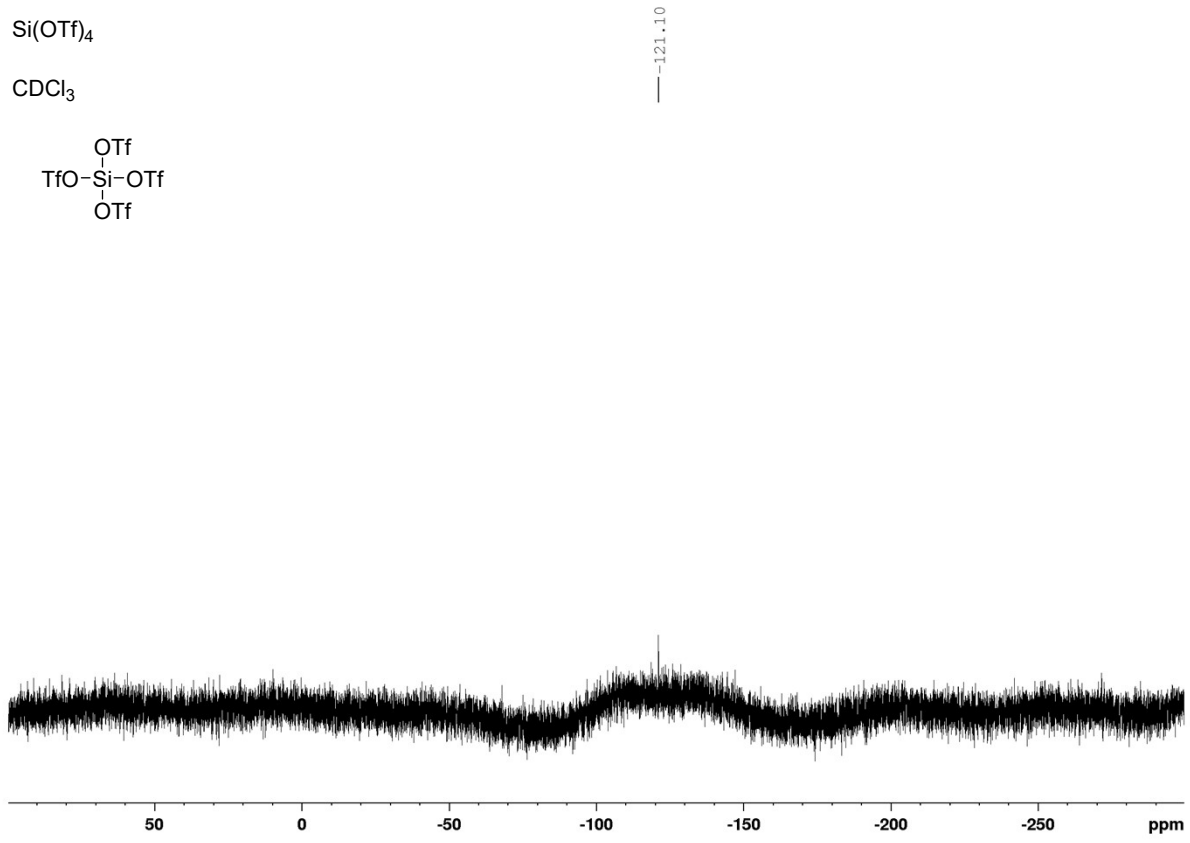

Figure S7. $^{29}Si\{^{1}H\}$ NMR ($CDCl_3$, 99 MHz): $Si(OTf)_4$.

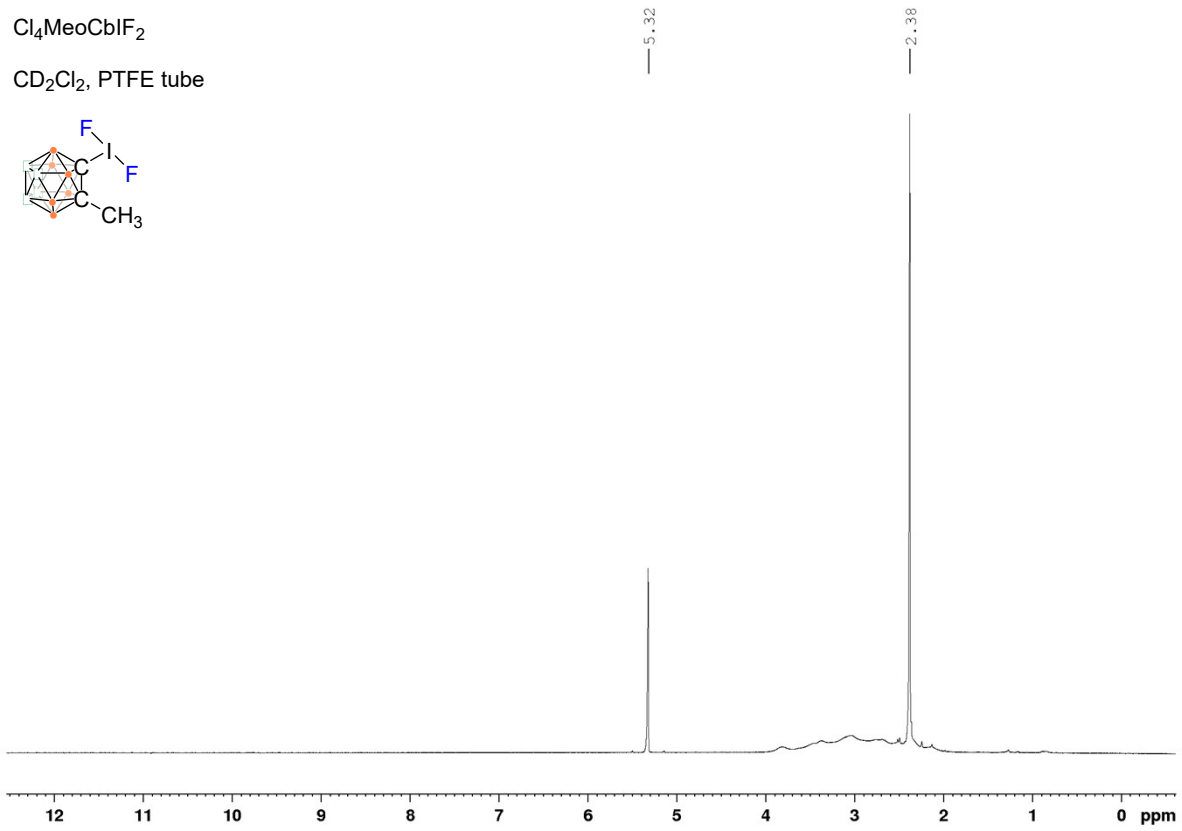

Figure S8. ^{1}H NMR (CD_2Cl_2, PTFE tube, 500 MHz): Cl_4MeoCb-IF_2.

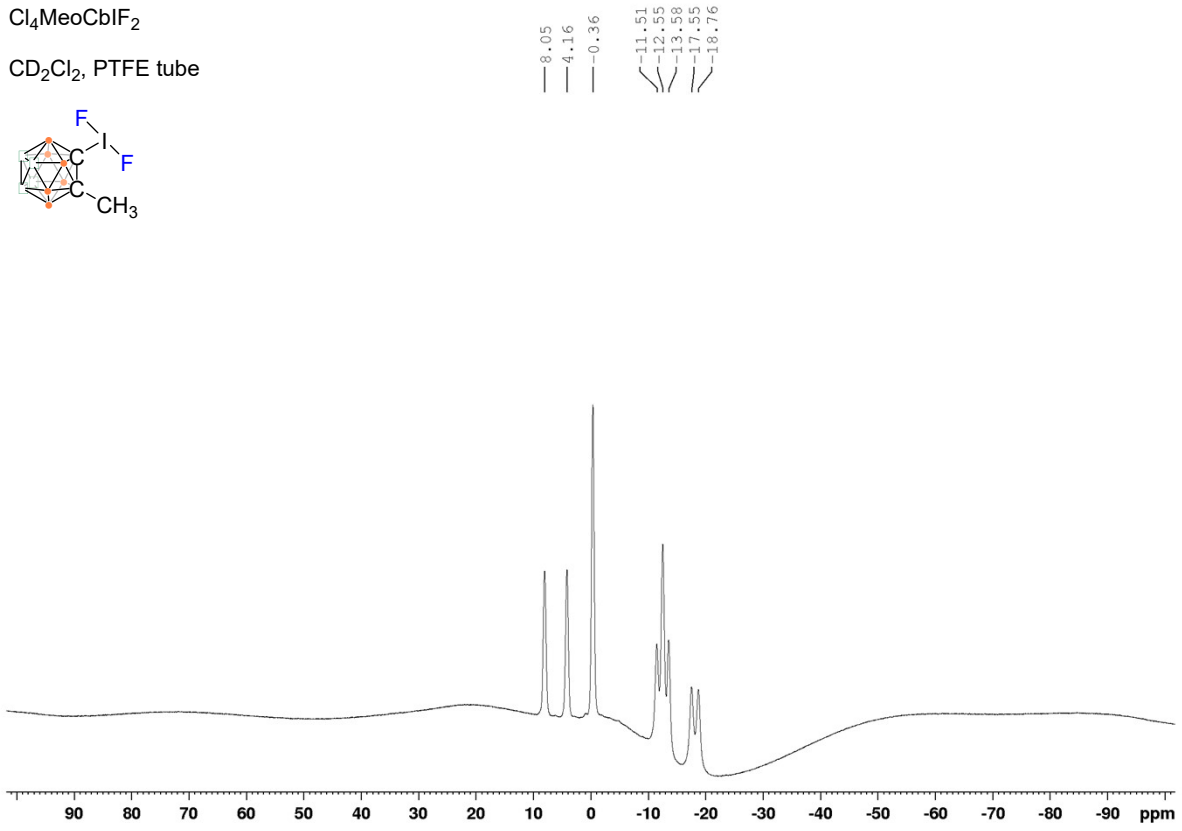

Figure S9. ^{11}B NMR (CD_2Cl_2, PTFE tube, 160 MHz): Cl_4MeoCb-IF_2.

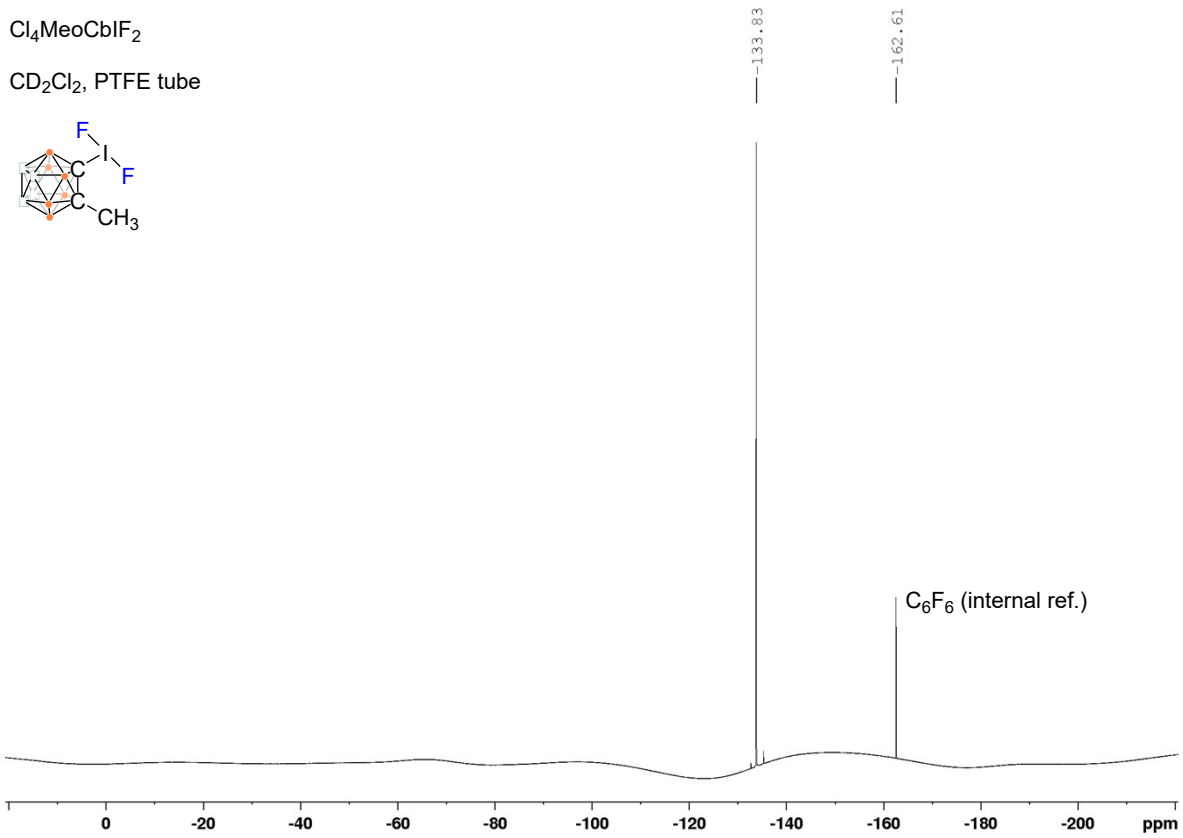

Figure S10. ^{19}F NMR (CD_2Cl_2, PTFE tube, 470 MHz): $Cl_4MeoCb\text{-}IF_2$.

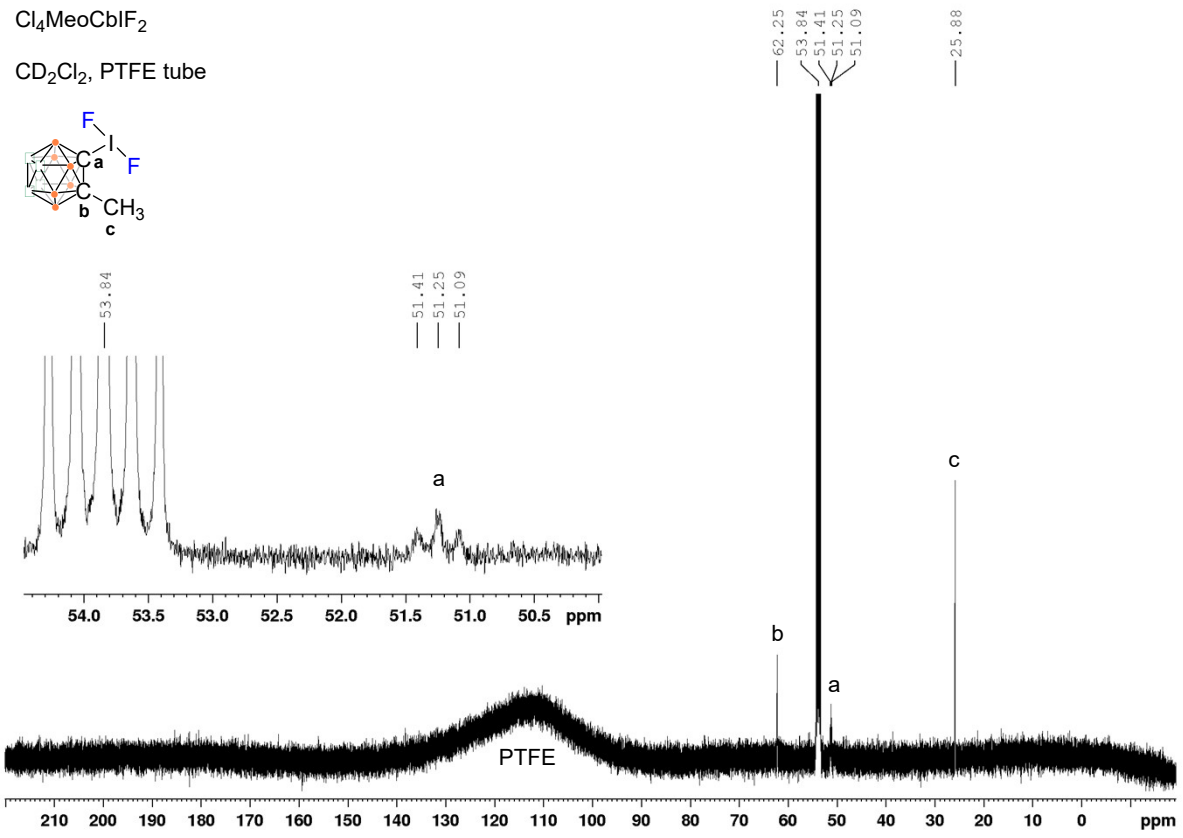

Figure S11. $^{13}C\{^1H\}$ NMR (CD_2Cl_2, PTFE tube, 126 MHz): $Cl_4MeoCb\text{-}IF_2$.

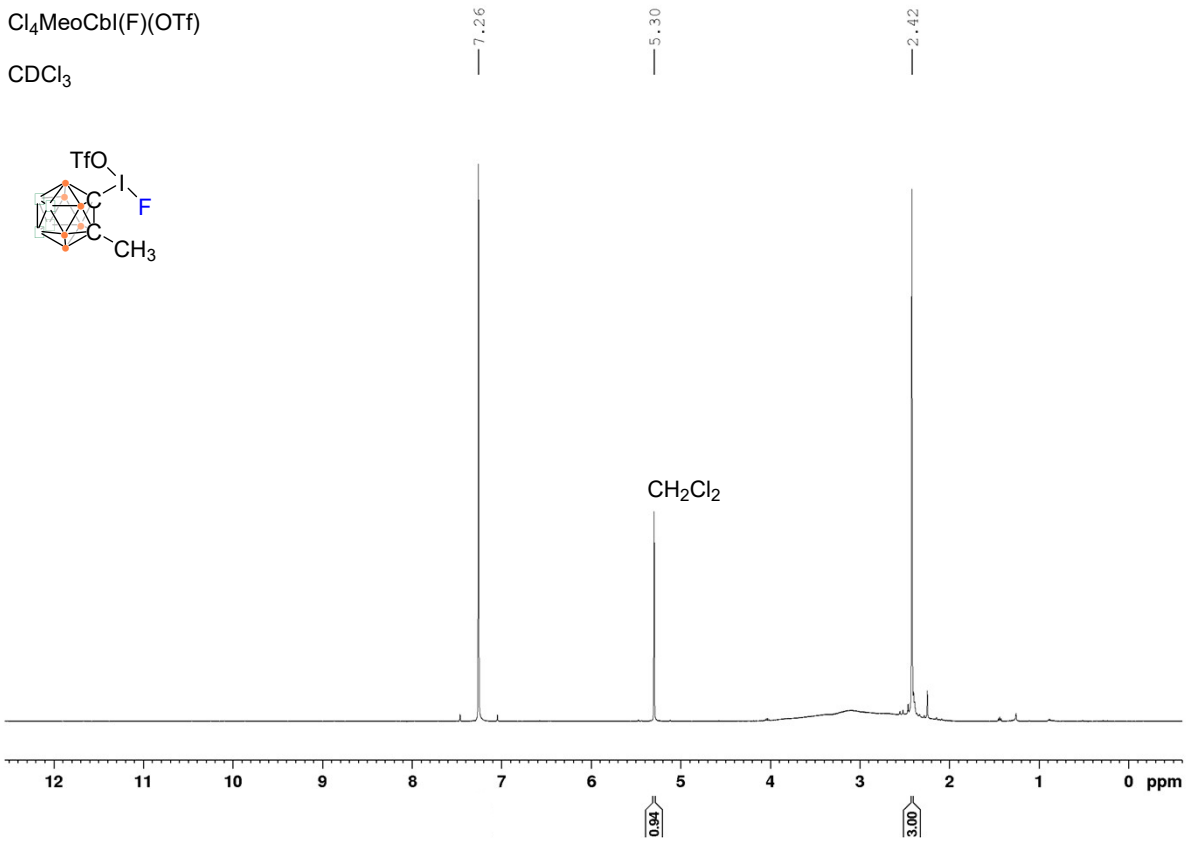

Figure S12. ^{1}H NMR ($CDCl_3$, 500 MHz): Cl_4MeoCb-I(F)(OTf).

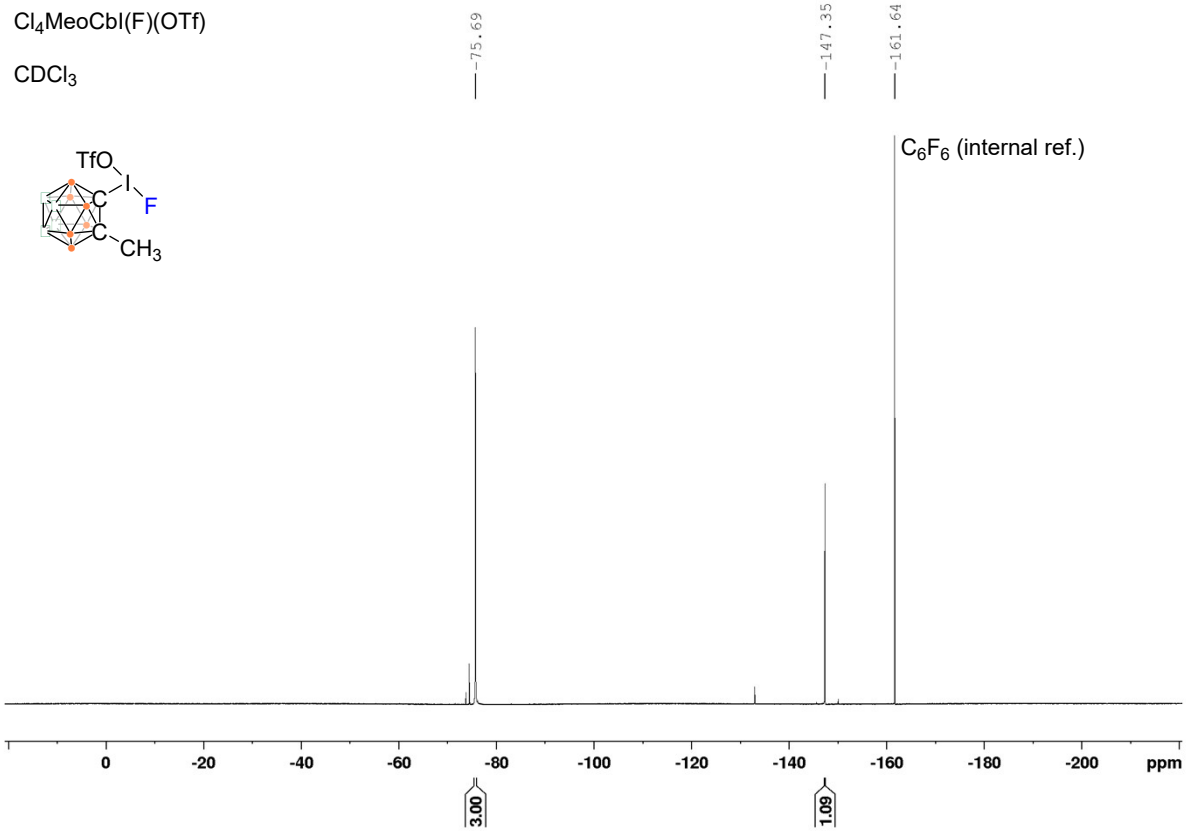

Figure S13. ^{19}F NMR ($CDCl_3$, 470 MHz): Cl_4MeoCb-I(F)(OTf). D1 set to 3 seconds.

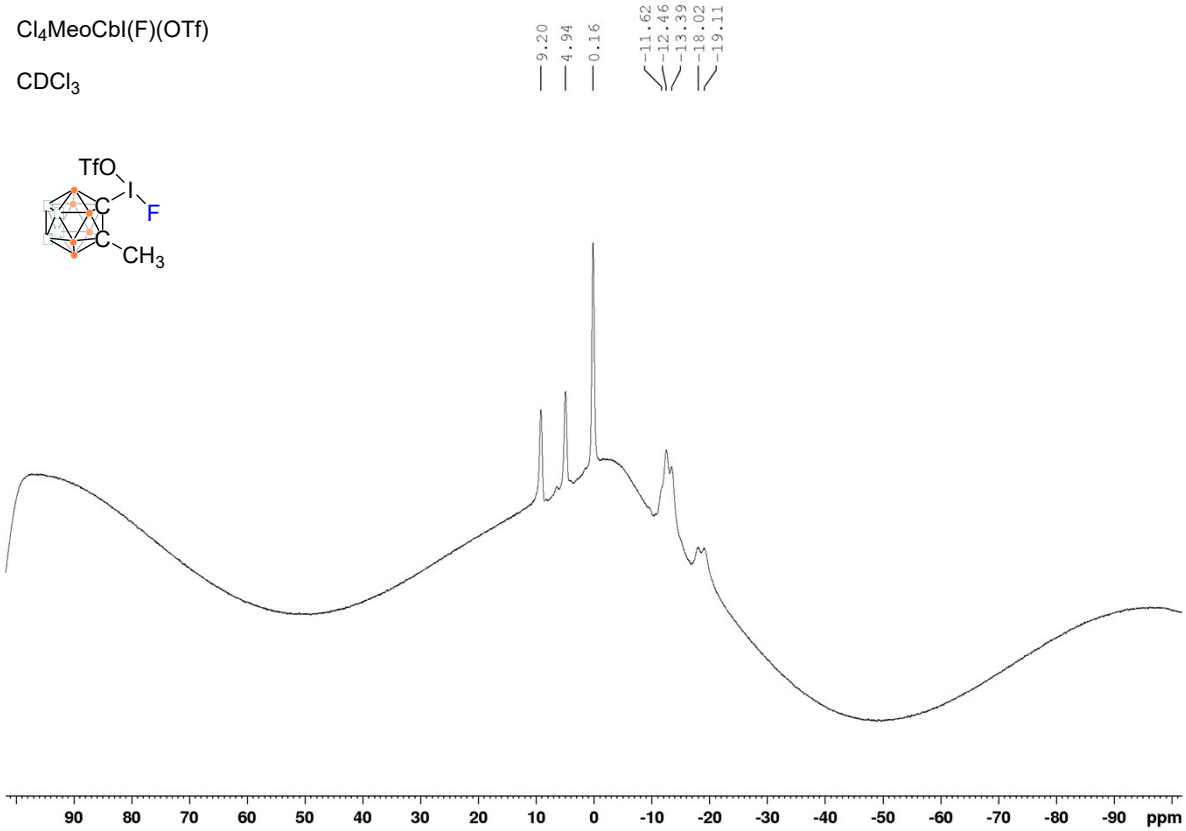

Figure S14. ^{11}B NMR ($CDCl_3$, 160 MHz): Cl_4MeoCb-I(F)(OTf).

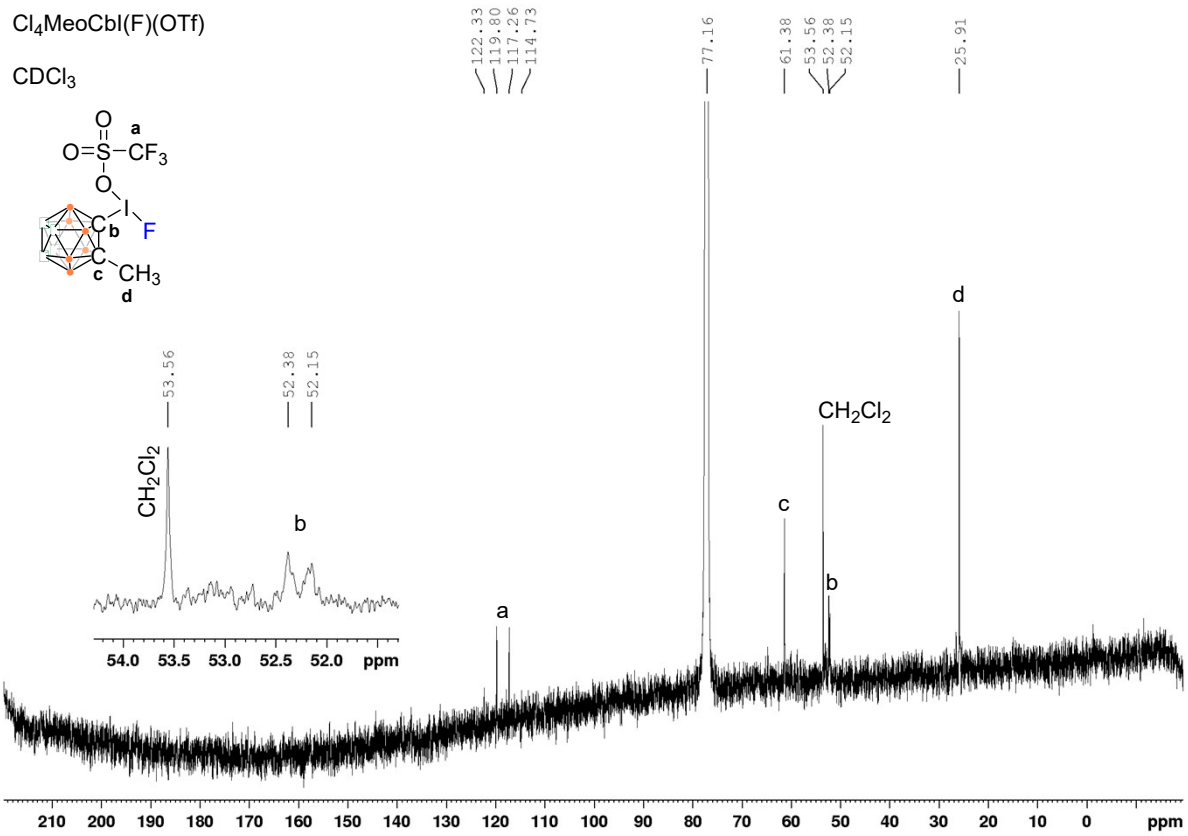

Figure S15. $^{13}C\{^{1}H\}$ NMR ($CDCl_3$, 126 MHz): Cl_4MeoCbI-(F)(OTf). Line broadening set to 2 Hz to increase visibility of carbon **b**.

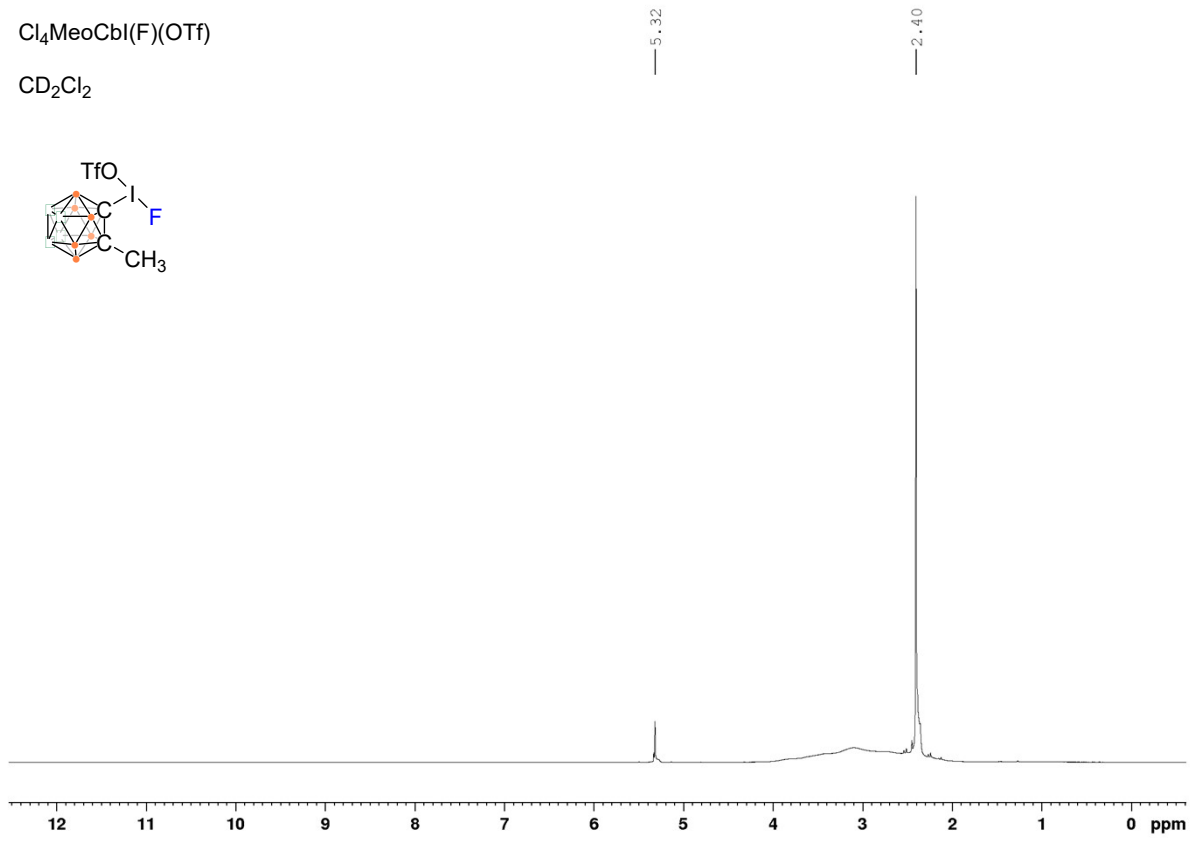

Figure S16. ^{1}H NMR (CD_2Cl_2, 500 MHz): Cl_4MeoCb-I(F)(OTf).

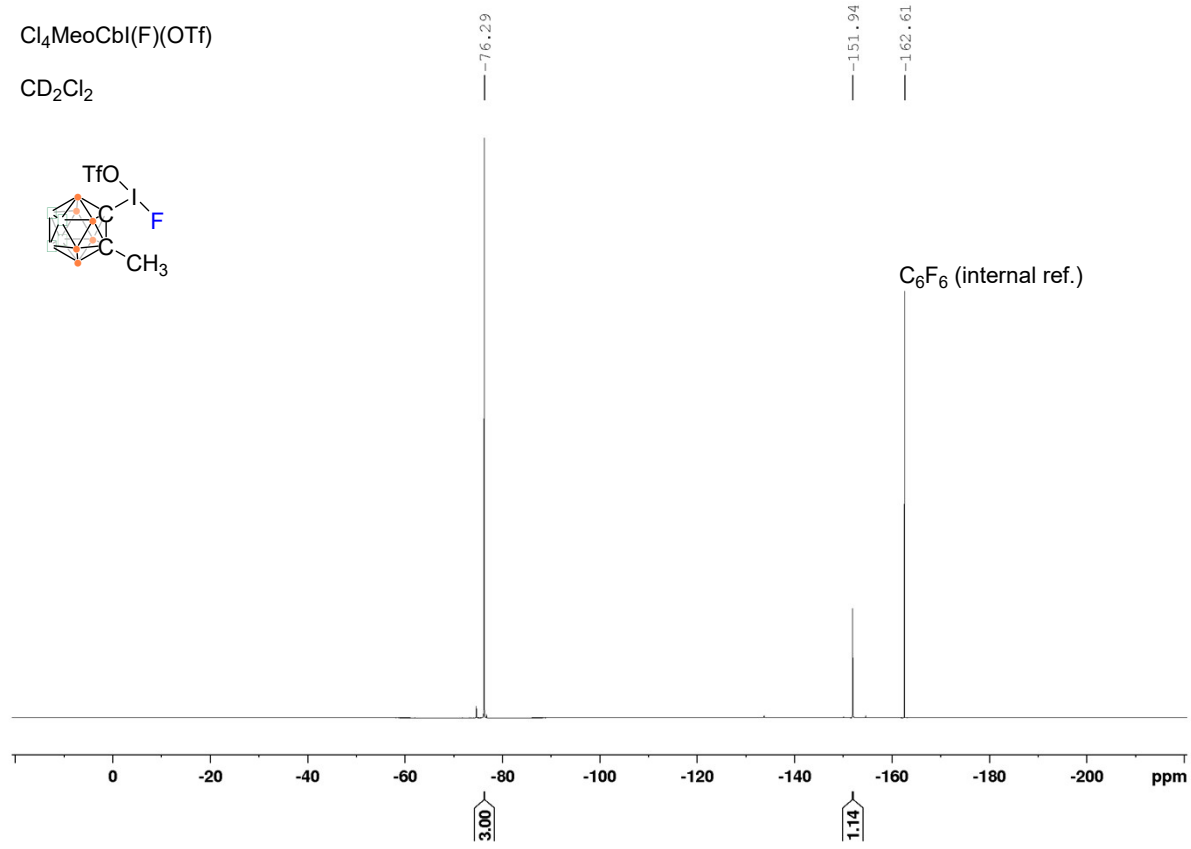

Figure S17. ^{19}F NMR (CD_2Cl_2, 470 MHz): Cl_4MeoCb-I(F)(OTf). D1 set to 3 seconds.

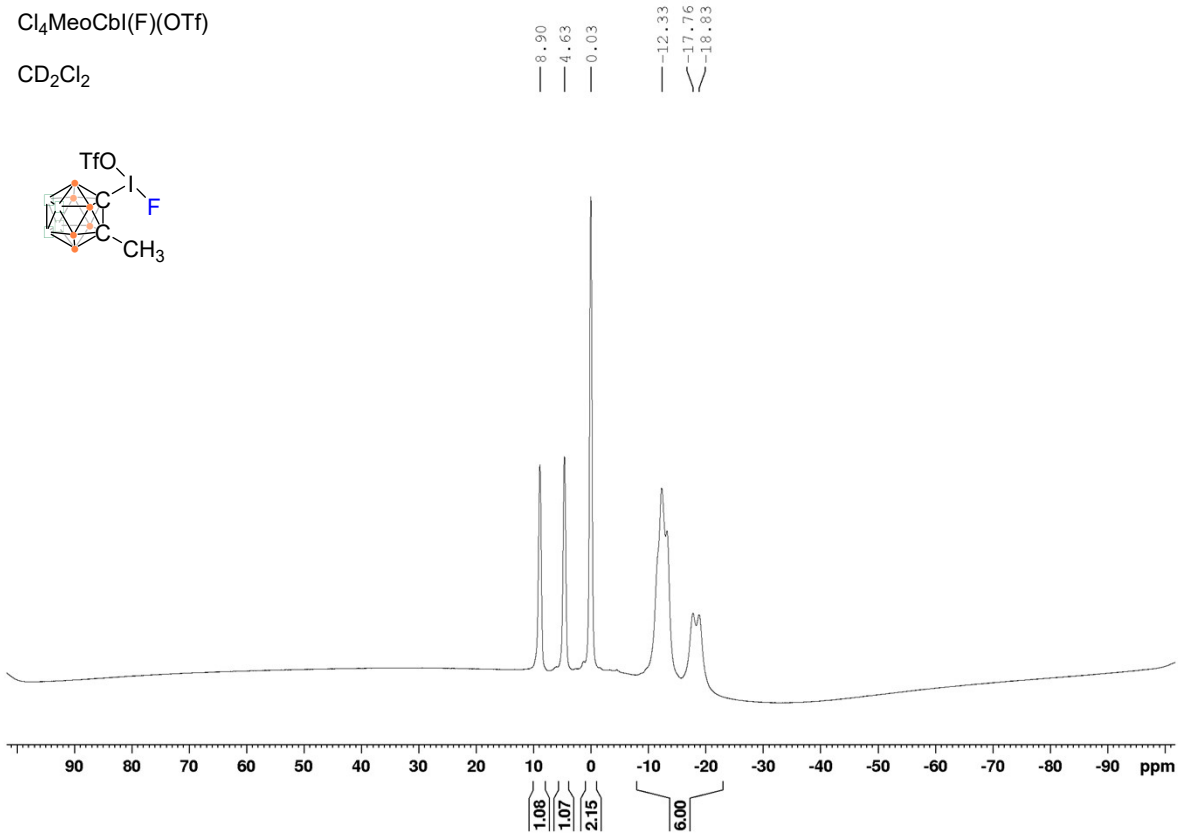

Figure S18. ^{11}B NMR (CD_2Cl_2, 160 MHz): Cl_4MeoCb-I(F)(OTf). Integrals use baseline correction.

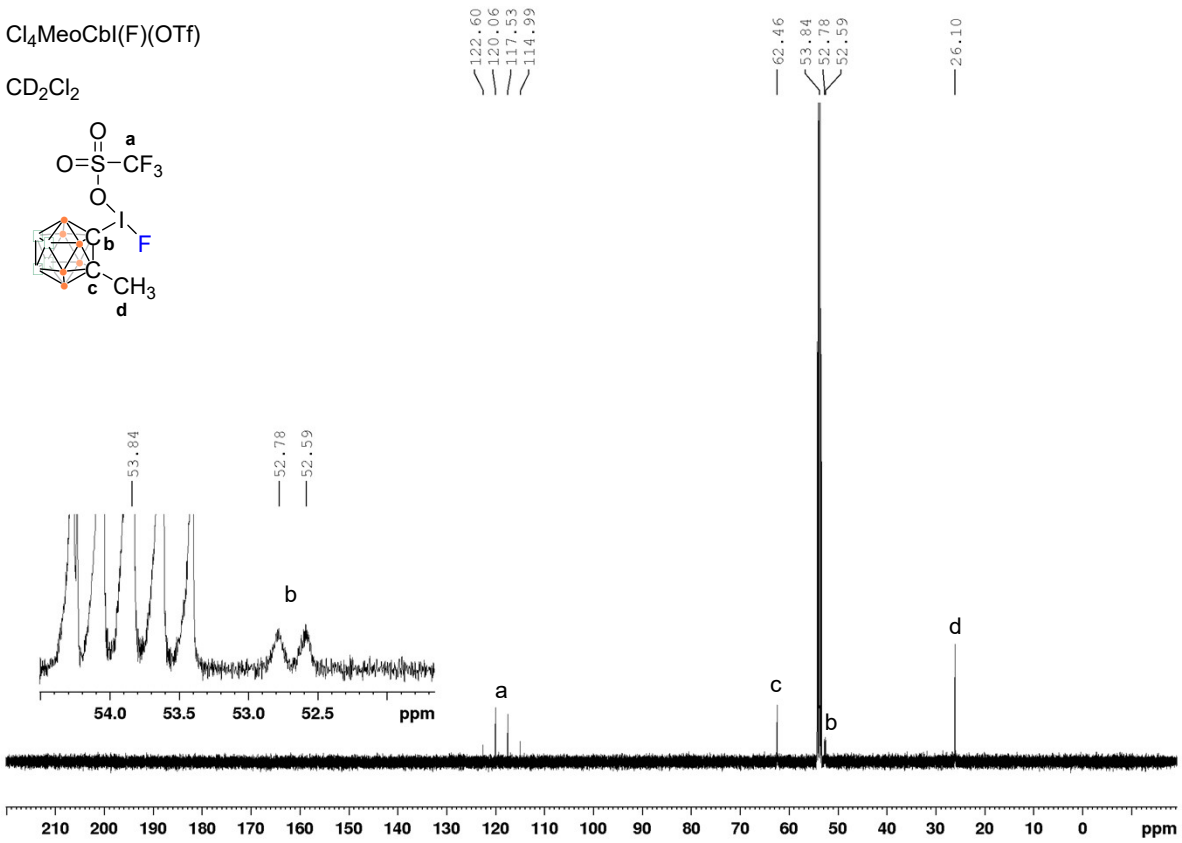

Figure S19. $^{13}C\{^{1}H\}$ NMR (CD_2Cl_2, 126 MHz): Cl_4MeoCbI-(F)(OTf).

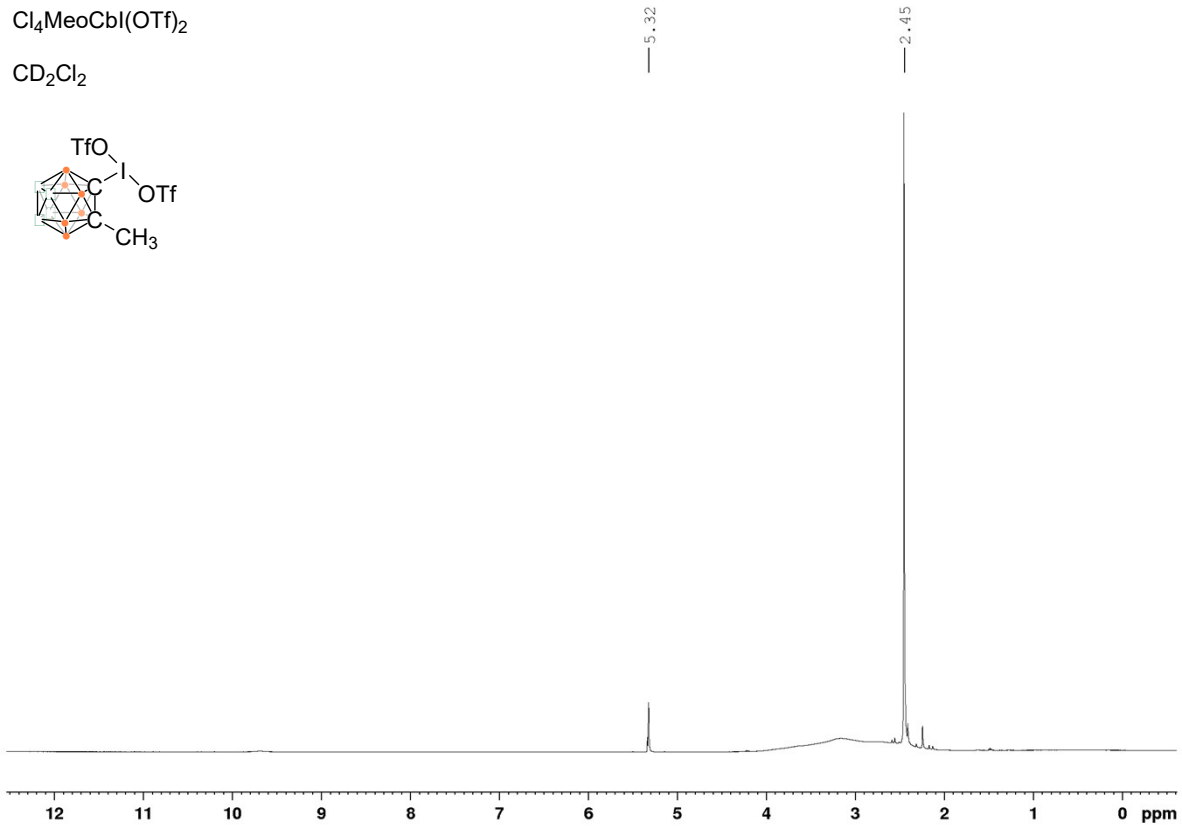

Figure S20. ^{1}H NMR (CD_2Cl_2, 500 MHz): $Cl_4MeoCb\text{-}I(OTf)_2$.

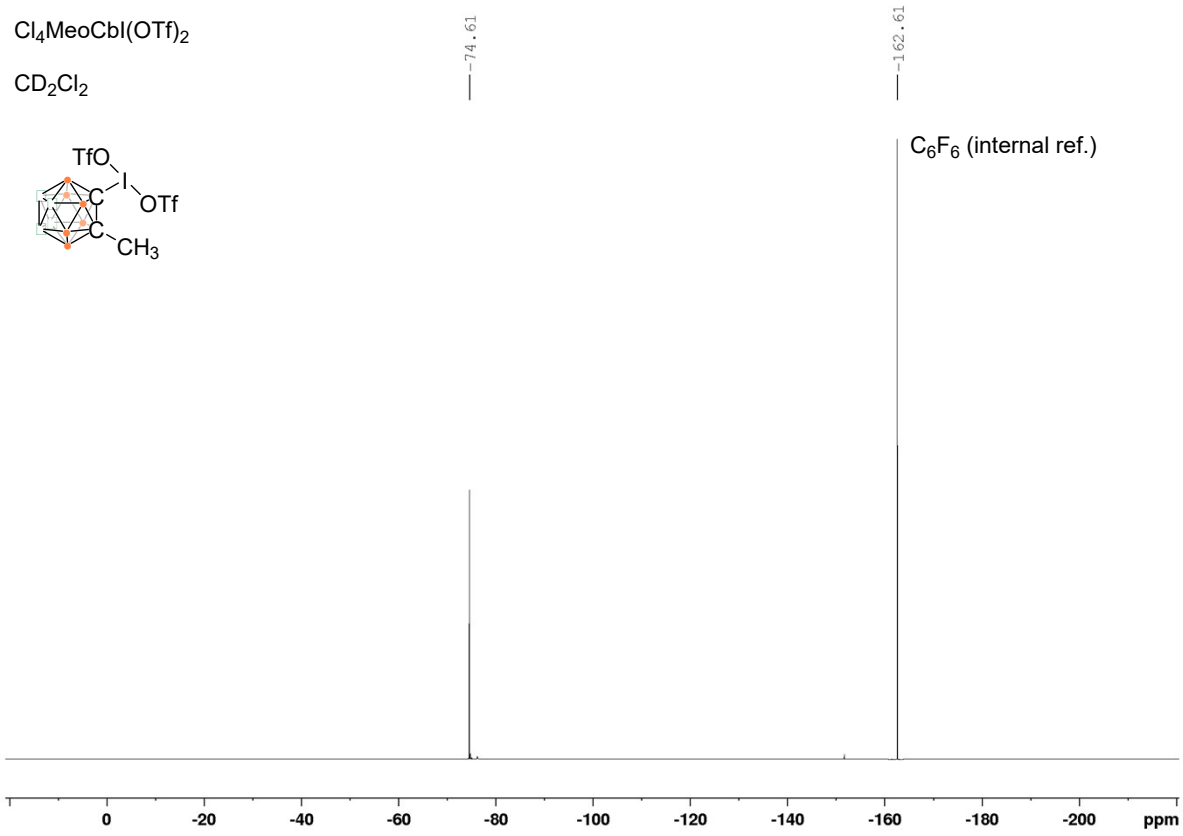

Figure S21. ^{19}F NMR (CD_2Cl_2, 470 MHz): Cl_4MeoCb-I$(OTf)_2$.

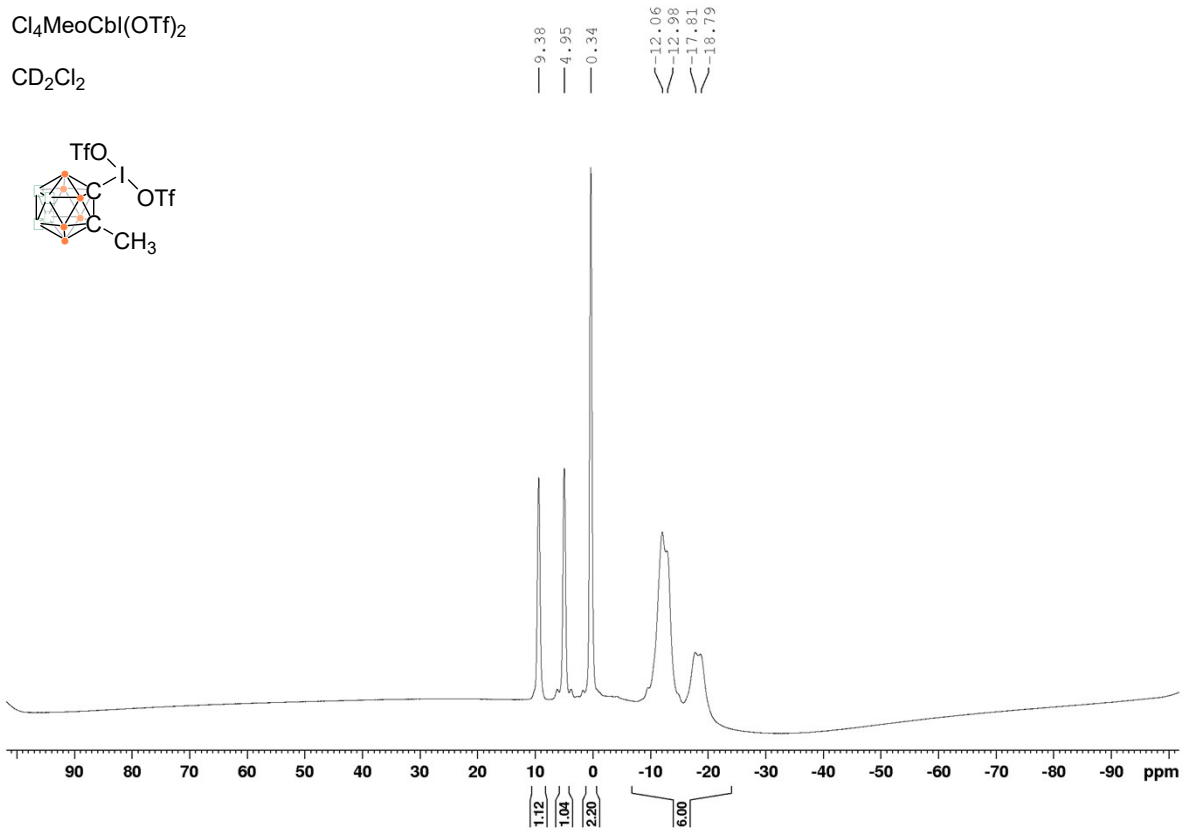

Figure S22. ^{11}B NMR (CD_2Cl_2, 160 MHz): Cl_4MeoCb-I(OTf)$_2$. Integrals use baseline correction.

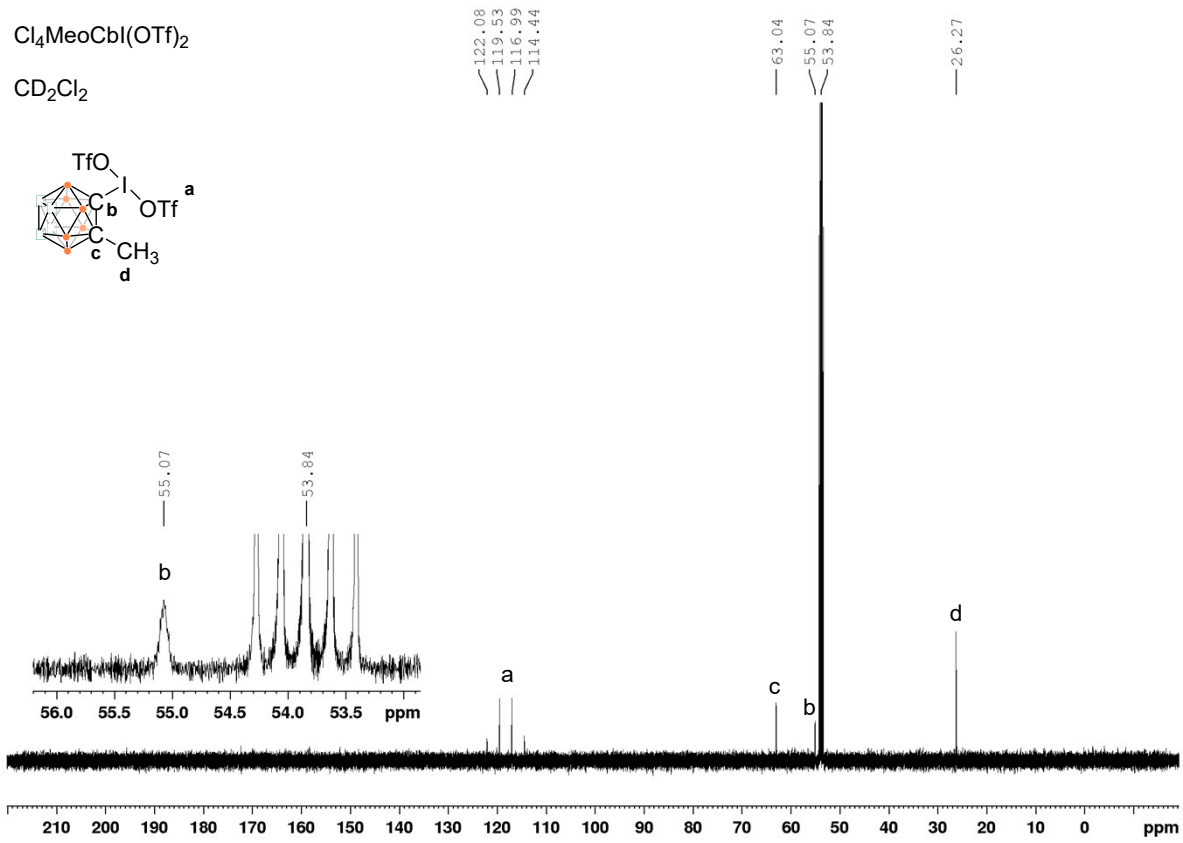

Figure S23. $^{13}C\{^{1}H\}$ NMR (CD_2Cl_2, 126 MHz): Cl_4MeoCb-I$(OTf)_2$.

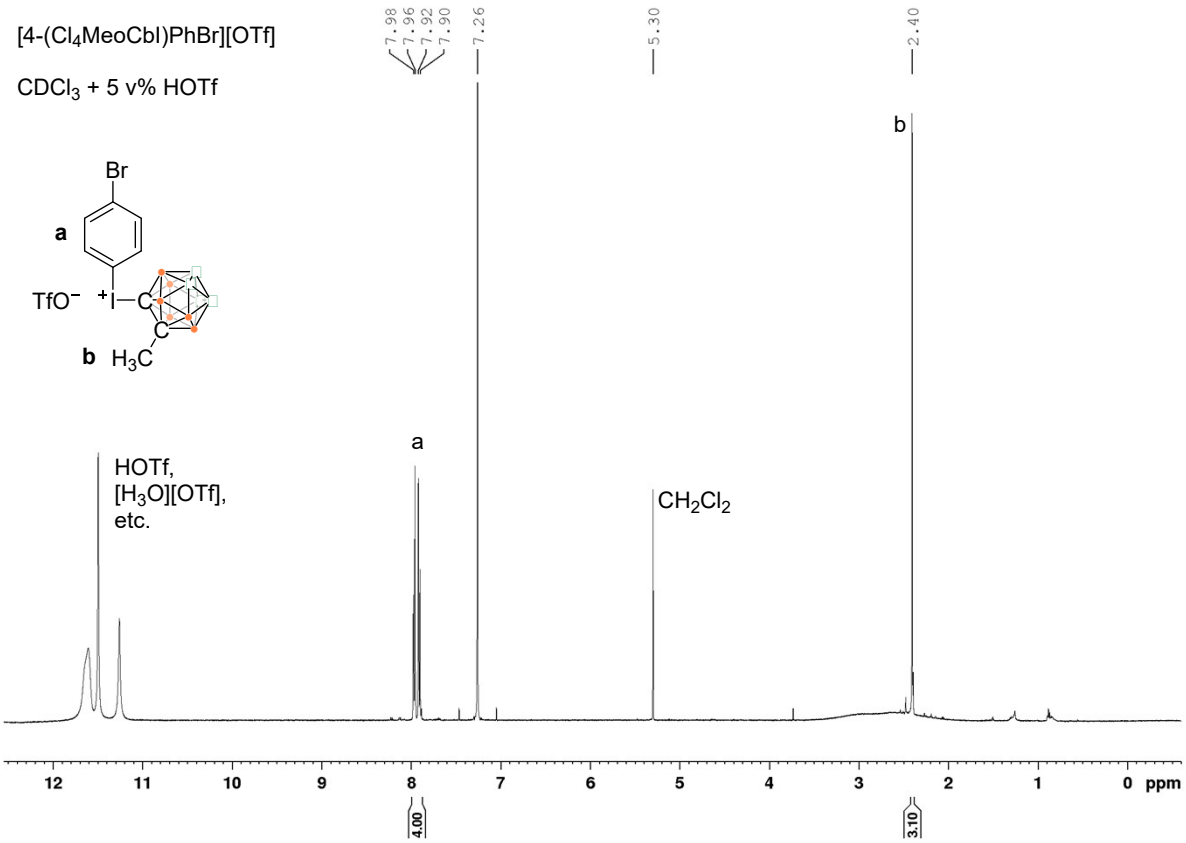

Figure S24. ^{1}H NMR ($CDCl_3$ + 5 v% HOTf, 500 MHz): [4-(Cl_4MeoCbI)PhBr][OTf].

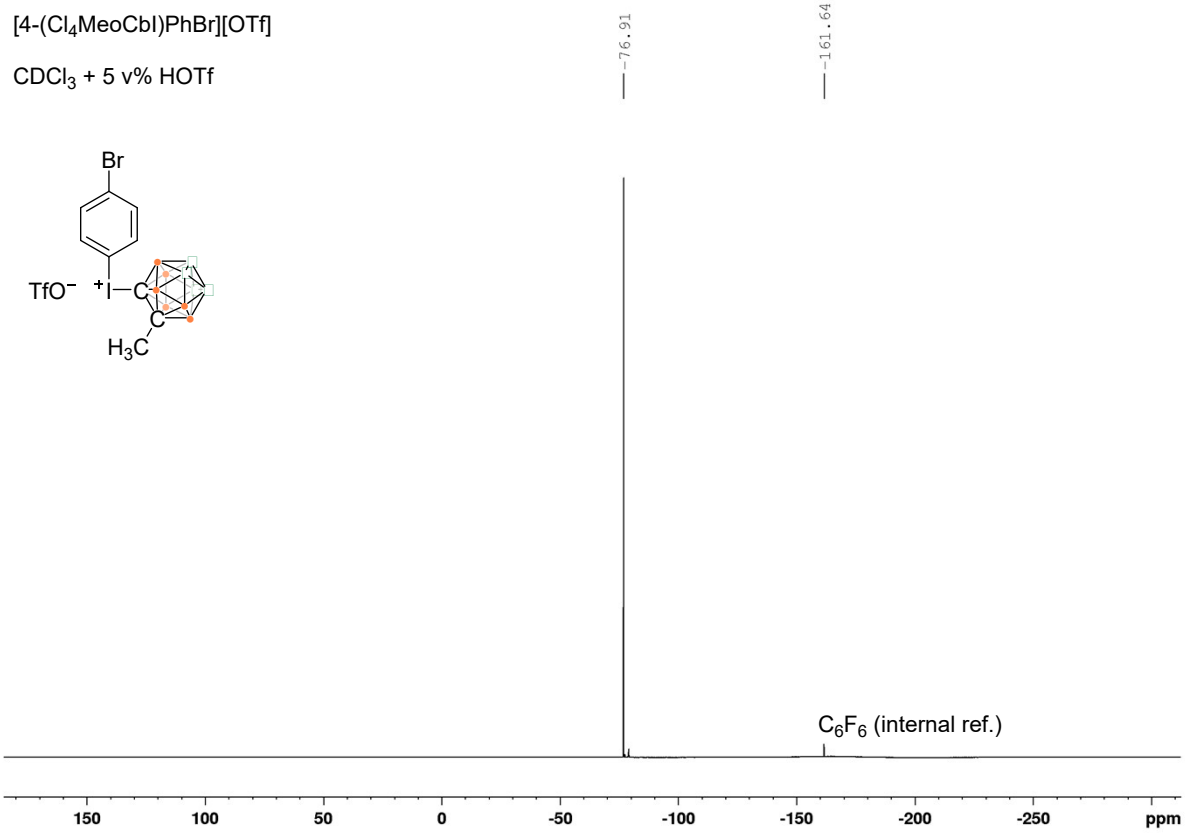

Figure S25. ^{19}F NMR ($CDCl_3$ + 5 v% HOTf, 376 MHz): [4-(Cl_4MeoCbI)PhBr][OTf].

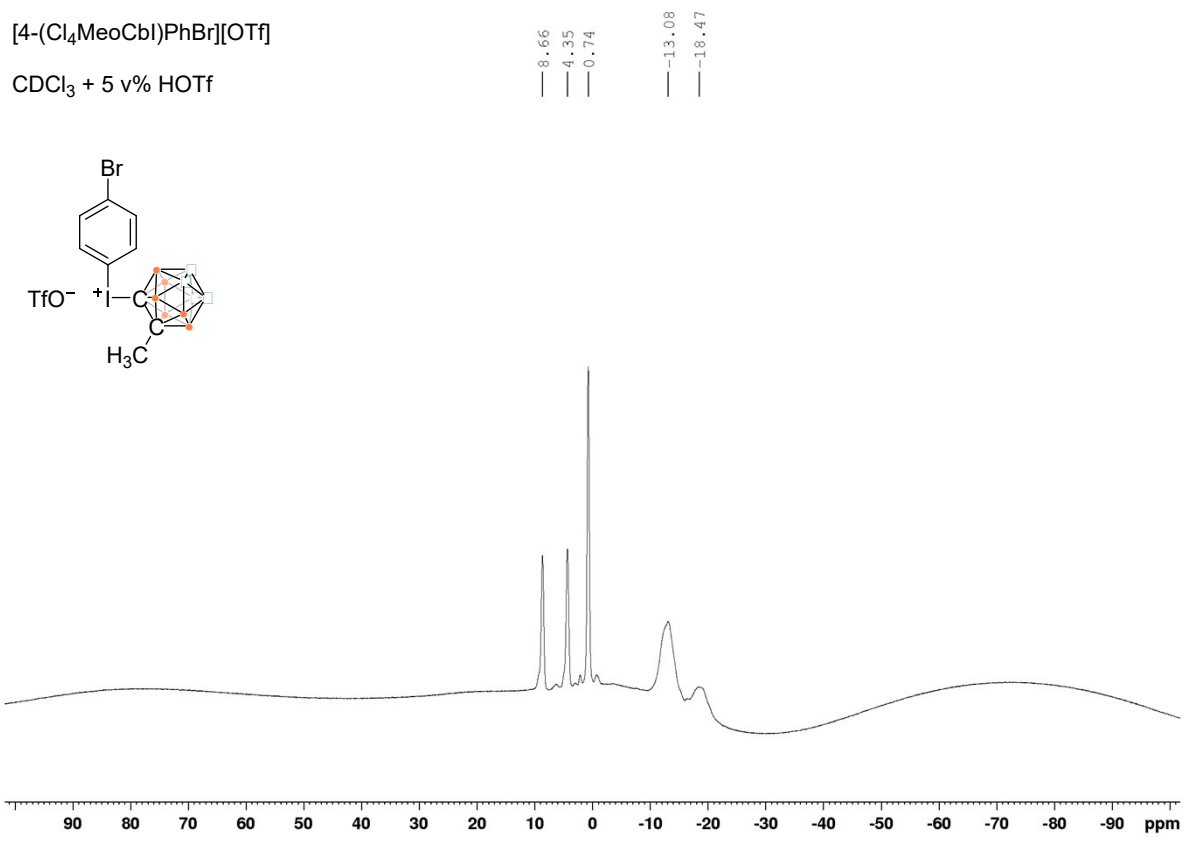

Figure S26. ^{11}B NMR ($CDCl_3$ + 5 v% HOTf, 160 MHz): [4-(Cl_4MeoCbI)PhBr][OTf].

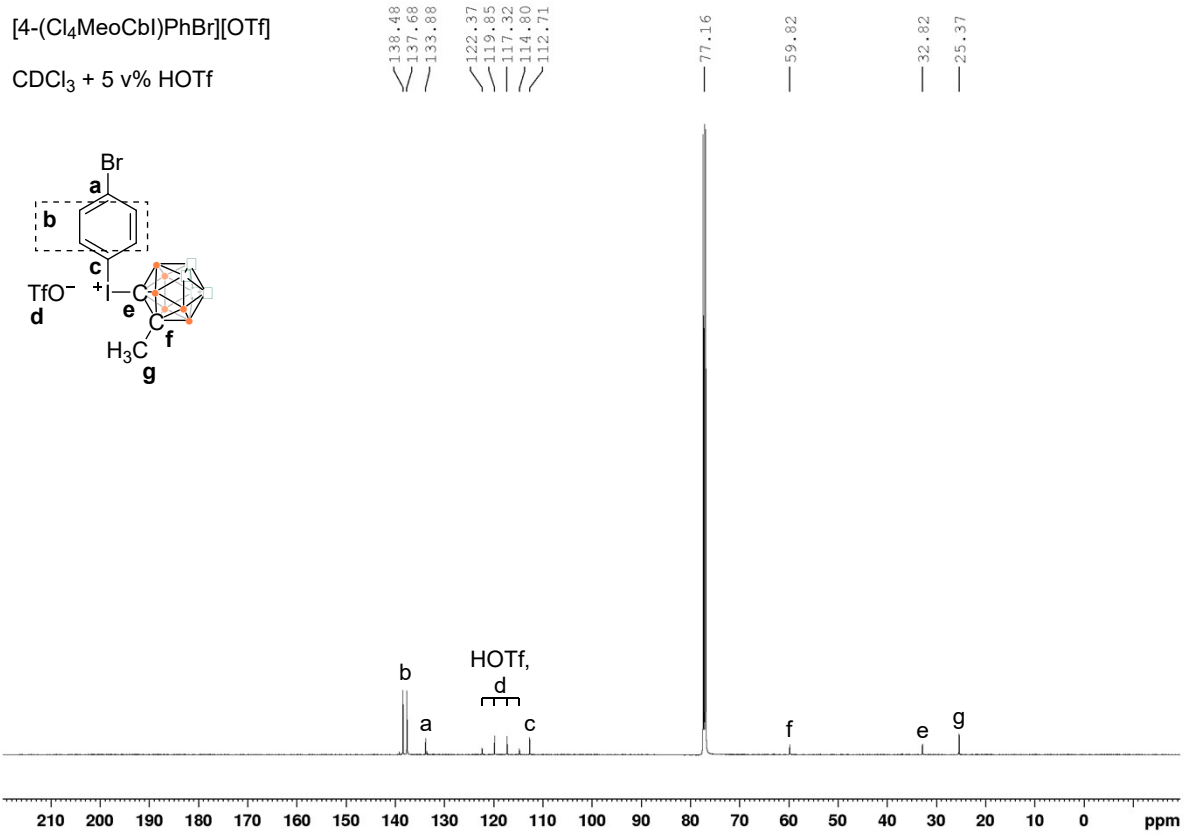

Figure S27. $^{13}C\{^1H\}$ NMR ($CDCl_3$ + 5 v% HOTf, 126 MHz): [4-(Cl_4MeoCbI)PhBr][OTf].

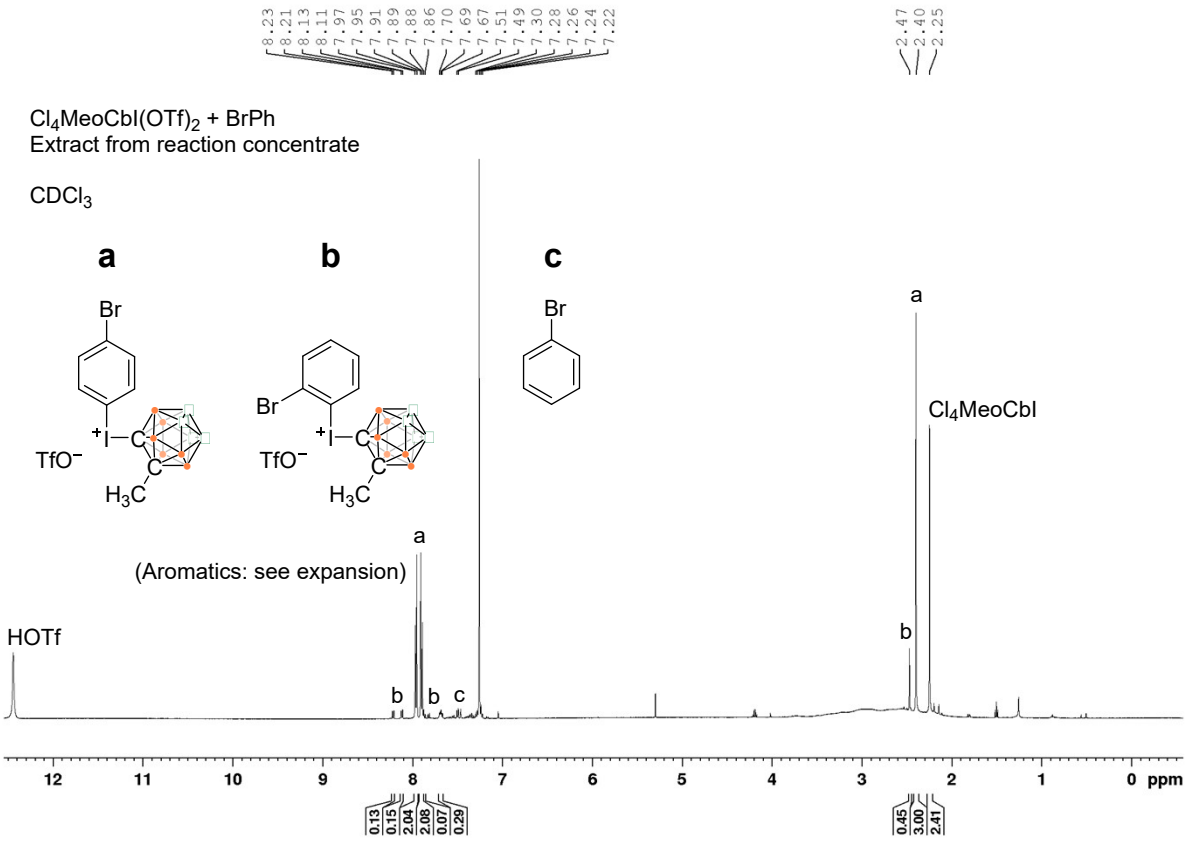

Figure S28. ^{1}H NMR ($CDCl_3$, 500 MHz): Unoptimized (room temperature) reaction of Cl_4MeoCb-I(OTf)$_2$ with BrPh, showing the o-isomer (b). Spectrum 1 of 2 (full).

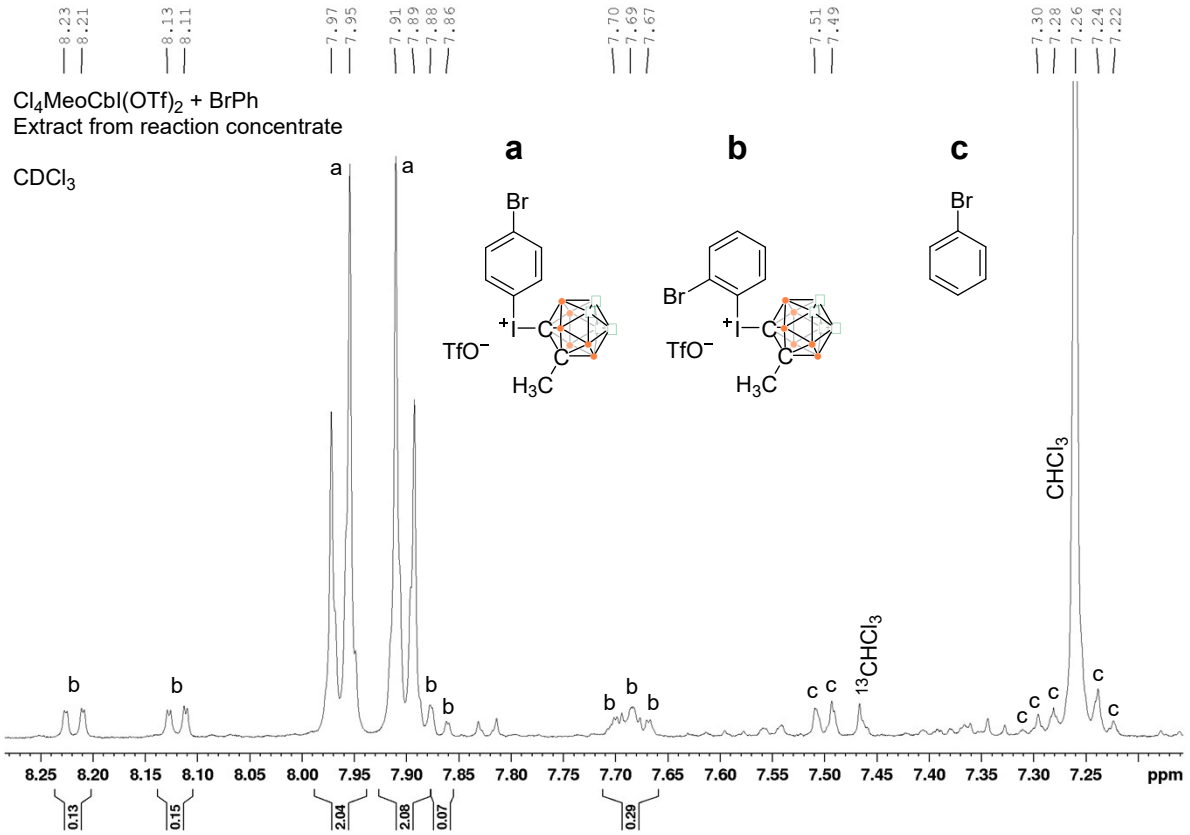

Figure S29. ^{1}H NMR ($CDCl_3$, 500 MHz): Unoptimized (room temperature) reaction of $Cl_4MeoCb\text{-}I(OTf)_2$ with BrPh, showing the o-isomer (b). Spectrum 2 of 2 (aromatics expansion).

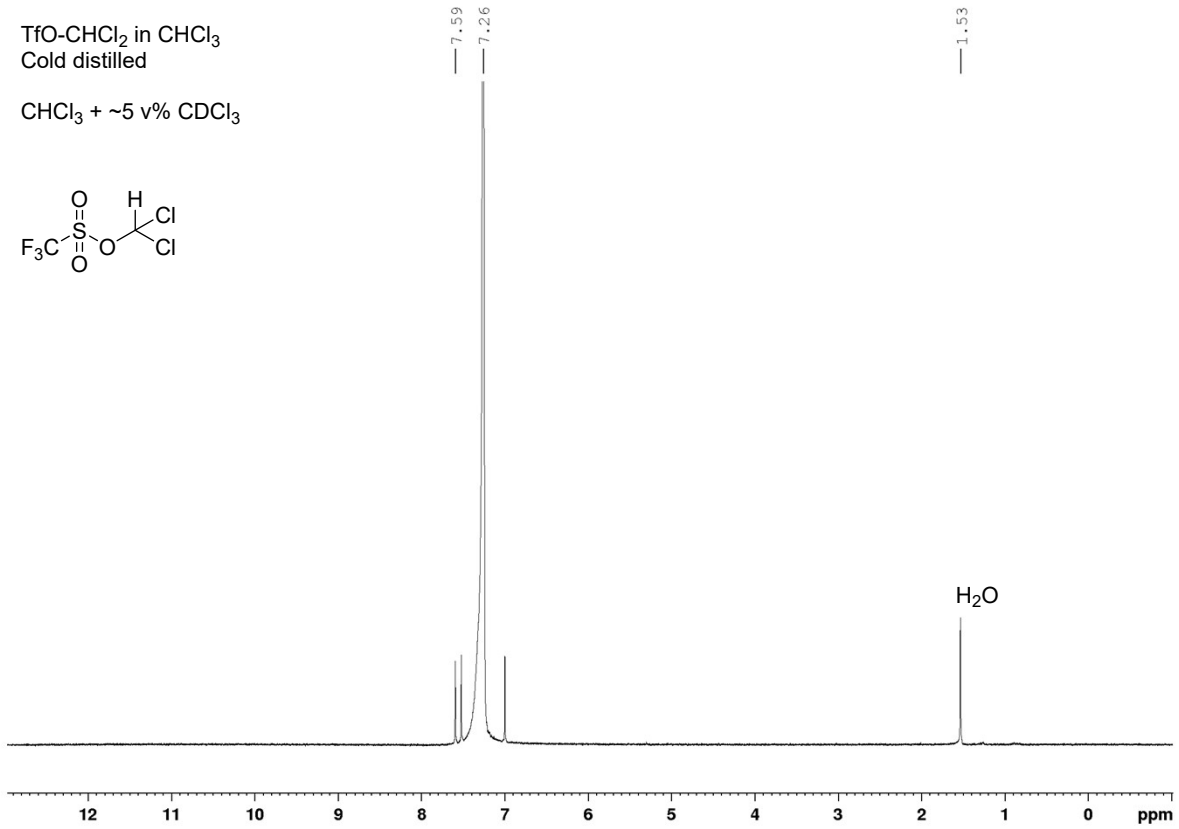

Figure S30. ^{1}H NMR ($CHCl_3$ + ~5 v% $CDCl_3$, 400 MHz): TfO-$CHCl_2$ isolated in $CHCl_3$.

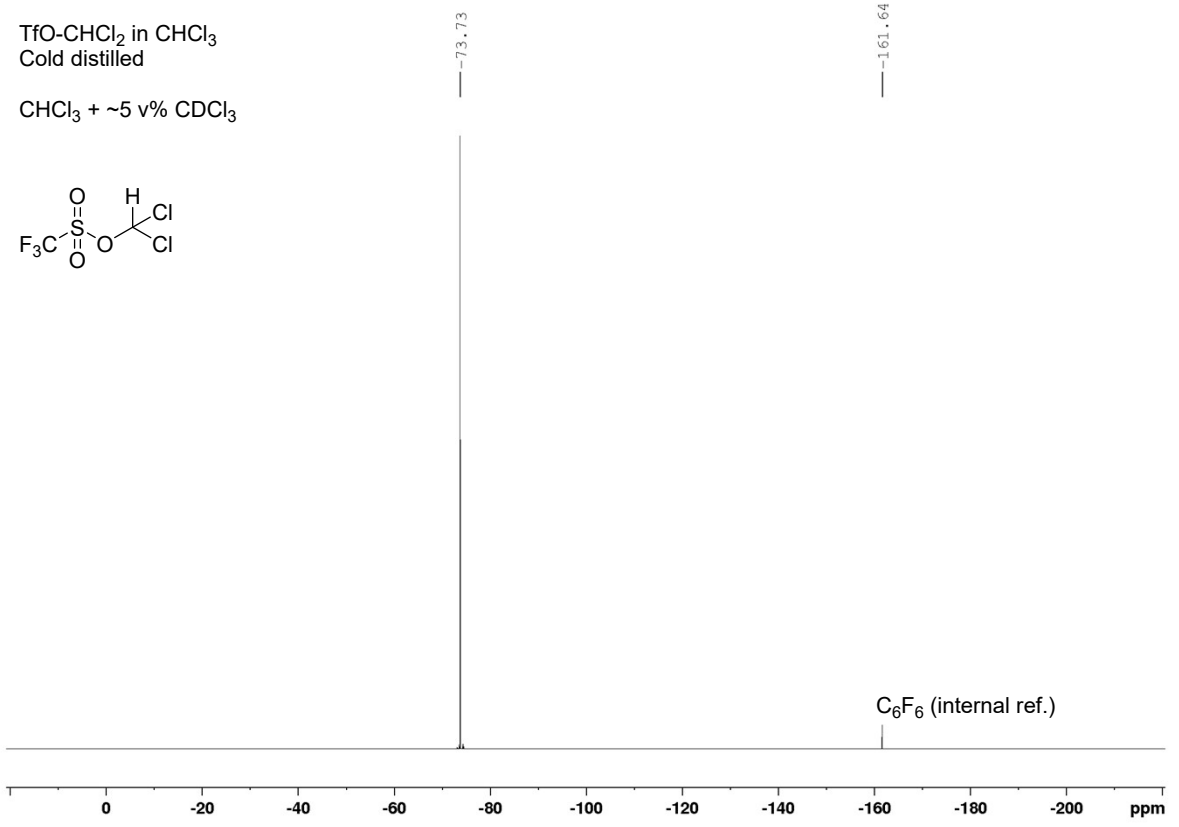

Figure S31. ^{19}F NMR ($CHCl_3$ + ~5 v% $CDCl_3$, 470 MHz): TfO-$CHCl_2$ isolated in $CHCl_3$.

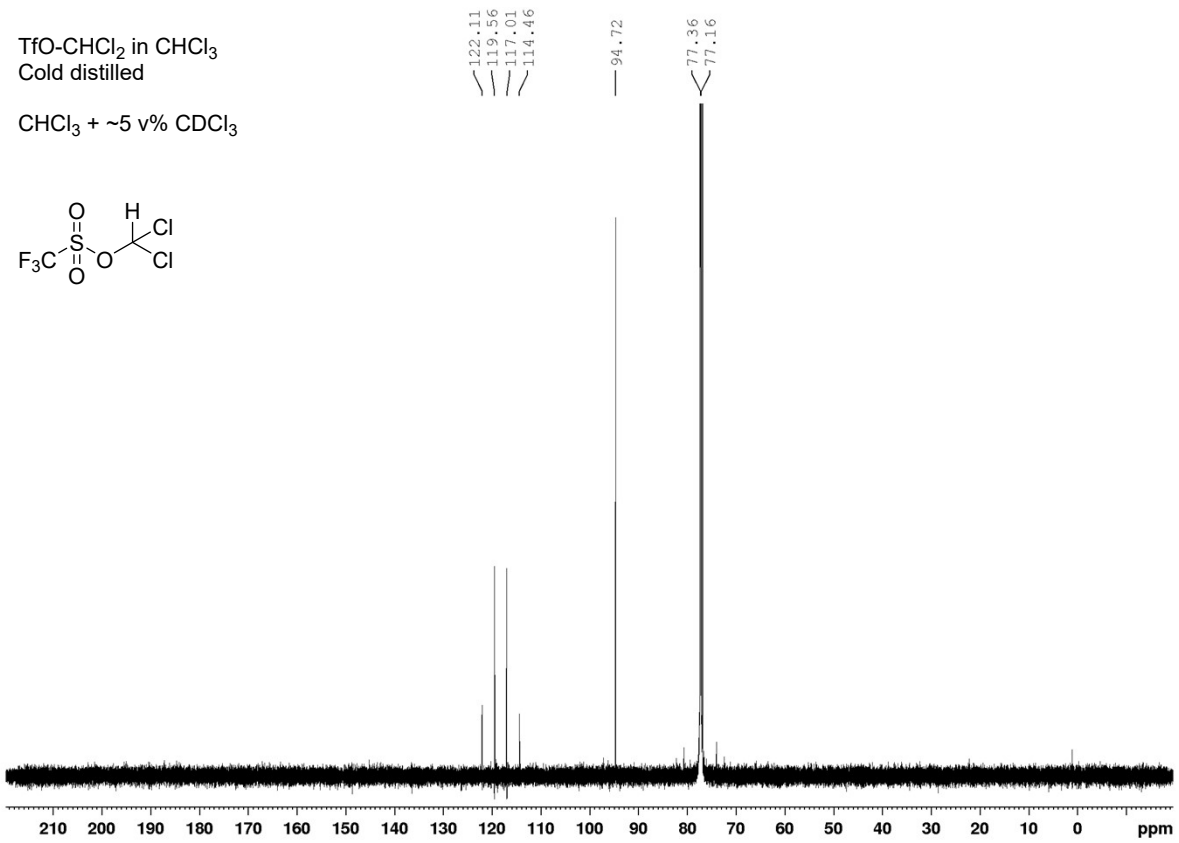

Figure S32. $^{13}C\{^{1}H\}$ NMR ($CHCl_3$ + ~ 5 v% $CDCl_3$, 126 MHz): TfO-$CHCl_2$ isolated in $CHCl_3$.

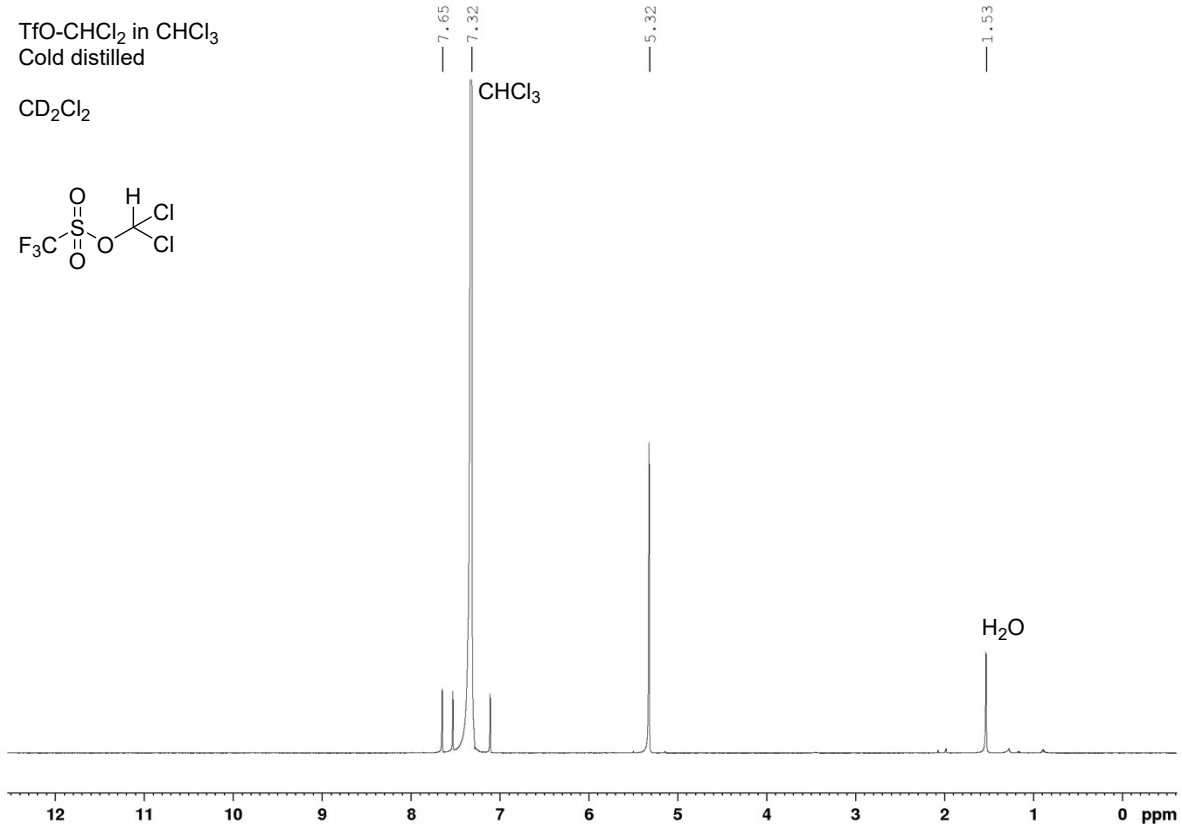

Figure S33. ^{1}H NMR (CD_2Cl_2 + ~5 v% $CHCl_3$, 500 MHz): TfO-$CHCl_2$ isolated in $CHCl_3$.

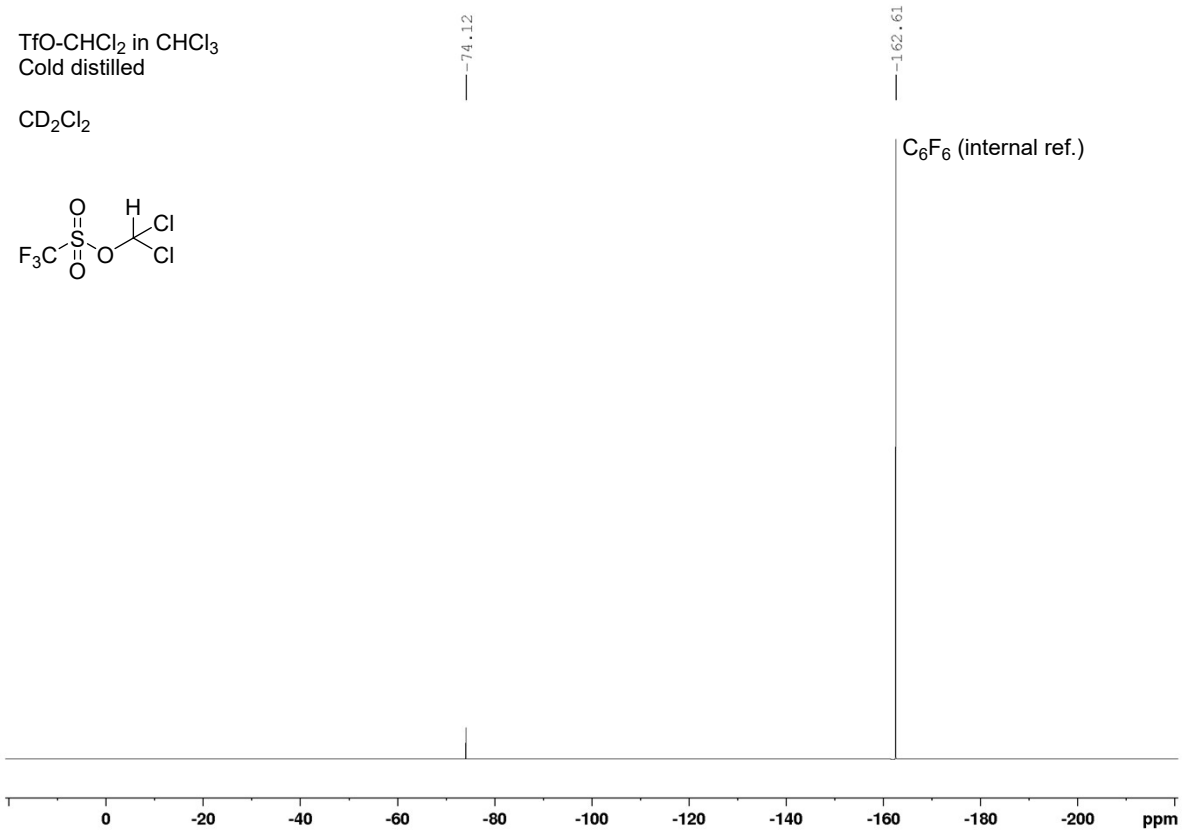

Figure S34. ^{19}F NMR (CD_2Cl_2 + ~5 v% $CHCl_3$, 470 MHz): TfO-$CHCl_2$ isolated in $CHCl_3$.

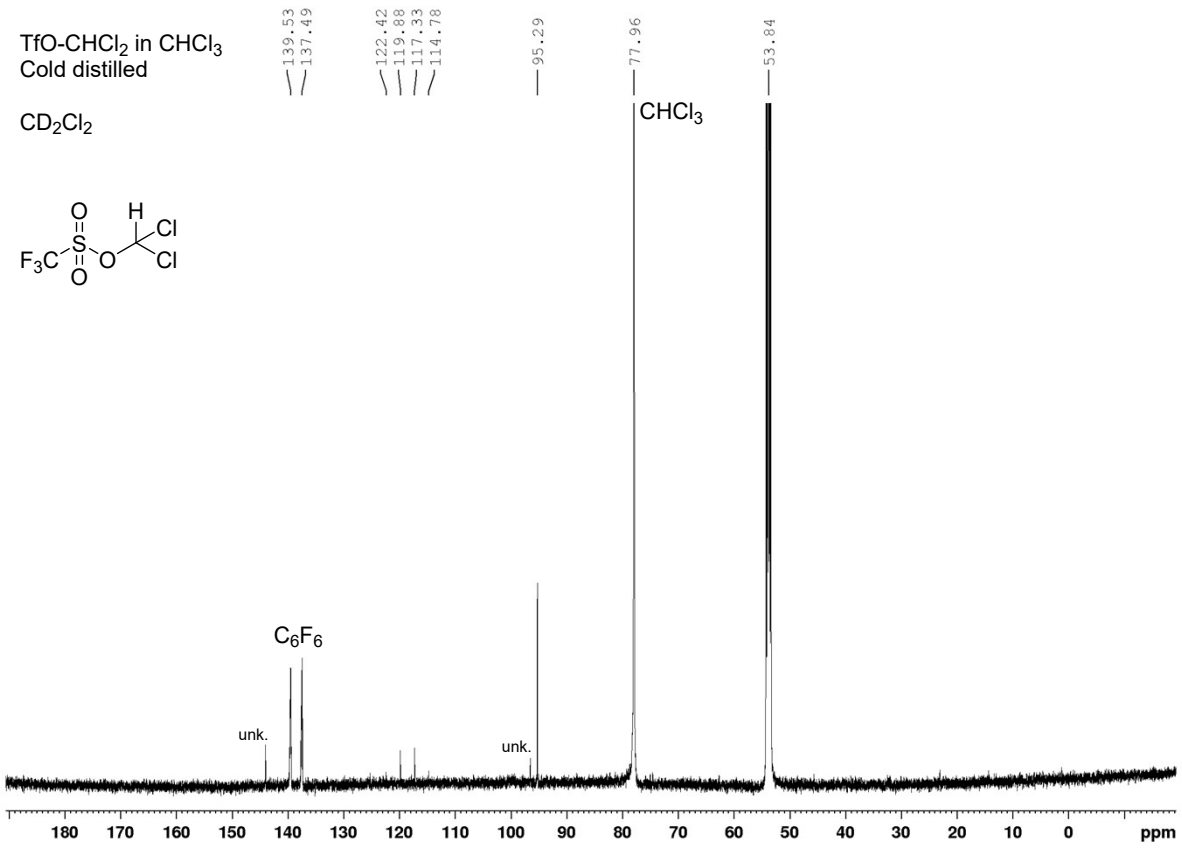

Figure S35. $^{13}C\{^{1}H\}$ NMR (CD_2Cl_2 + ~ 5 v% $CHCl_3$, 126 MHz): TfO-$CHCl_2$ isolated in $CHCl_3$. An unknown contaminant likely introduced with the C_6F_6 spike appears at 144.0 and 96.6 ppm.

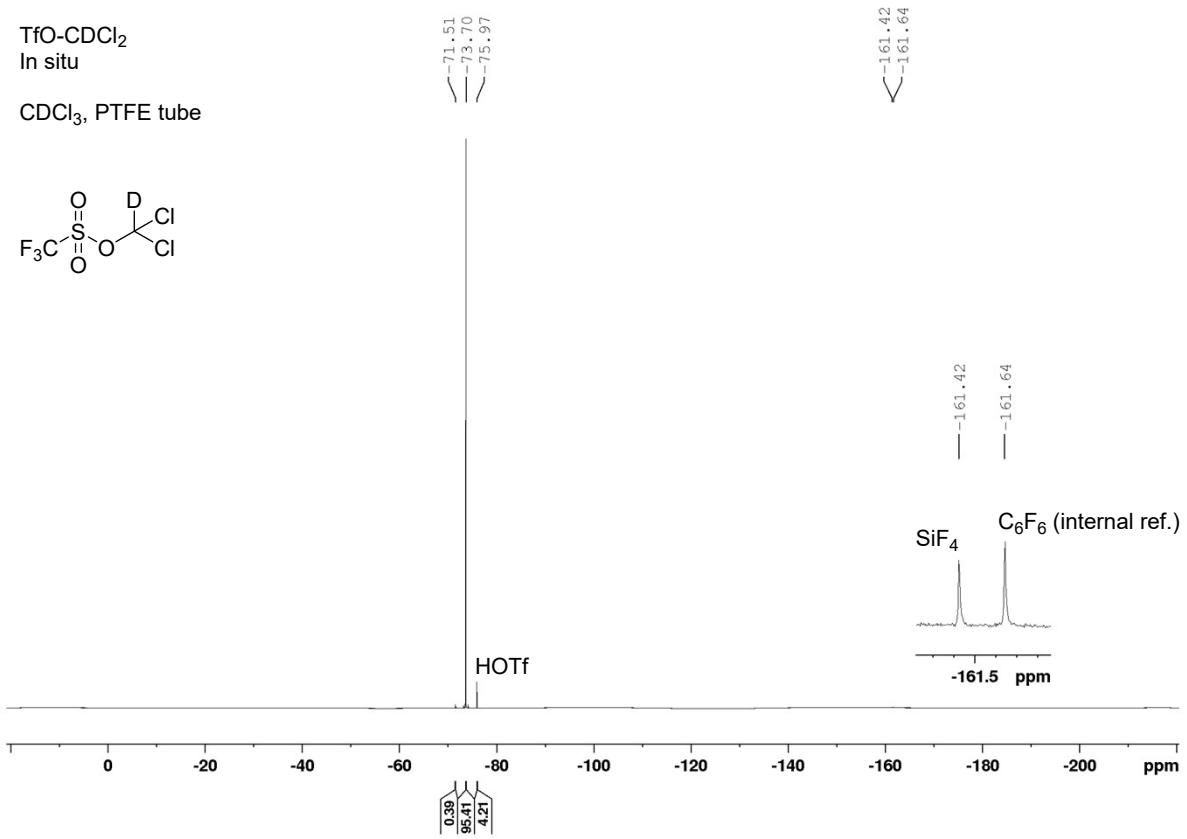

Figure S36. ^{19}F NMR ($CDCl_3$, PTFE tube, 470 MHz): TfO-$CDCl_2$ generated in PTFE (*in situ*).

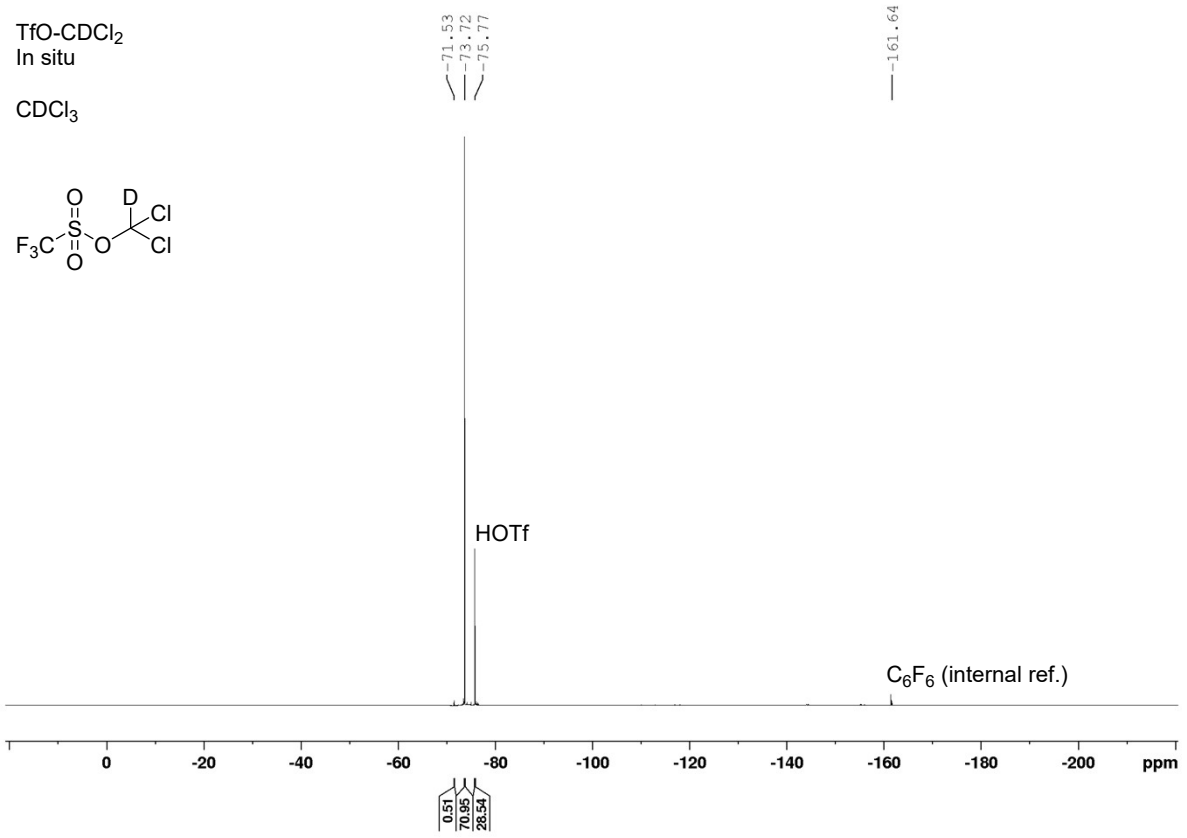

Figure S37. ^{19}F NMR ($CDCl_3$, 470 MHz): TfO-$CDCl_2$ generated in glass (*in situ*).

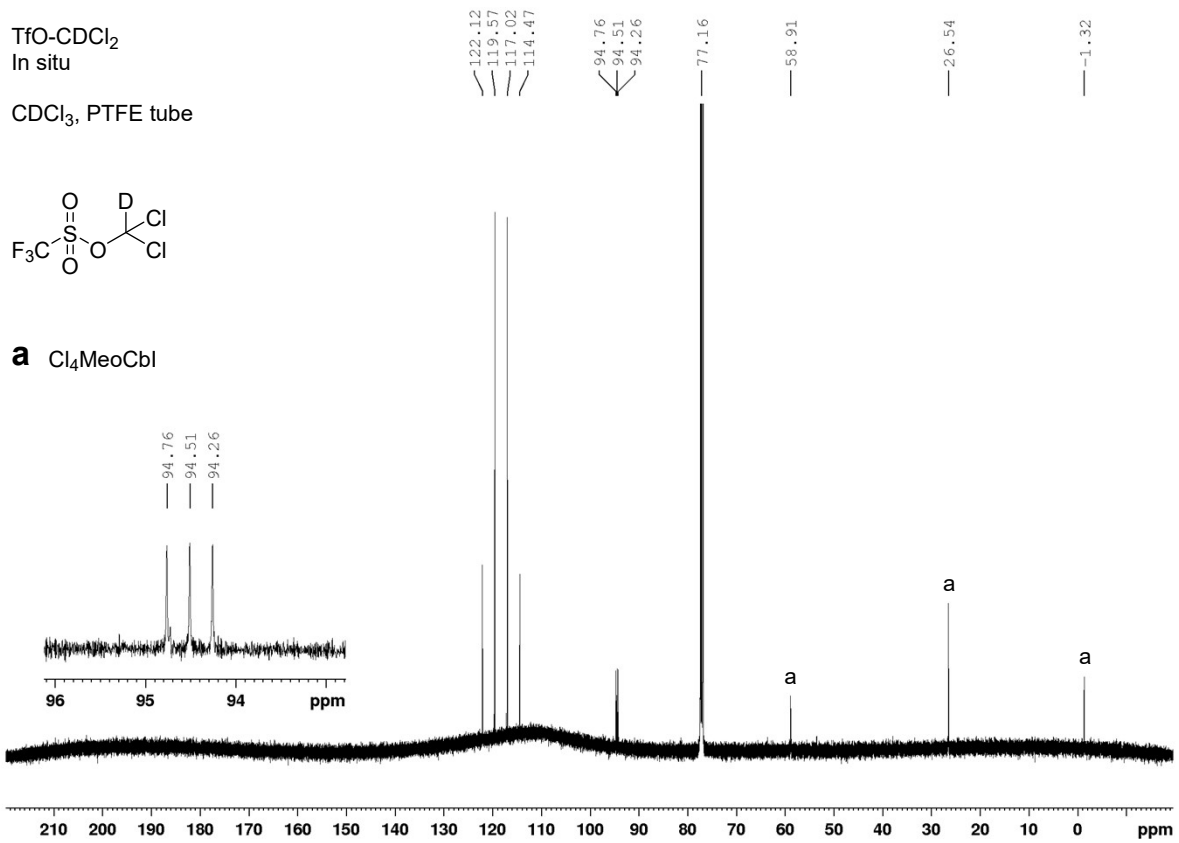

Figure S38. $^{13}C\{^{1}H\}$ NMR ($CDCl_3$, PTFE tube, 126 MHz): TfO-$CDCl_2$ generated *in situ*.

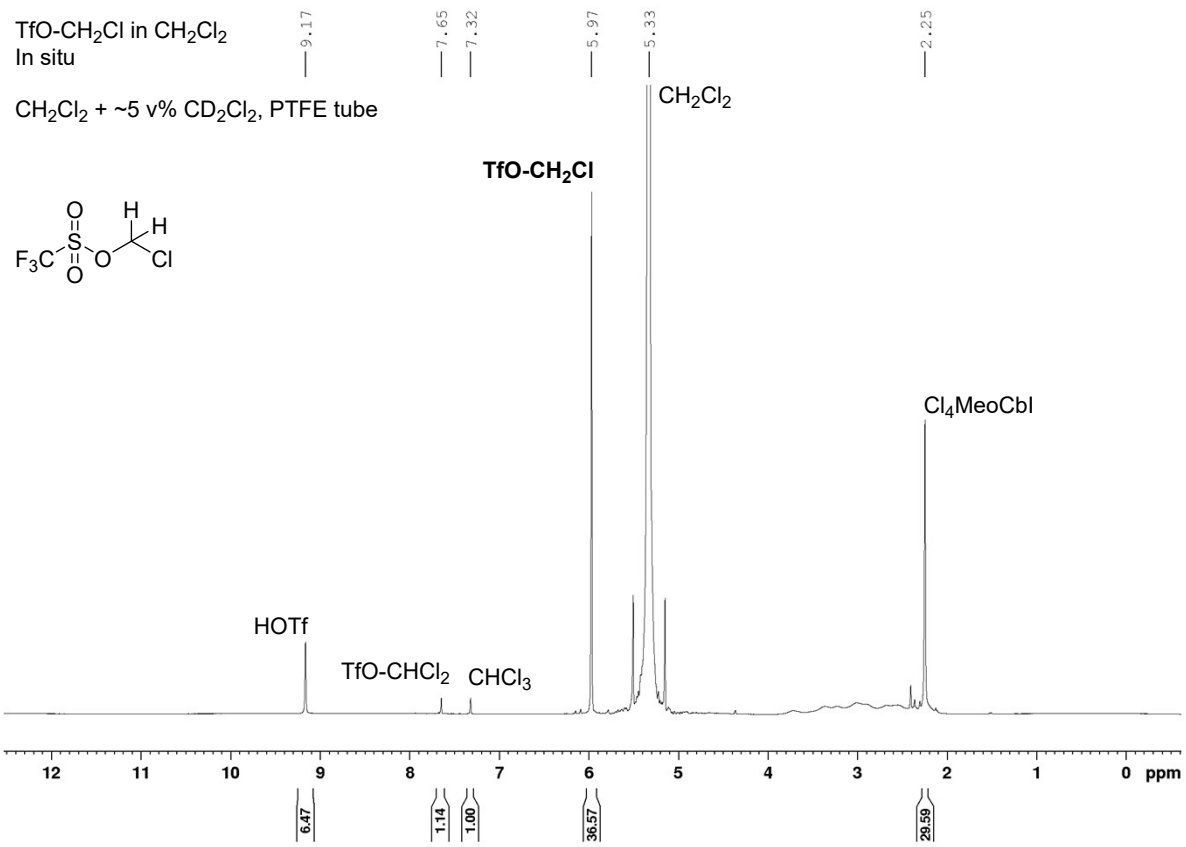

Figure S39. ^{1}H NMR (CH_2Cl_2 + CD_2Cl_2, PTFE tube, 500 MHz): TfO-CH_2Cl and related products generated *in situ*.

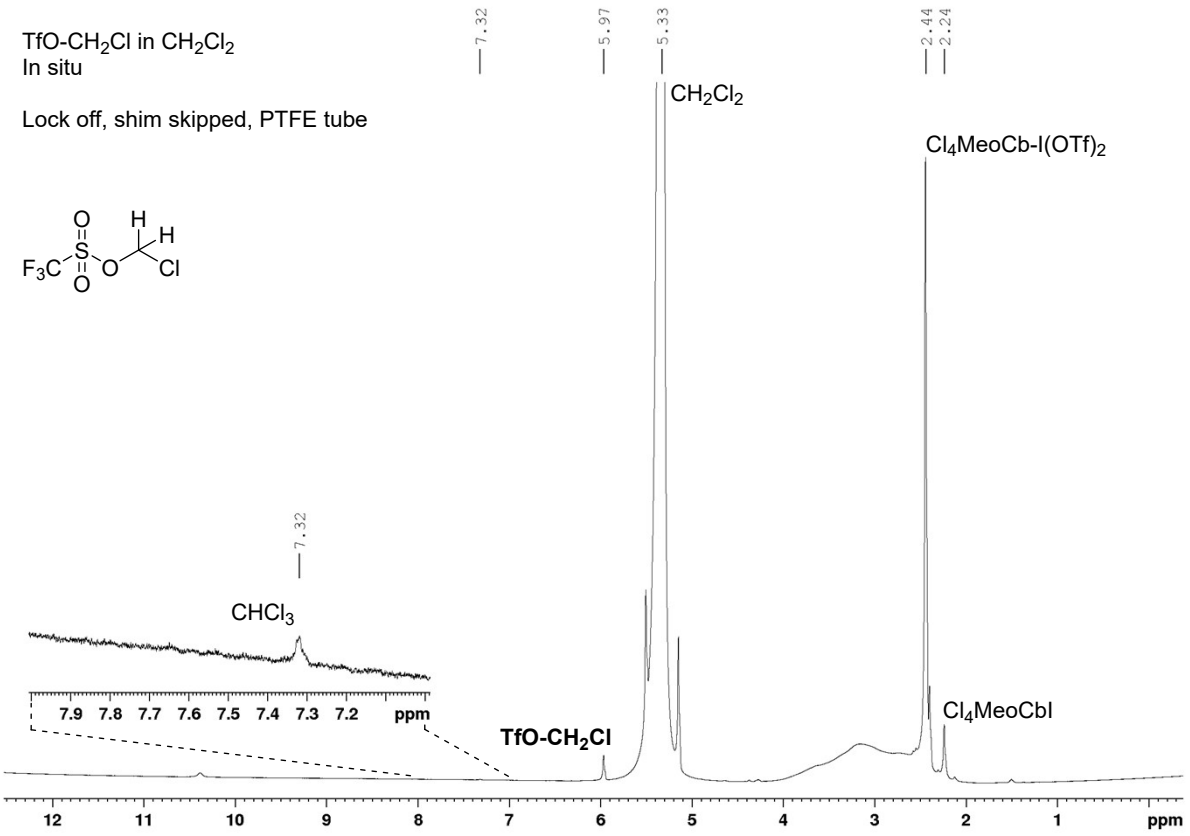

Figure S40. ^{1}H NMR (CH_2Cl_2, unlocked, PTFE tube, 500 MHz): In progress reaction between $Cl_4MeoCb\text{-}I(OTf)_2$ and CH_2Cl_2 at approx. 15 minutes. Shows generation of $CHCl_3$ occurring before $TfO\text{-}CHCl_2$ is detectable.

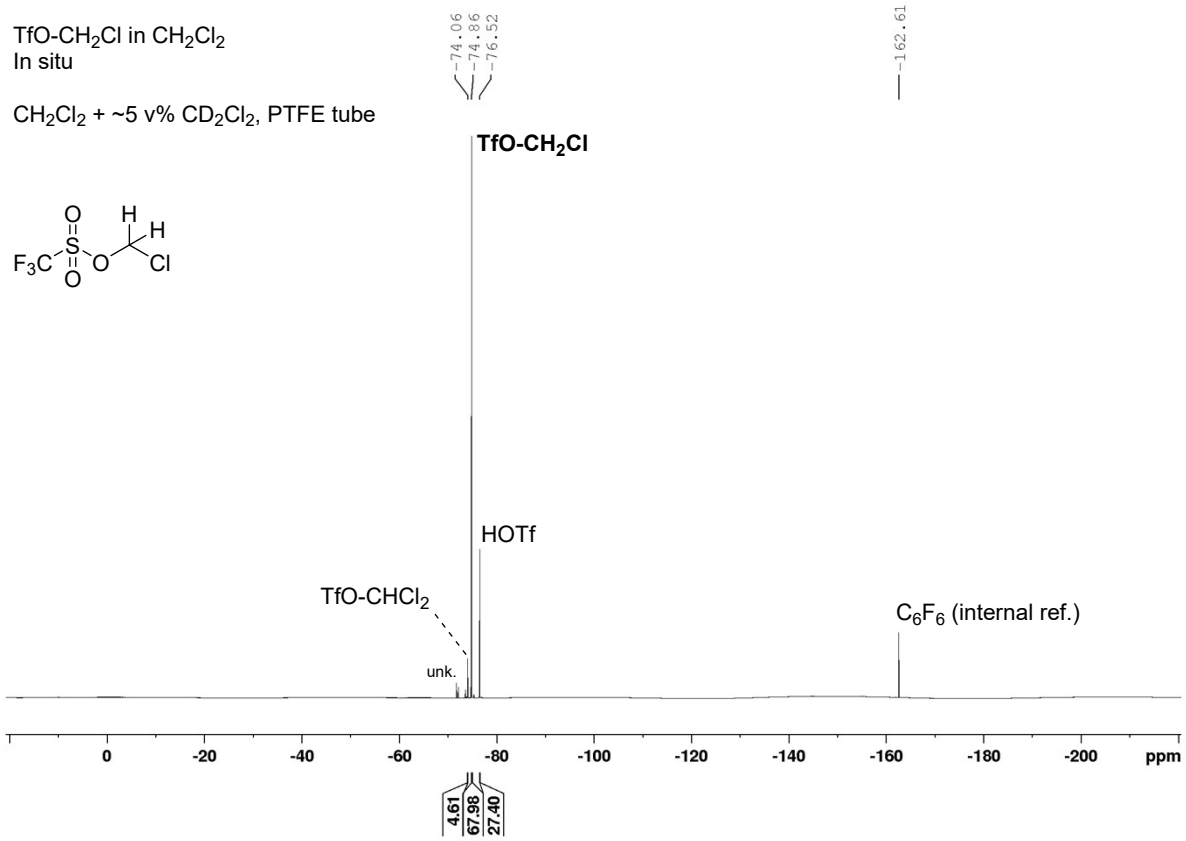

Figure S41. ^{19}F NMR (CH_2Cl_2 + CD_2Cl_2, PTFE tube, 470 MHz): TfO-CH_2Cl and related products generated *in situ*.

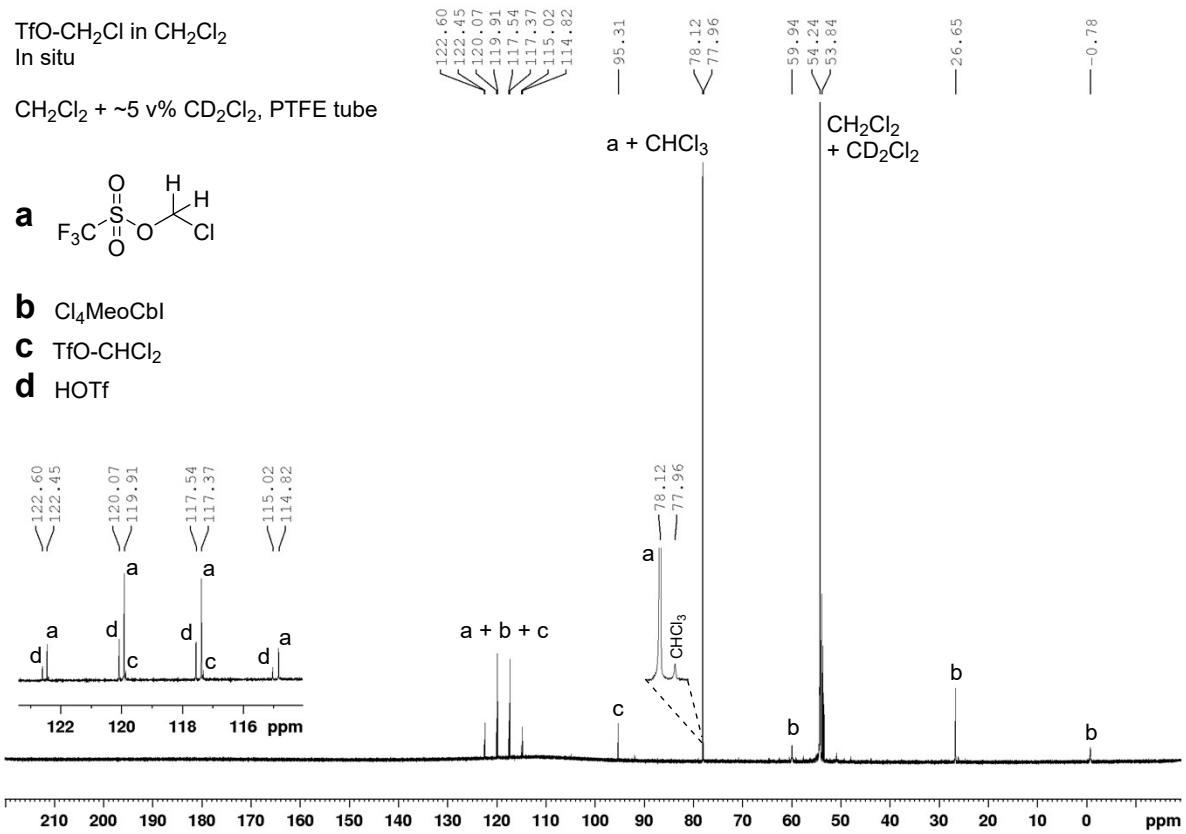

Figure S42. $^{13}C\{^{1}H\}$ NMR (CH_2Cl_2 + CD_2Cl_2, PTFE tube, 126 MHz): TfO-CH_2Cl and related products generated *in situ*.

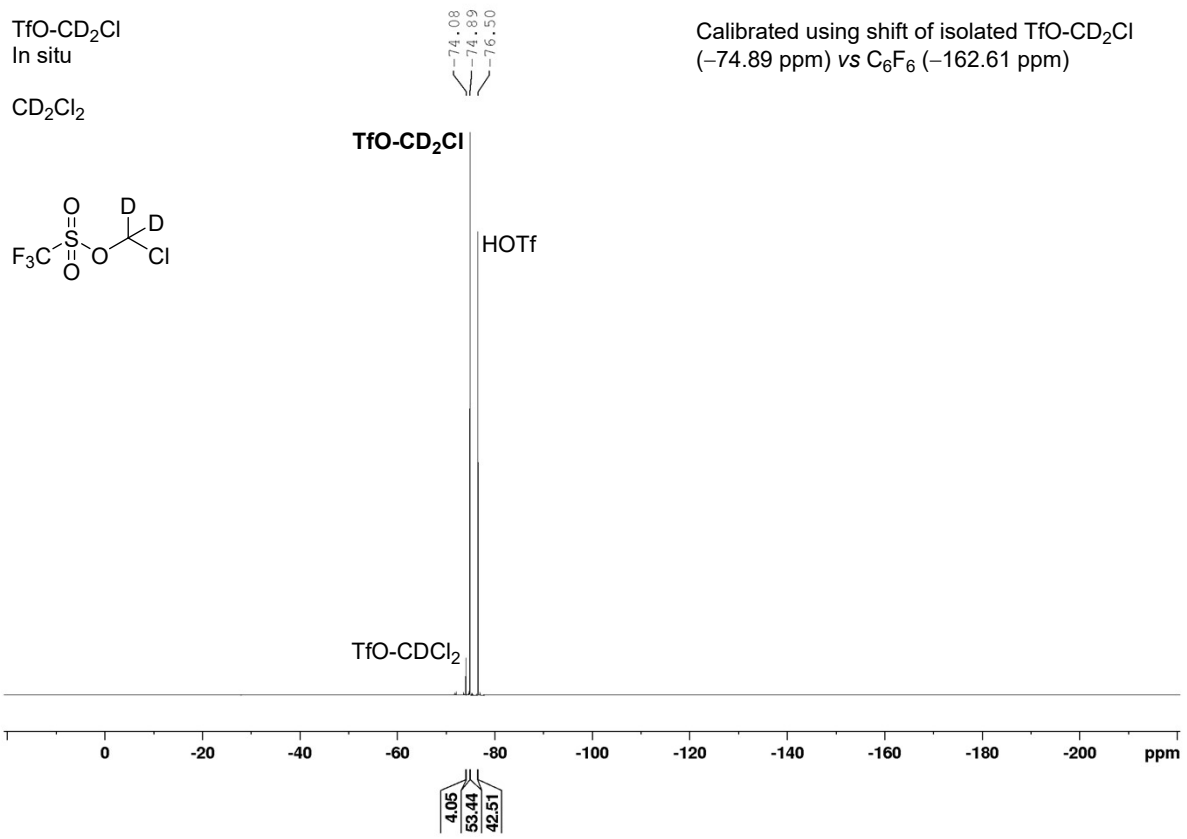

Figure S43. ^{19}F NMR (CD_2Cl_2, 470 MHz): TfO-CD_2Cl generated *in situ*.

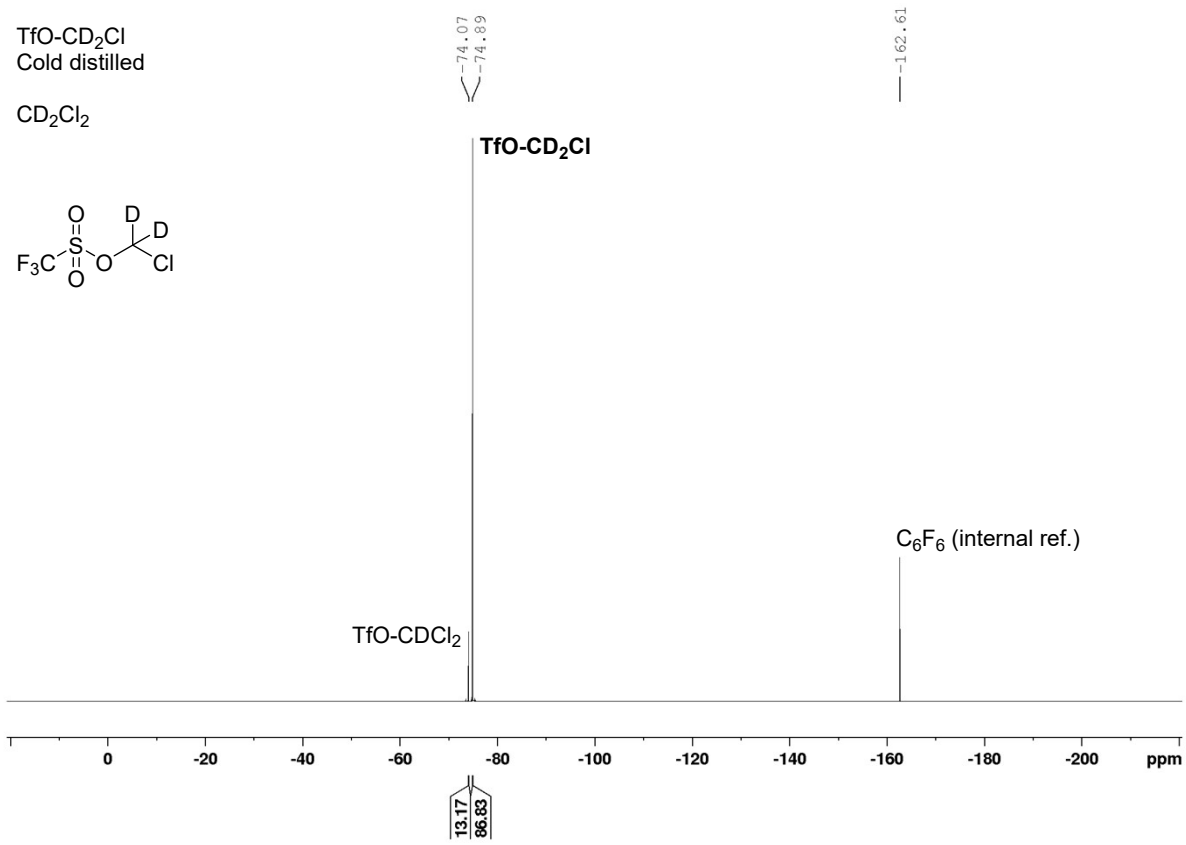

Figure S44. ^{19}F NMR (CD_2Cl_2, 470 MHz): TfO-CD_2Cl cold distilled alongside TfO-$CDCl_2$ and the reaction solvent, CD_2Cl_2.

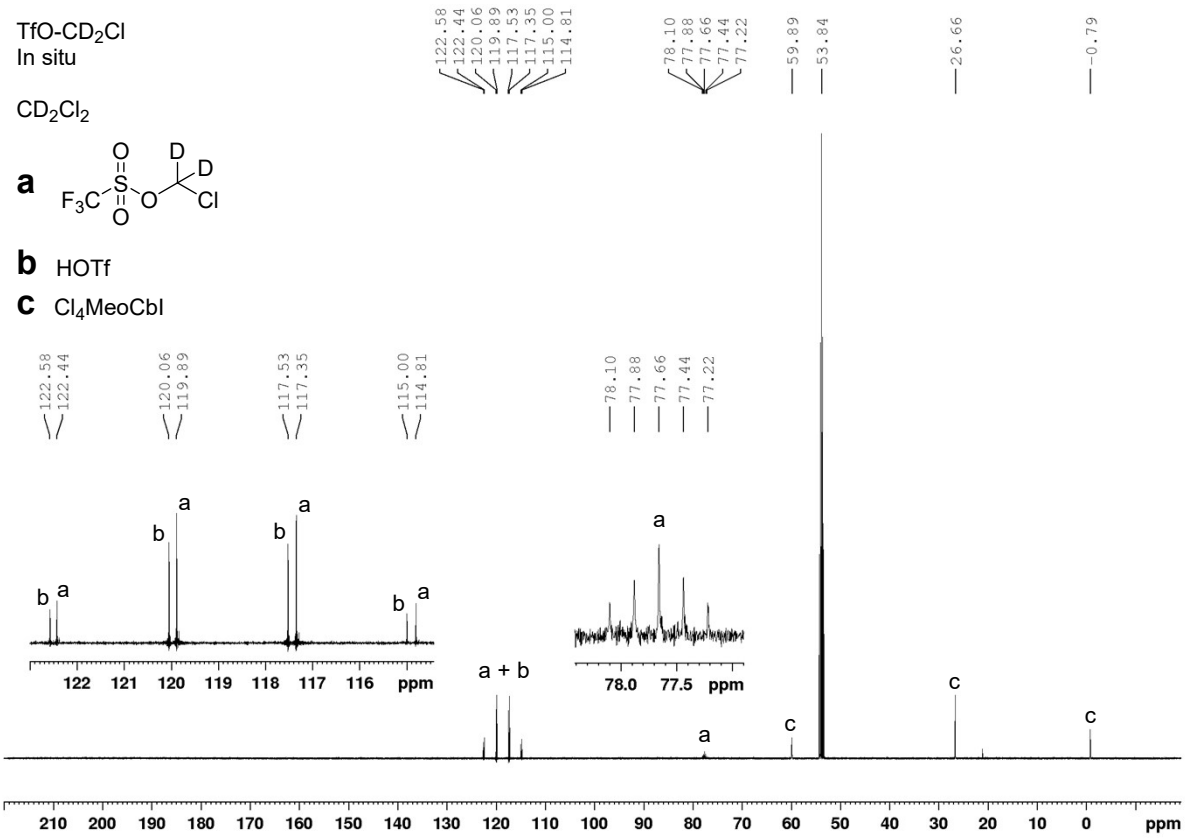

Figure S45. $^{13}C\{^{1}H\}$ NMR (CD_2Cl_2, 126 MHz): TfO-CD_2Cl_2 generated *in situ*.

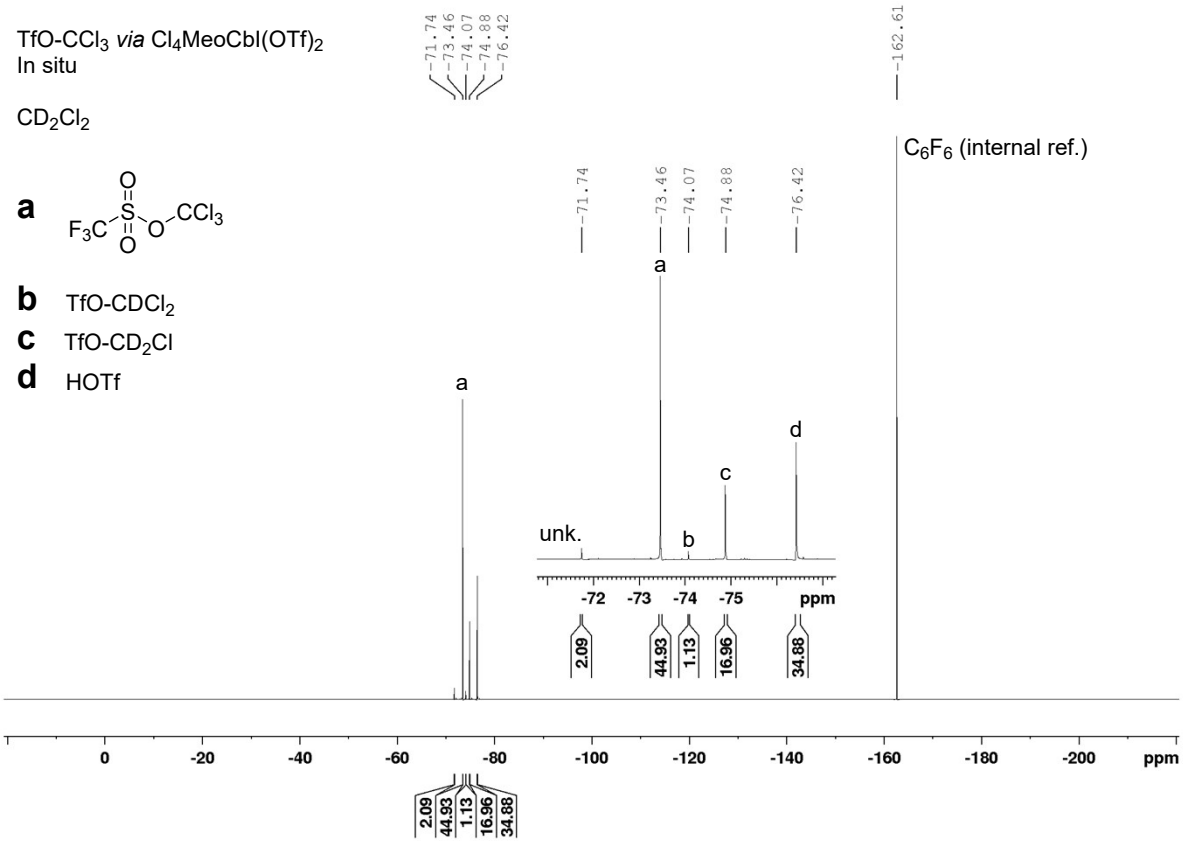

Figure S46. ^{19}F NMR (CD_2Cl_2, 470 MHz): TfO-CCl_3 and side products generated *via* Cl_4MeOCbI$(OTf)_2$.

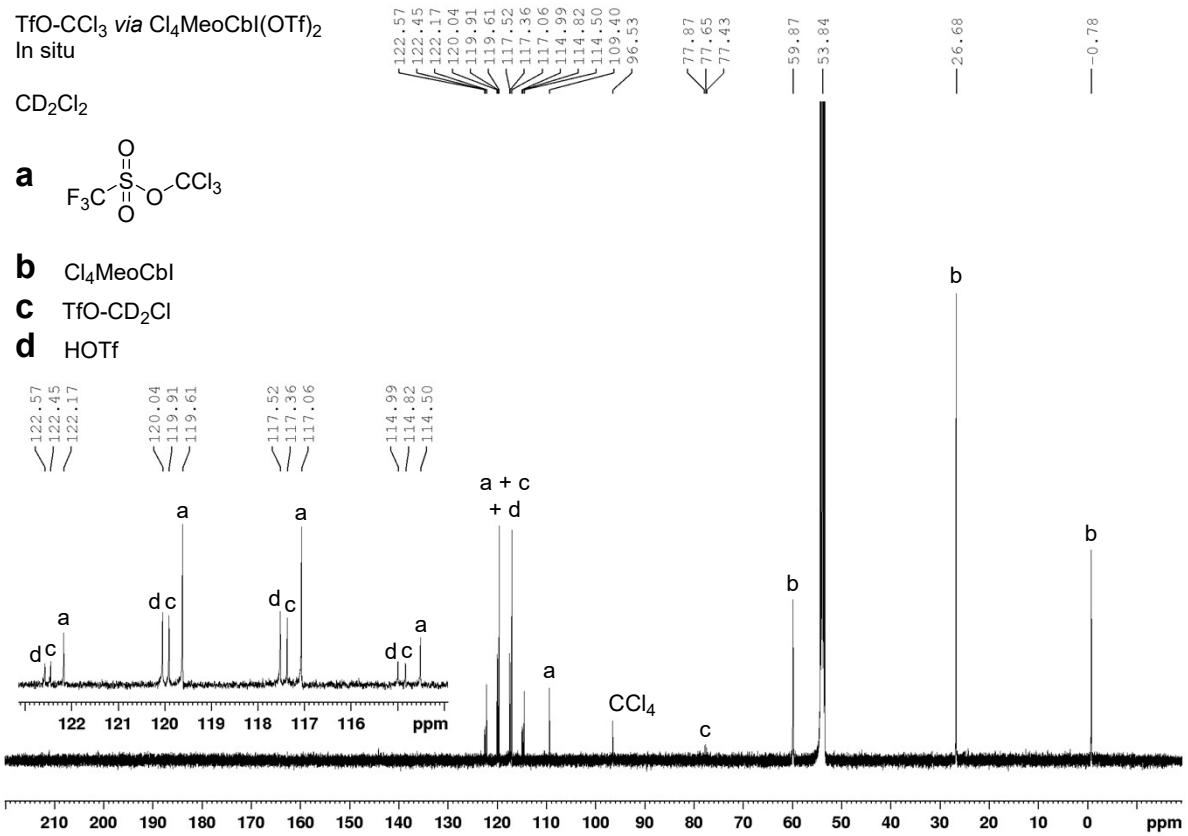

Figure S47. $^{13}C\{^{1}H\}$ NMR (CD_2Cl_2, 126 MHz): TfO-CCl_3 and side products generated *via* Cl_4MeoCb-I$(OTf)_2$.

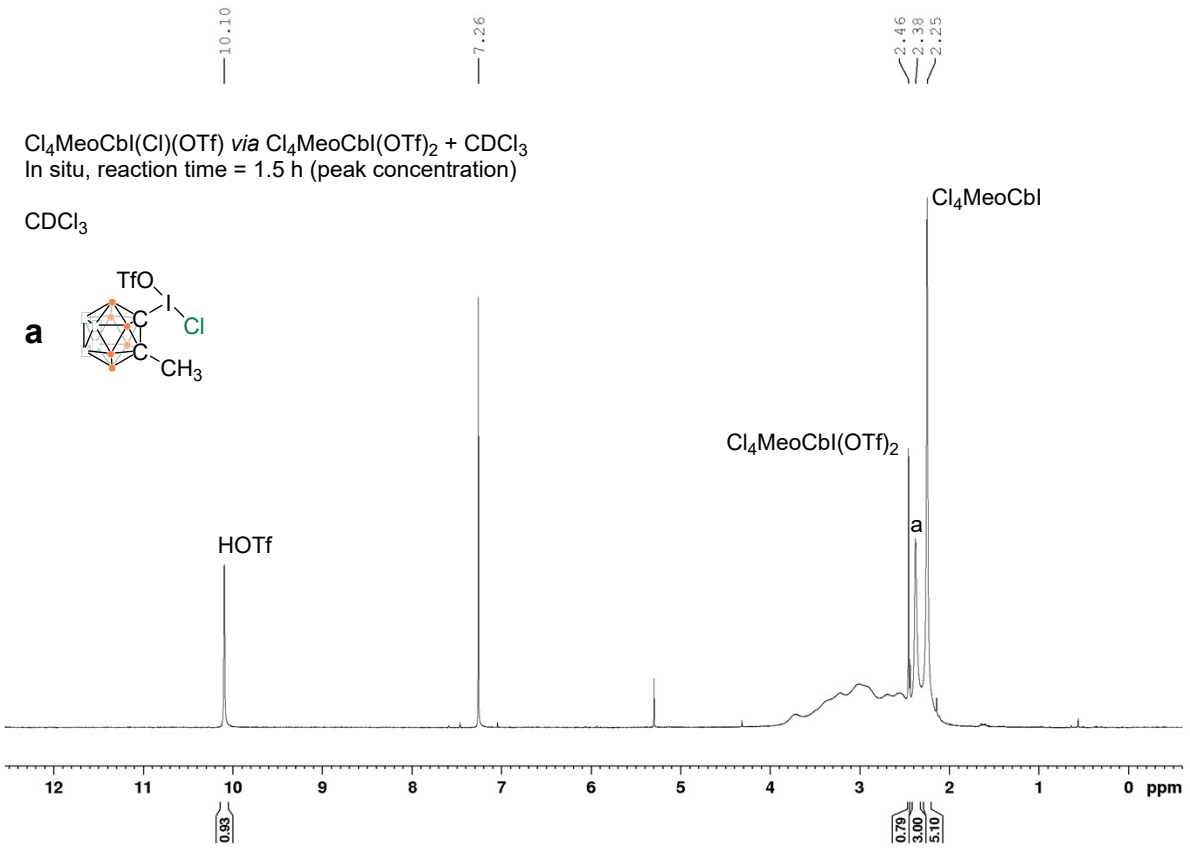

Figure S48. ^{1}H NMR ($CDCl_3$, 500 MHz): Cl_4MeoCb-I(OTf)$_2$ + $CDCl_3$ at 1.5 h with Cl_4MeoCb-I(Cl)(OTf) at its peak concentration.

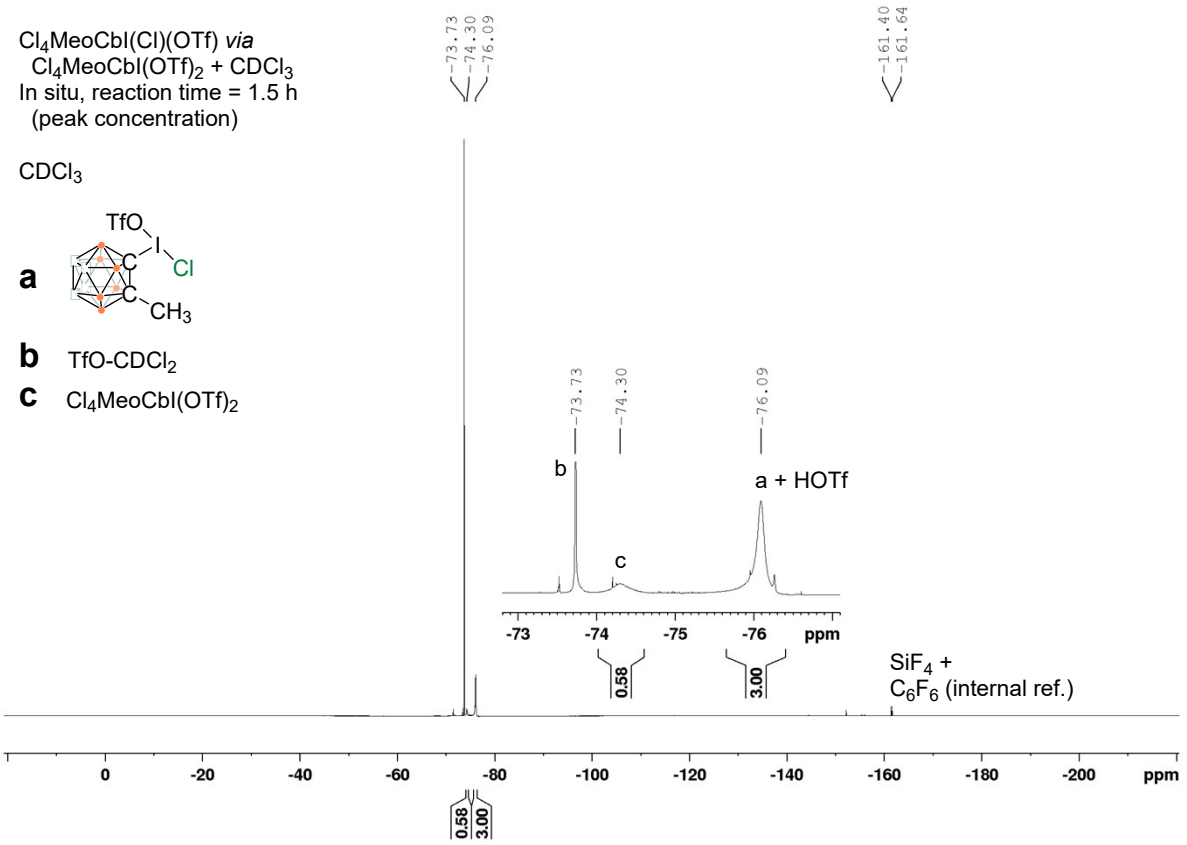

Figure S49. ^{19}F NMR ($CDCl_3$, PTFE tube, 470 MHz): $Cl_4MeoCb\text{-}I(OTf)_2$ + $CDCl_3$ at 1.5 h with $Cl_4MeoCb\text{-}I(Cl)(OTf)$ at its peak concentration.

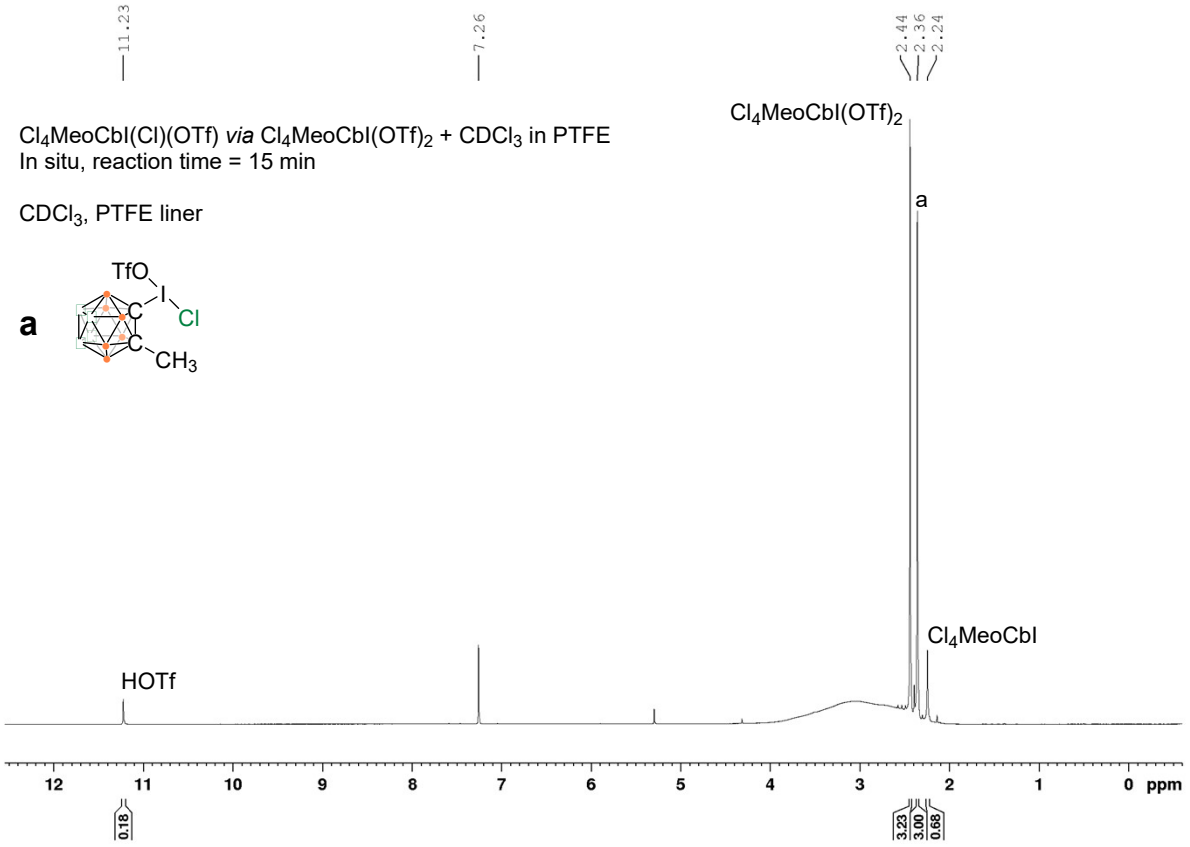

Figure S50. ^{1}H NMR ($CDCl_3$, PTFE tube, 500 MHz): Cl_4MeoCb-I$(OTf)_2$ + $CDCl_3$ in PTFE at 15 min. A large amount of Cl_4MeoCb-I(Cl)(OTf) is already visible.

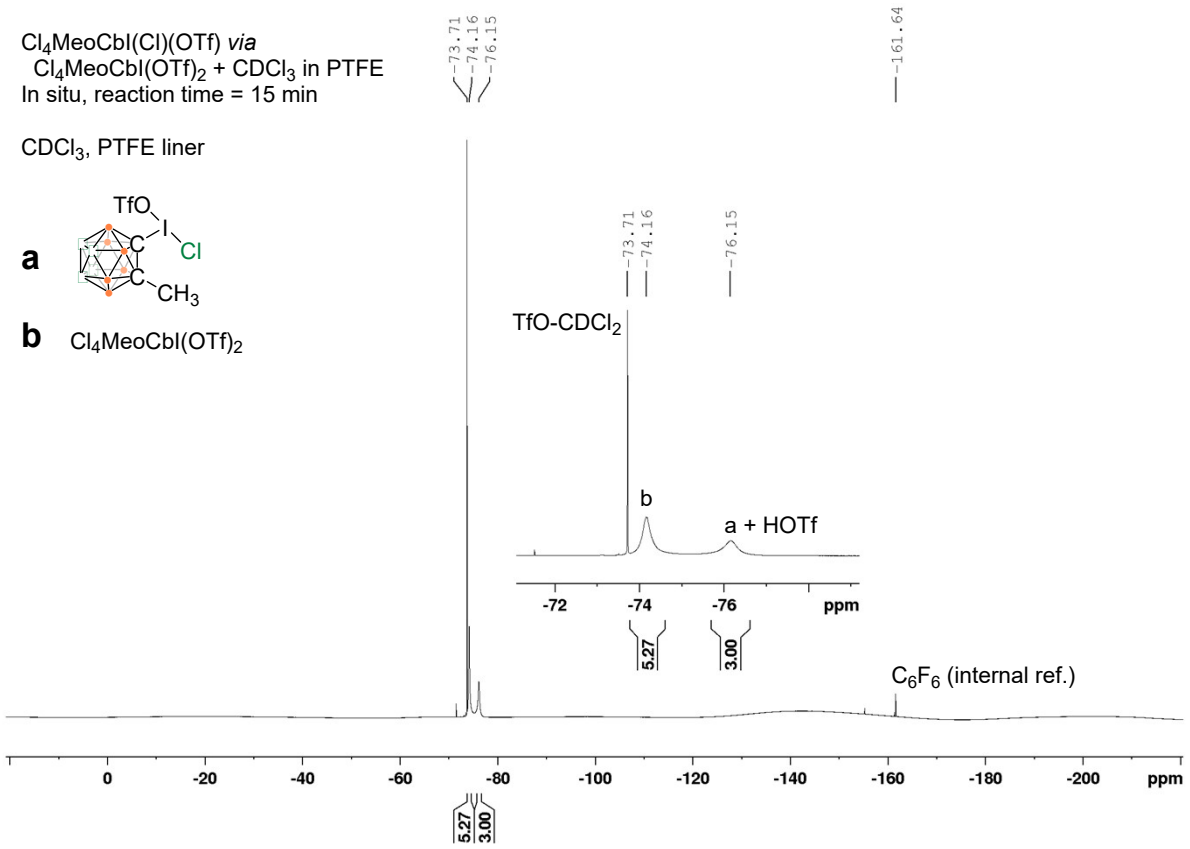

Figure S51. ^{19}F NMR ($CDCl_3$, PTFE tube, 470 MHz): $Cl_4MeoCb\text{-}I(OTf)_2$ + $CDCl_3$ in PTFE at 15 min. A large amount of $Cl_4MeoCb\text{-}I(Cl)(OTf)$ is already visible.

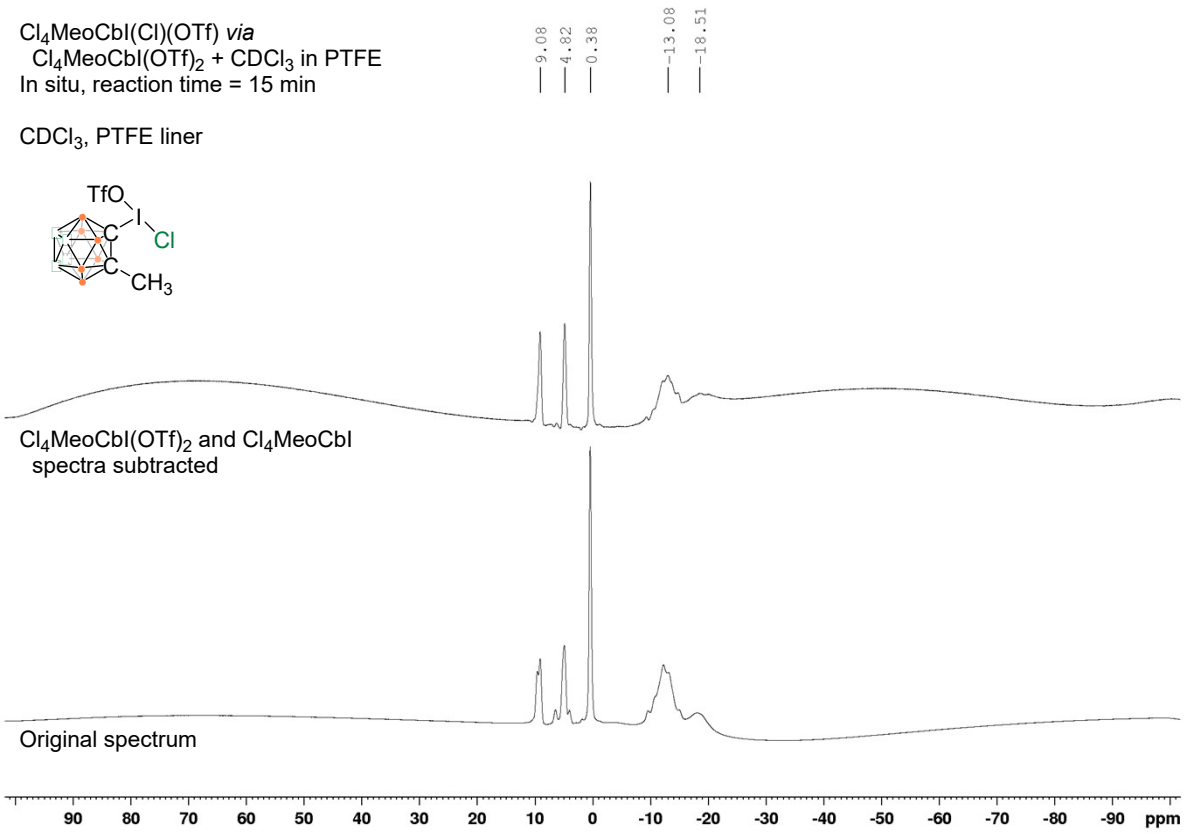

Figure S52. ^{11}B NMR ($CDCl_3$, PTFE tube, 160 MHz): Cl_4MeoCb-I$(OTf)_2$ + $CDCl_3$ in PTFE at 15 min. Top spectrum is remaining signals after subtraction of Cl_4MeoCb-I$(OTf)_2$ and Cl_4MeoCbI spectra in $CDCl_3$. The spectrum for Cl_4MeoCb-I$(OTf)_2$ in $CDCl_3$ was generated by the same method using a scan in glass where a greatly reduced quantity of Cl_4MeoCb-I(Cl)(OTf) is present.

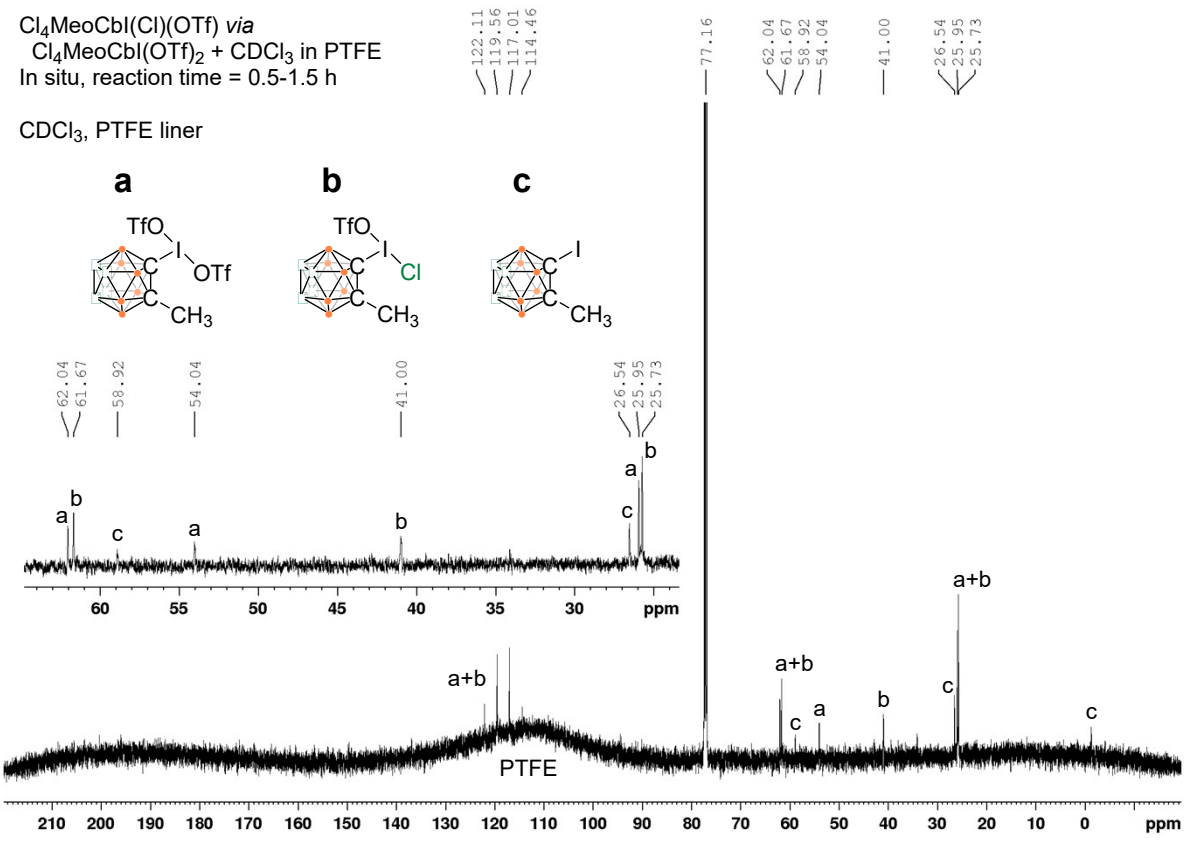

Figure S53. $^{13}C\{^{1}H\}$ NMR ($CDCl_3$, PTFE liner, 126 MHz): $Cl_4MeoCb\text{-}I(OTf)_2$ + $CDCl_3$ in PTFE at 0.5-1.5 h.

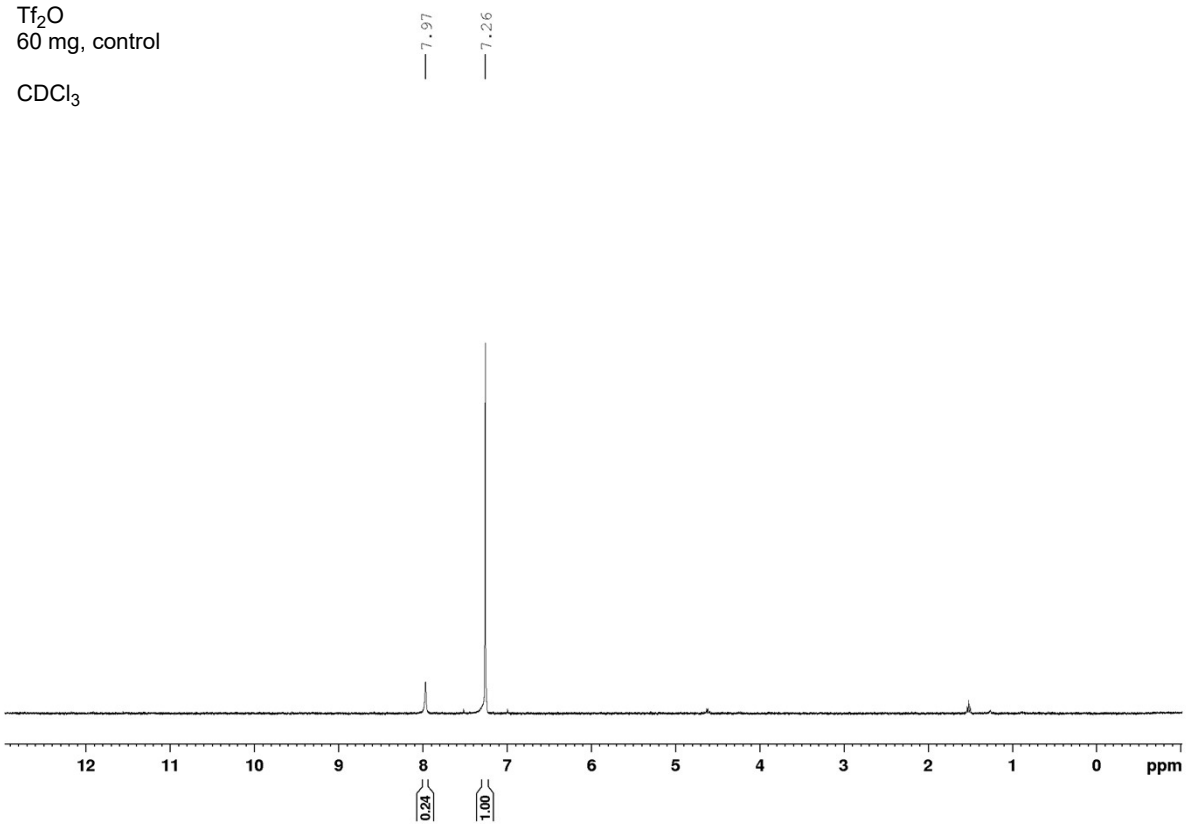

Figure S54. ^{1}H NMR ($CDCl_3$, 400 MHz): Concentrated Tf_2O to quantify H_2O contamination.

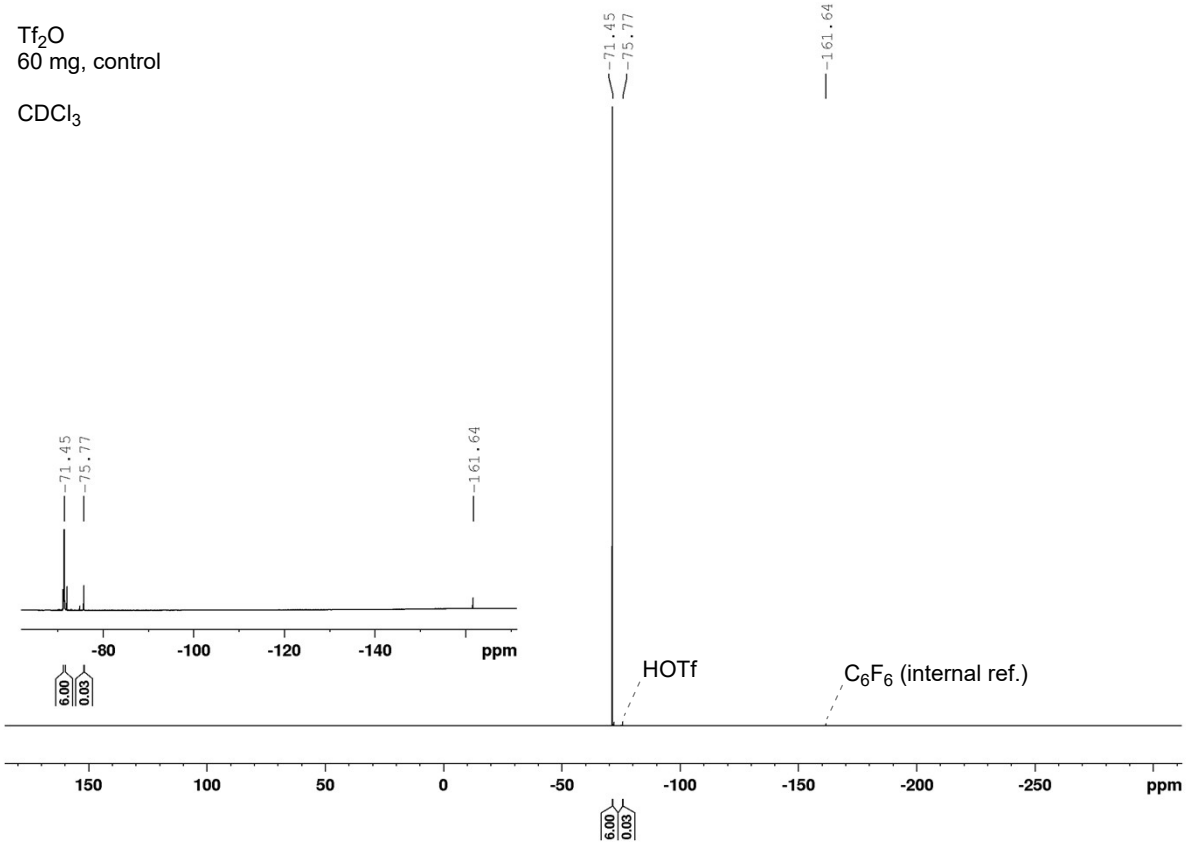

Figure S55. ^{19}F NMR ($CDCl_3$, 376 MHz): Concentrated Tf_2O to quantify H_2O contamination.

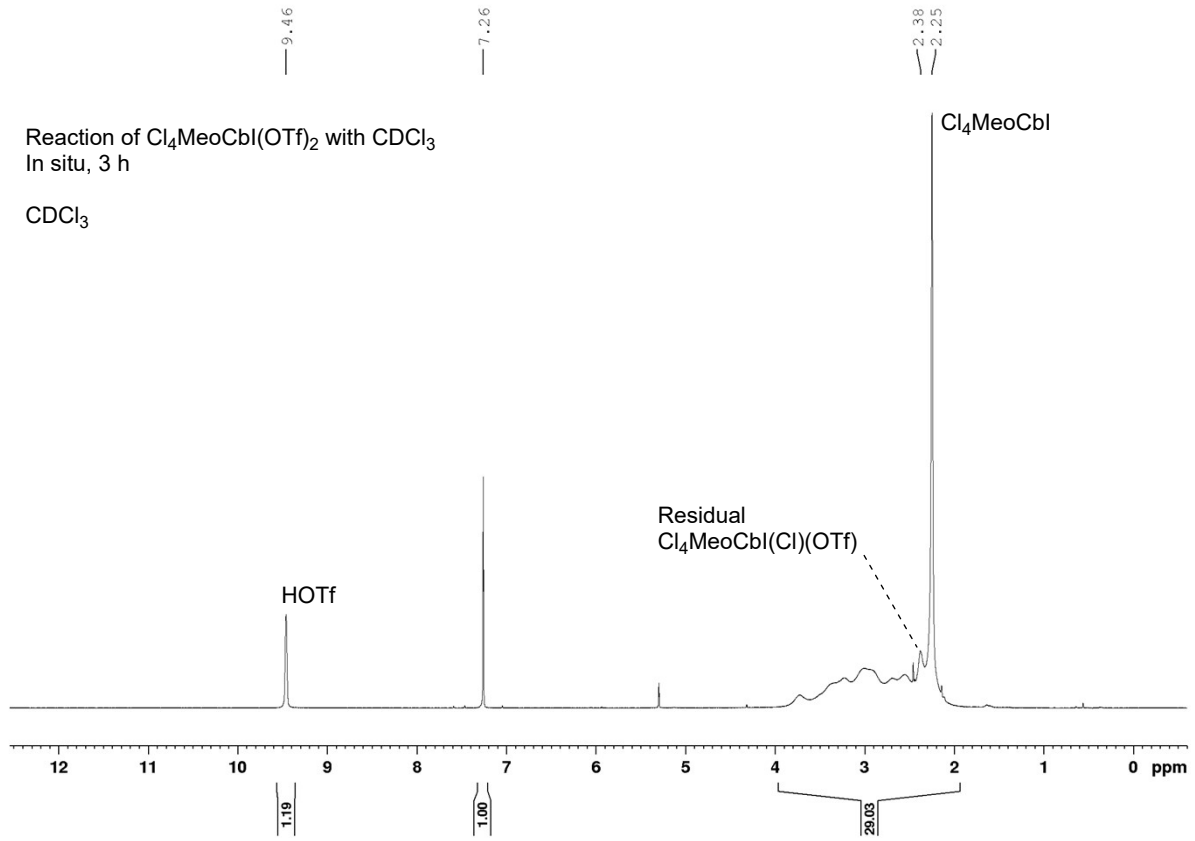

Figure S56. ^{1}H NMR ($CDCl_3$, 500 MHz): Reaction of $Cl_4MeoCb\text{-}I(OTf)_2$ with $CDCl_3$ in glass near completion at 3 h.

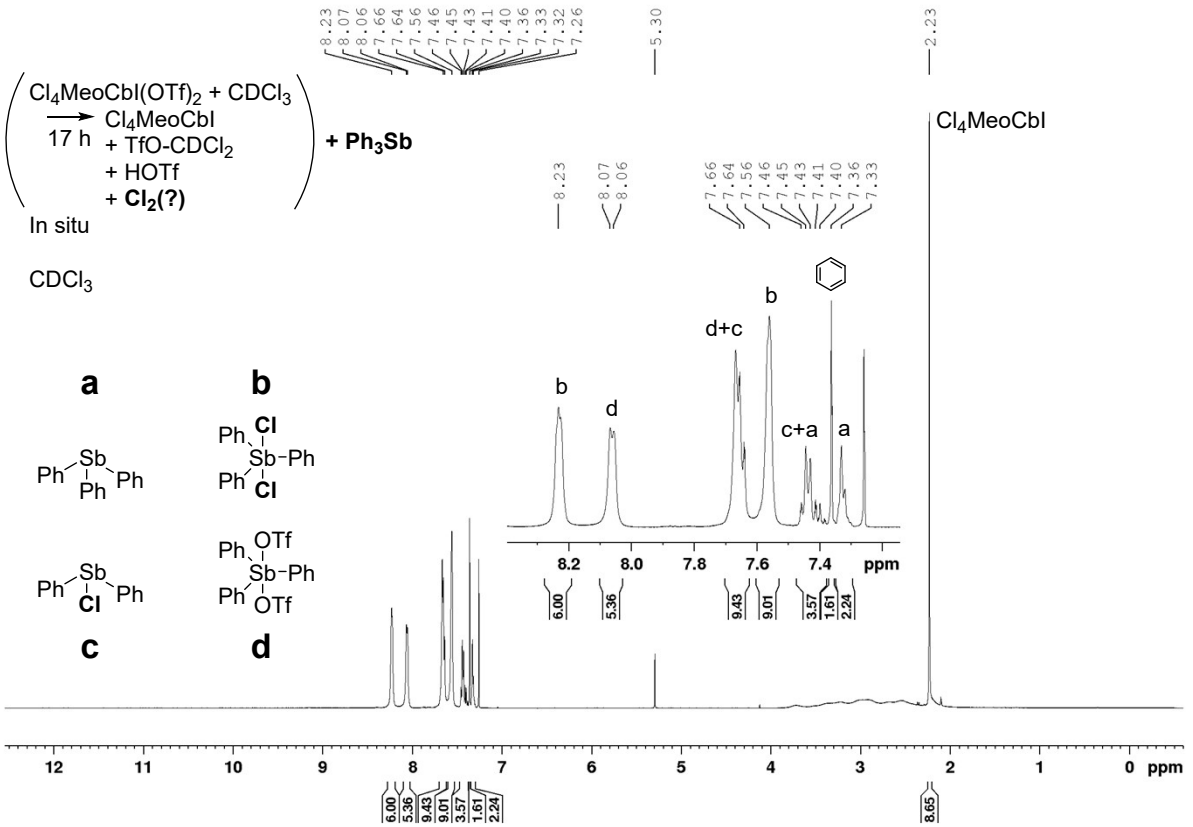

Figure S57. ^{1}H NMR ($CDCl_3$, 500 MHz): Addition of Ph_3Sb to a fully degraded sample of $Cl_4MeoCb\text{-}I(OTf)_2$ in $CDCl_3$.

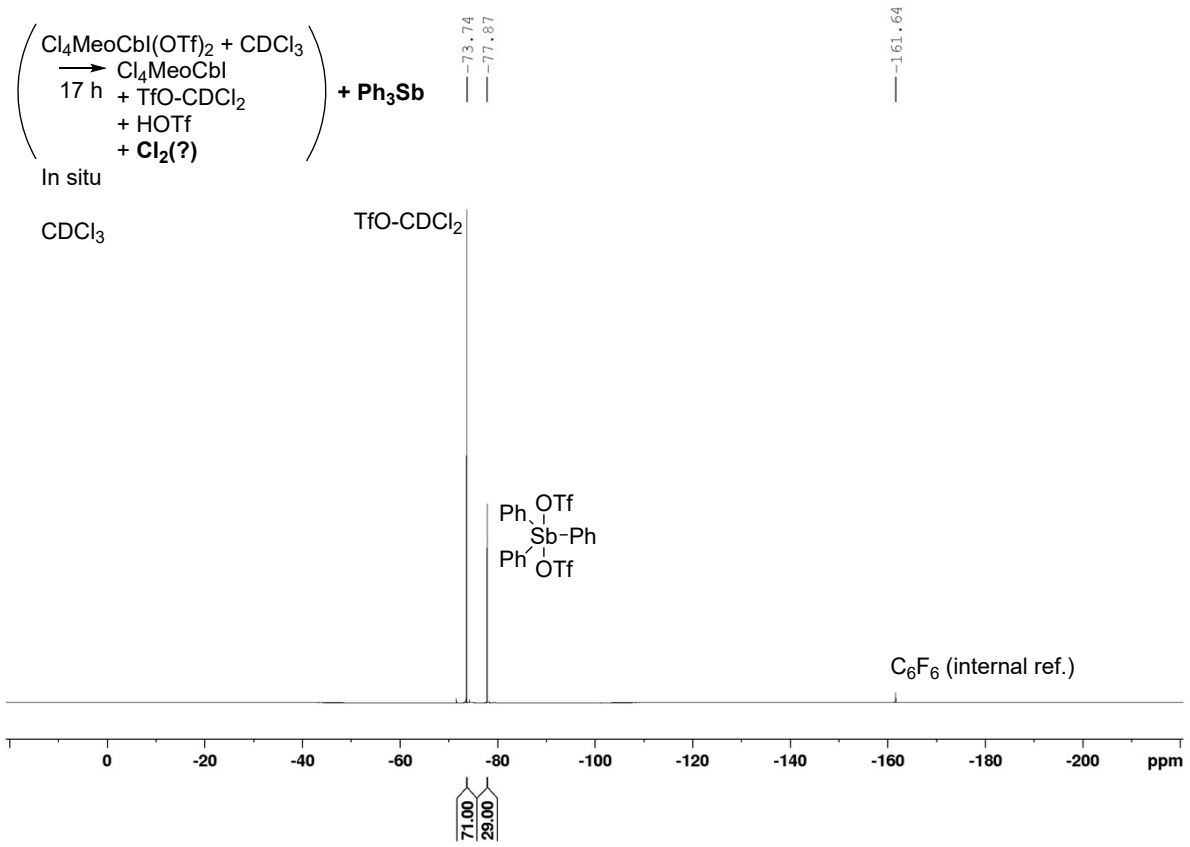

Figure S58. ^{19}F NMR ($CDCl_3$, 470 MHz): Addition of Ph_3Sb to a fully degraded sample of $Cl_4MeoCb\text{-}I(OTf)_2$ in $CDCl_3$.

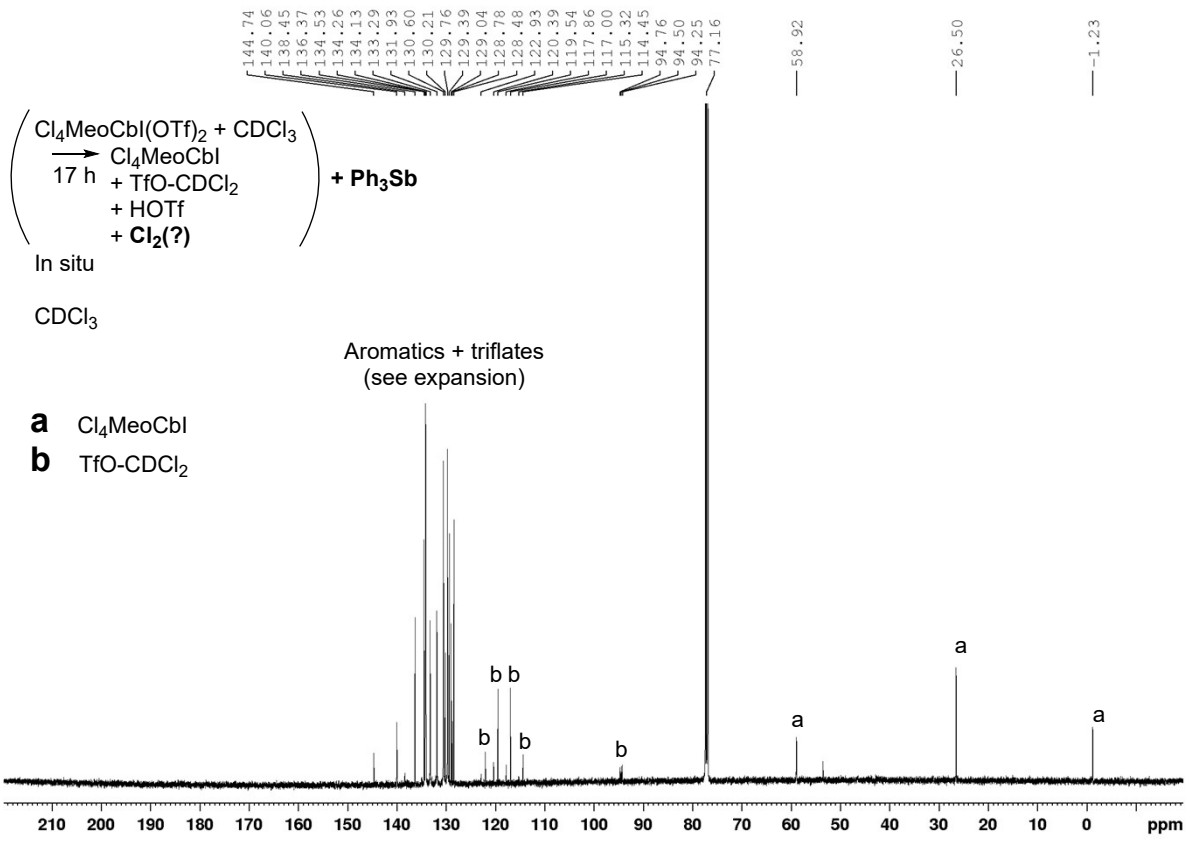

Figure S59. $^{13}C\{^{1}H\}$ NMR ($CDCl_3$, 126 MHz): Addition of Ph_3Sb to a fully degraded sample of $Cl_4MeoCb\text{-}I(OTf)_2$ in $CDCl_3$. Spectrum 1 of 2 (full).

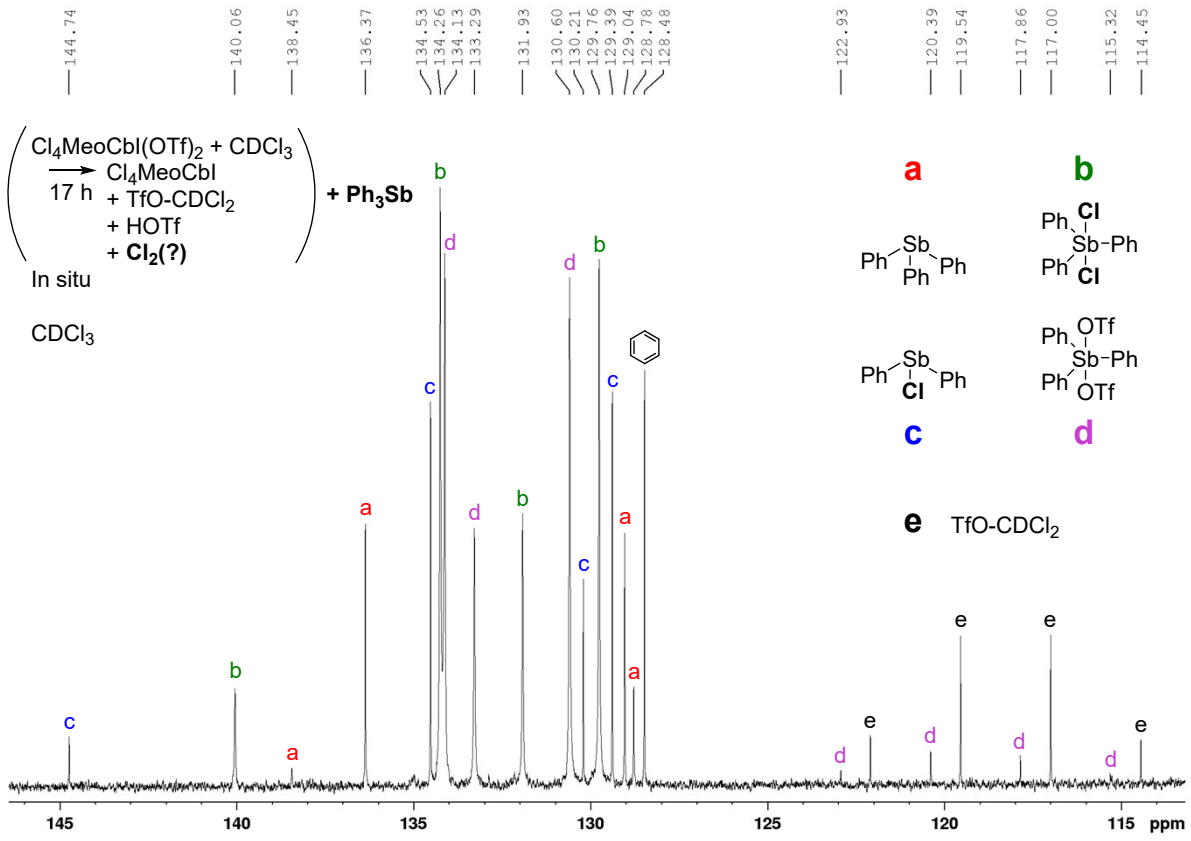

Figure S60. $^{13}C\{^{1}H\}$ NMR ($CDCl_3$, 126 MHz): Addition of Ph_3Sb to a fully degraded sample of $Cl_4MeoCb\text{-}I(OTf)_2$ in $CDCl_3$. Spectrum 2 of 2 (expansion).

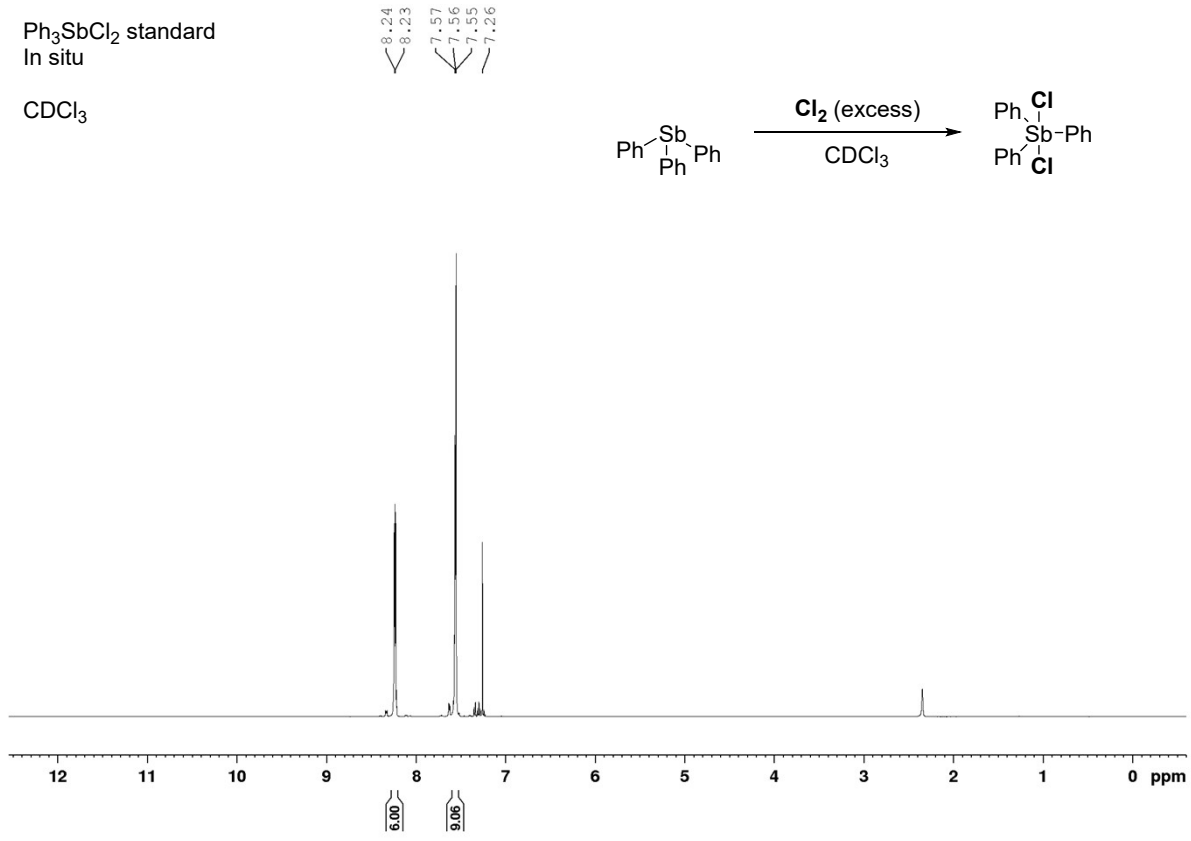

Figure S61. ^{1}H NMR ($CDCl_3$, 500 MHz): Ph_3SbCl_2 generated in situ from Ph_3Sb and Cl_2.

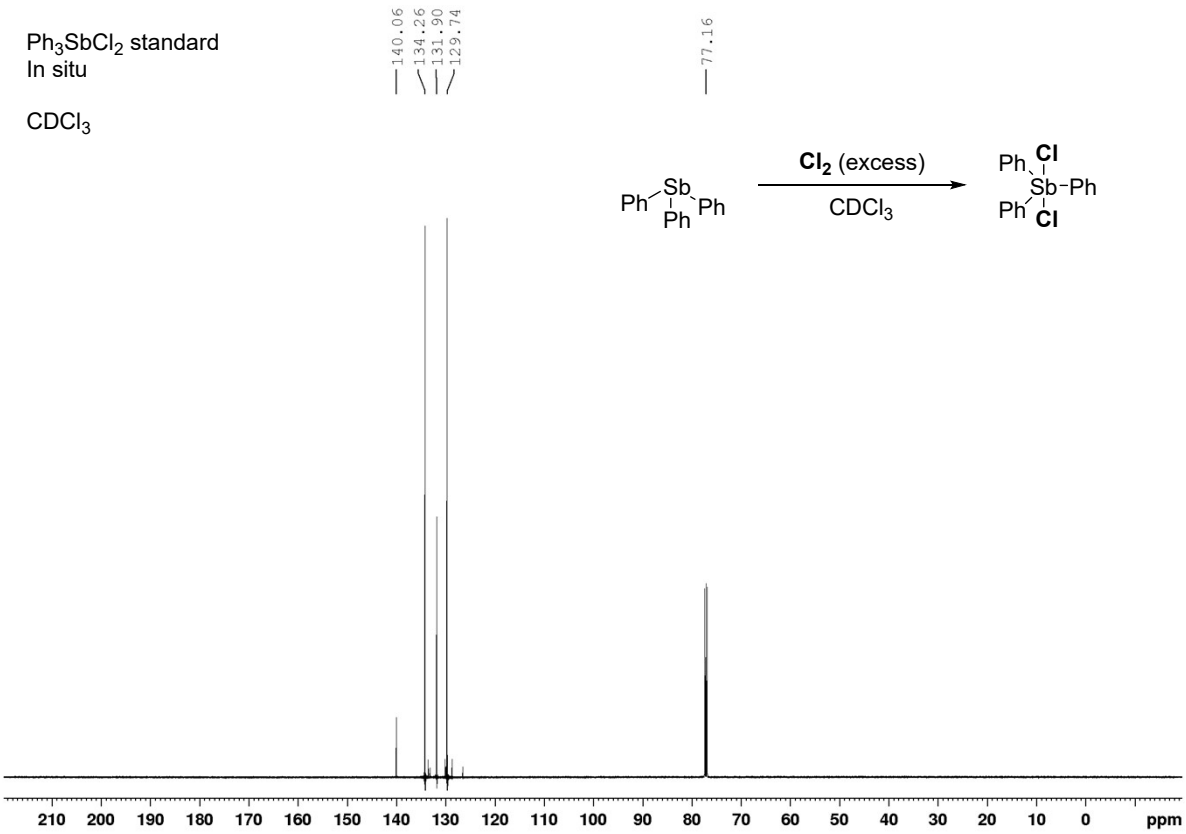

Figure S62. $^{13}C\{^{1}H\}$ NMR ($CDCl_3$, 126 MHz): Ph_3SbCl_2 generated in situ from Ph_3Sb and Cl_2.

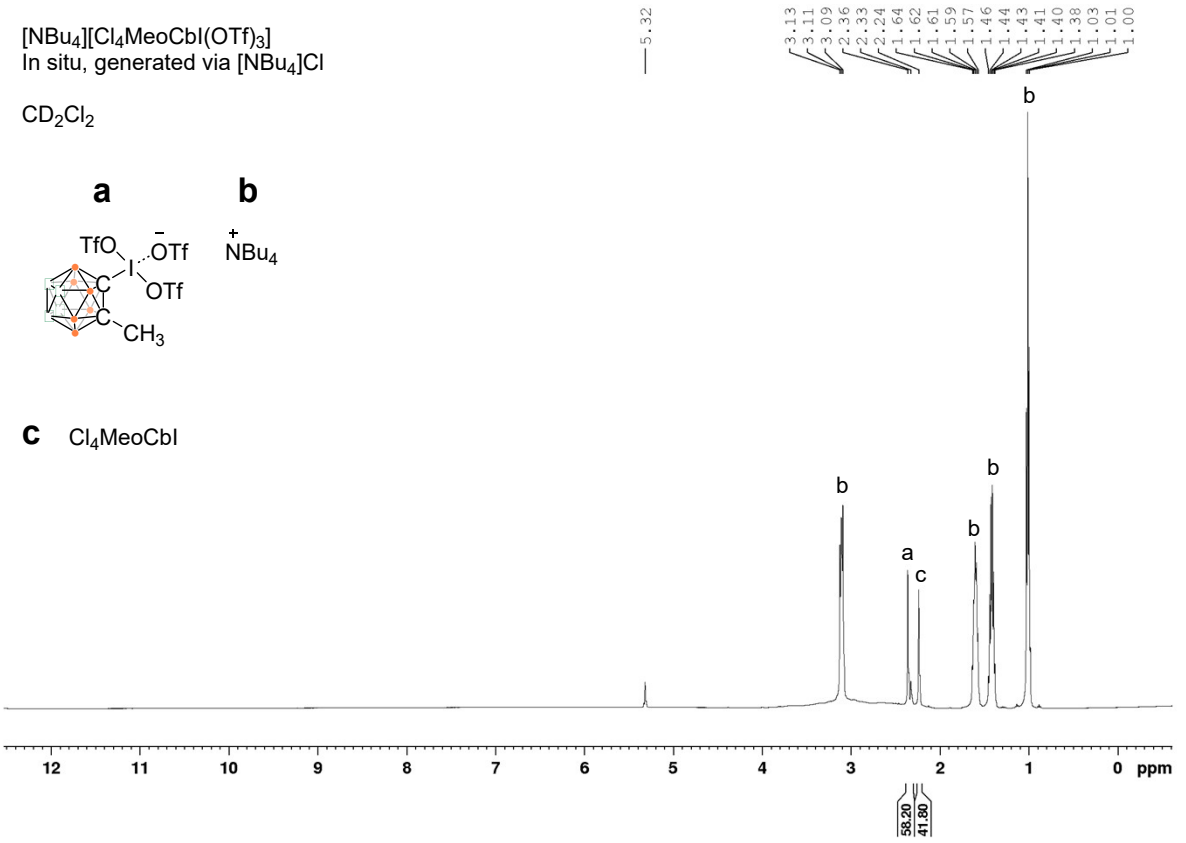

Figure S63. ^{1}H NMR (CD_2Cl_2, 500 MHz): $[NBu_4][Cl_4MeoCb\text{-}I(OTf)_3]$ generated *via* $[NBu_4]Cl$.

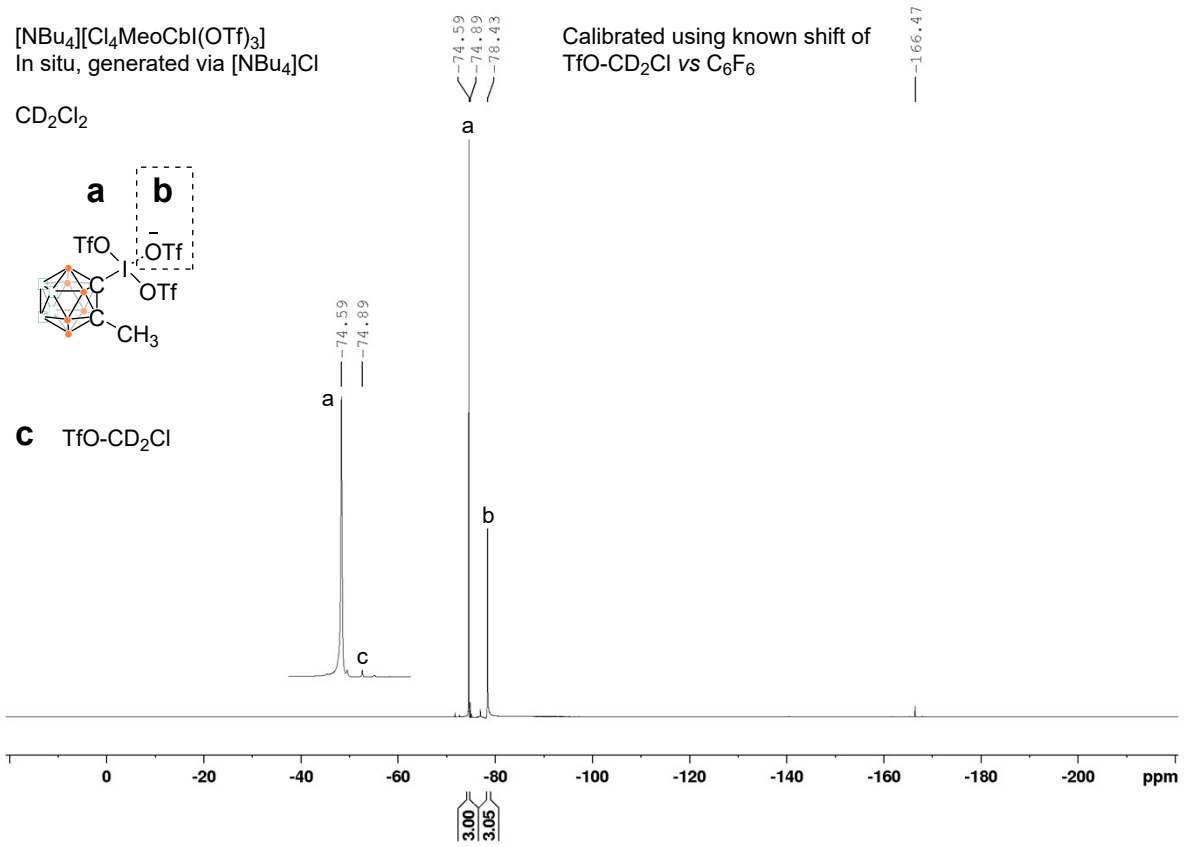

Figure S64. ^{19}F NMR (CD_2Cl_2, 470 MHz): $[NBu_4][Cl_4MeoCb\text{-}I(OTf)_3]$ generated *via* $[NBu_4]Cl$.

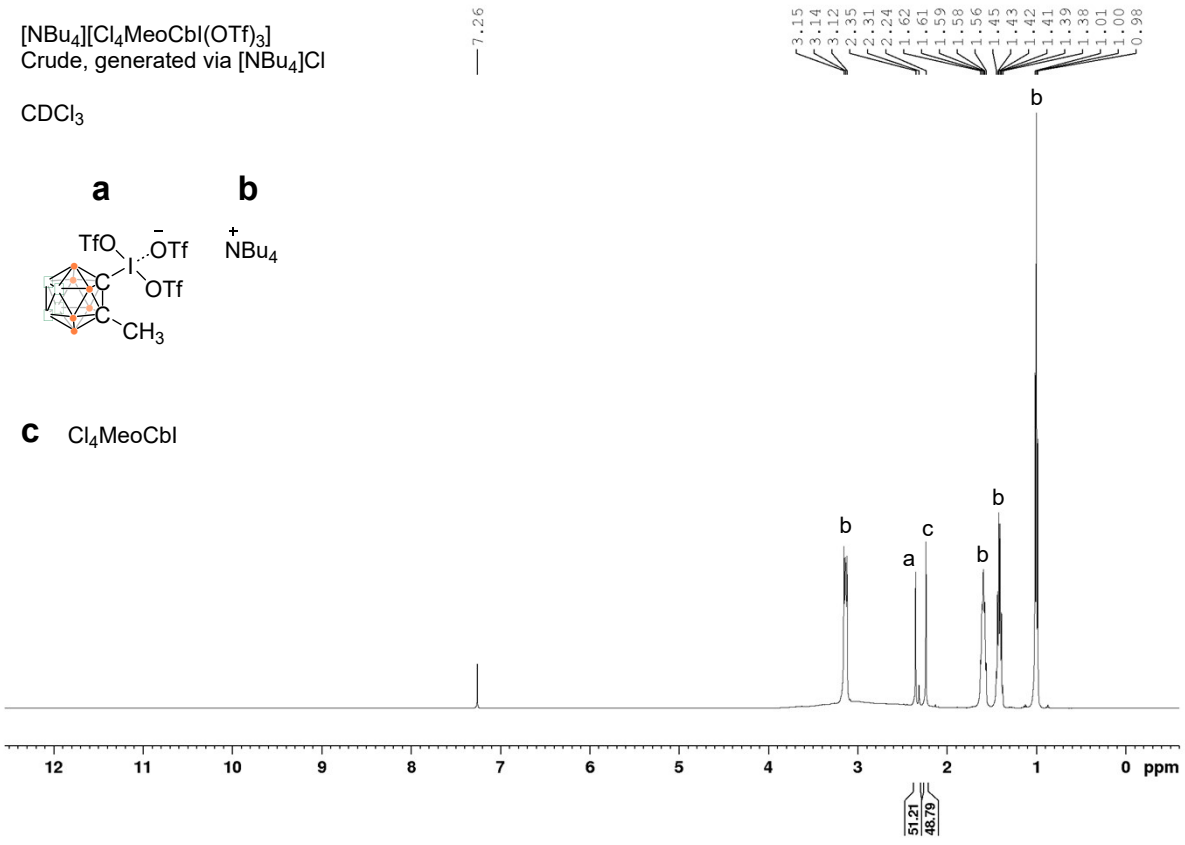

Figure S65. ^{1}H NMR ($CDCl_3$, 500 MHz): $[NBu_4][Cl_4MeoCb\text{-}I(OTf)_3]$ generated *via* $[NBu_4]Cl$.

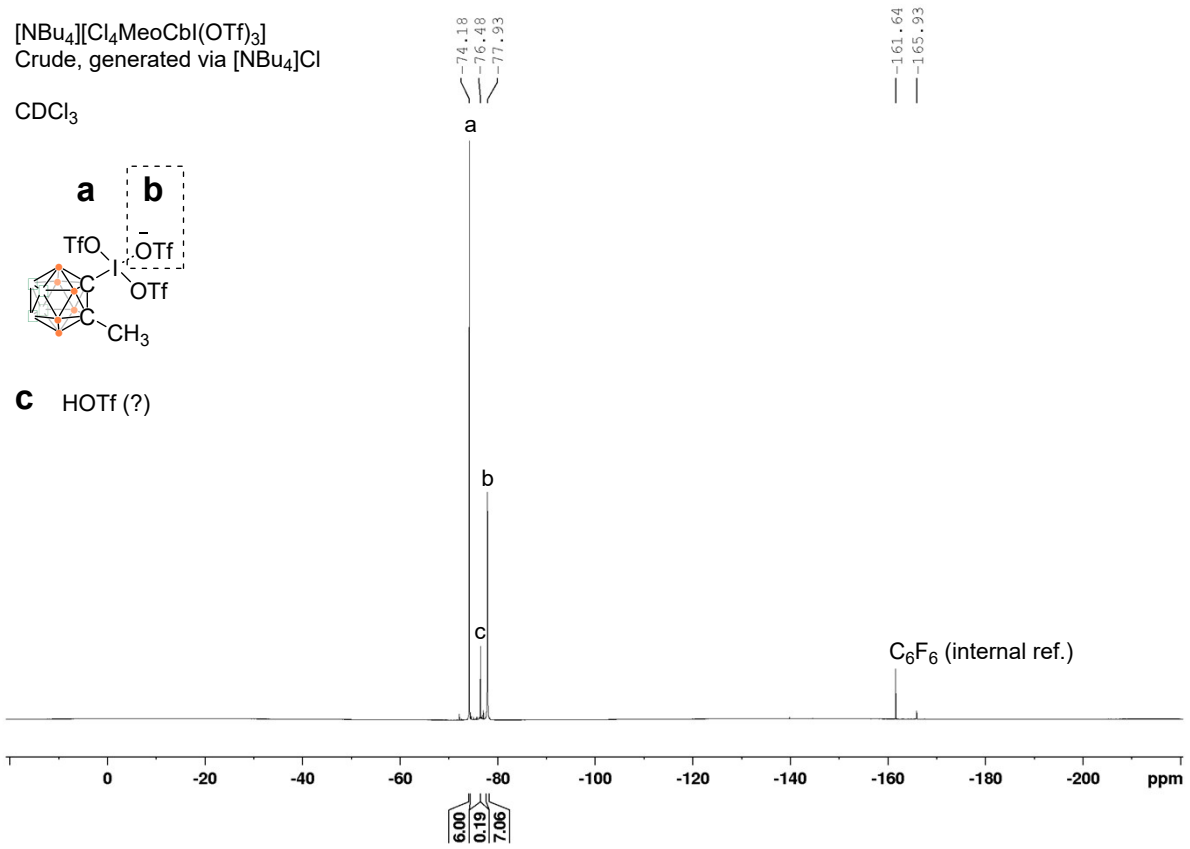

Figure S66. ^{19}F NMR ($CDCl_3$, 470 MHz): $[NBu_4][Cl_4MeoCb\text{-}I(OTf)_3]$ generated *via* $[NBu_4]Cl$.

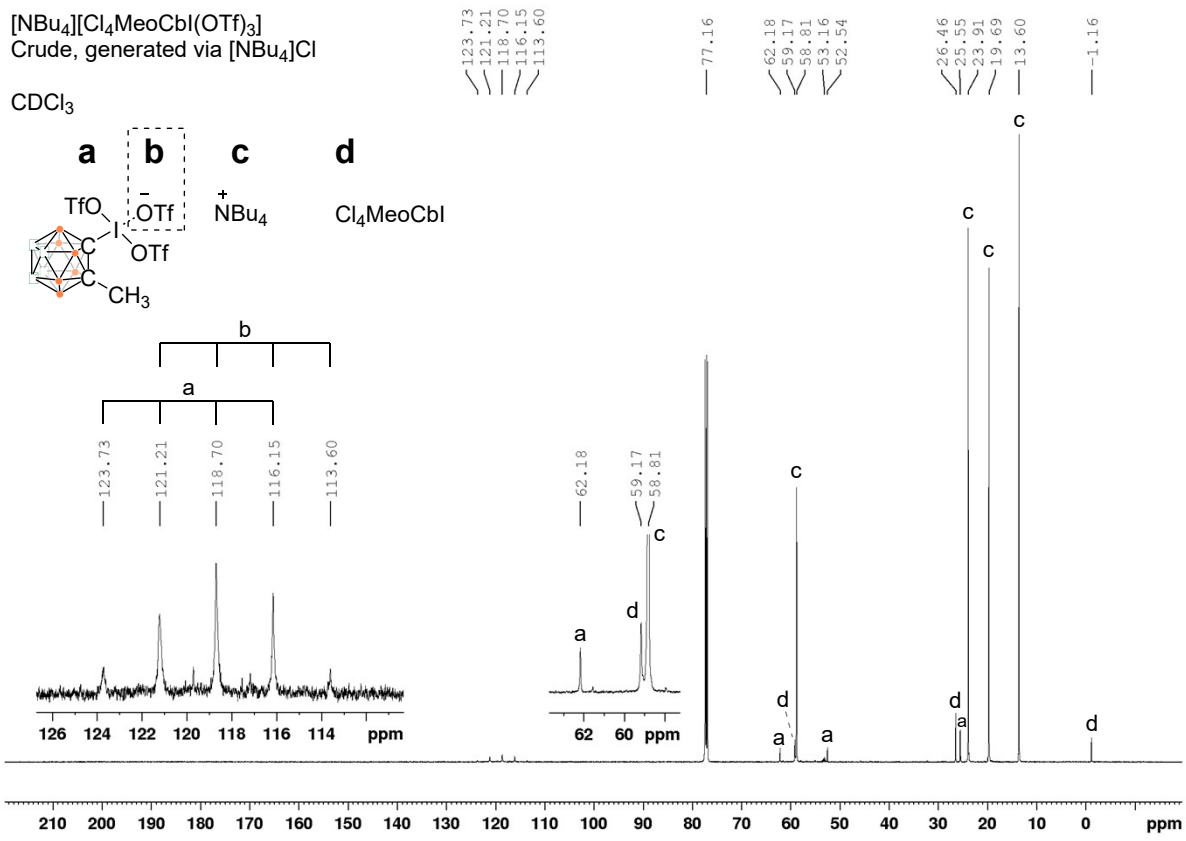

Figure S67. $^{13}C\{^{1}H\}$ NMR ($CDCl_3$, 126 MHz): $[NBu_4][Cl_4MeoCb\text{-}I(OTf)_3]$ generated *via* $[NBu_4]Cl$.

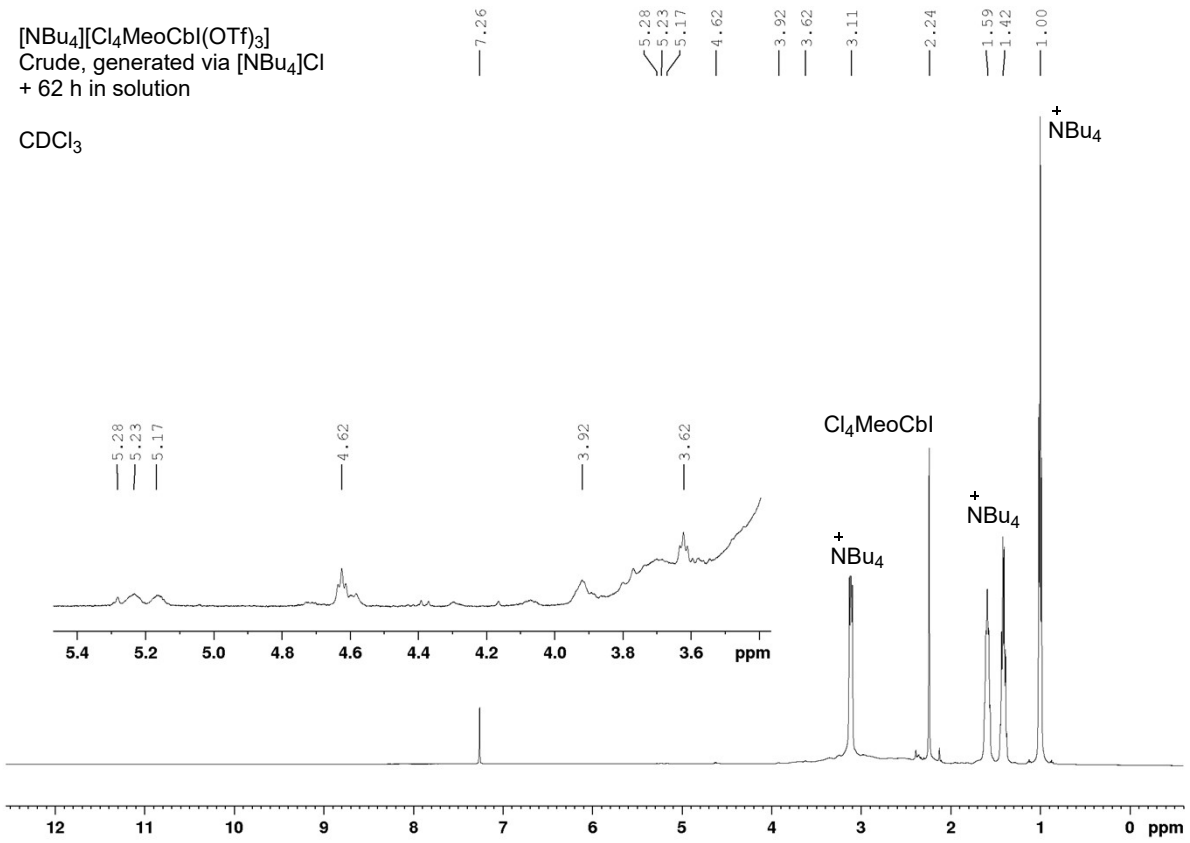

Figure S68. ^{1}H NMR ($CDCl_3$, 500 MHz): $[NBu_4][Cl_4MeoCb\text{-}I(OTf)_3]$ generated *via* $[NBu_4]Cl$ after 62 h in solution.

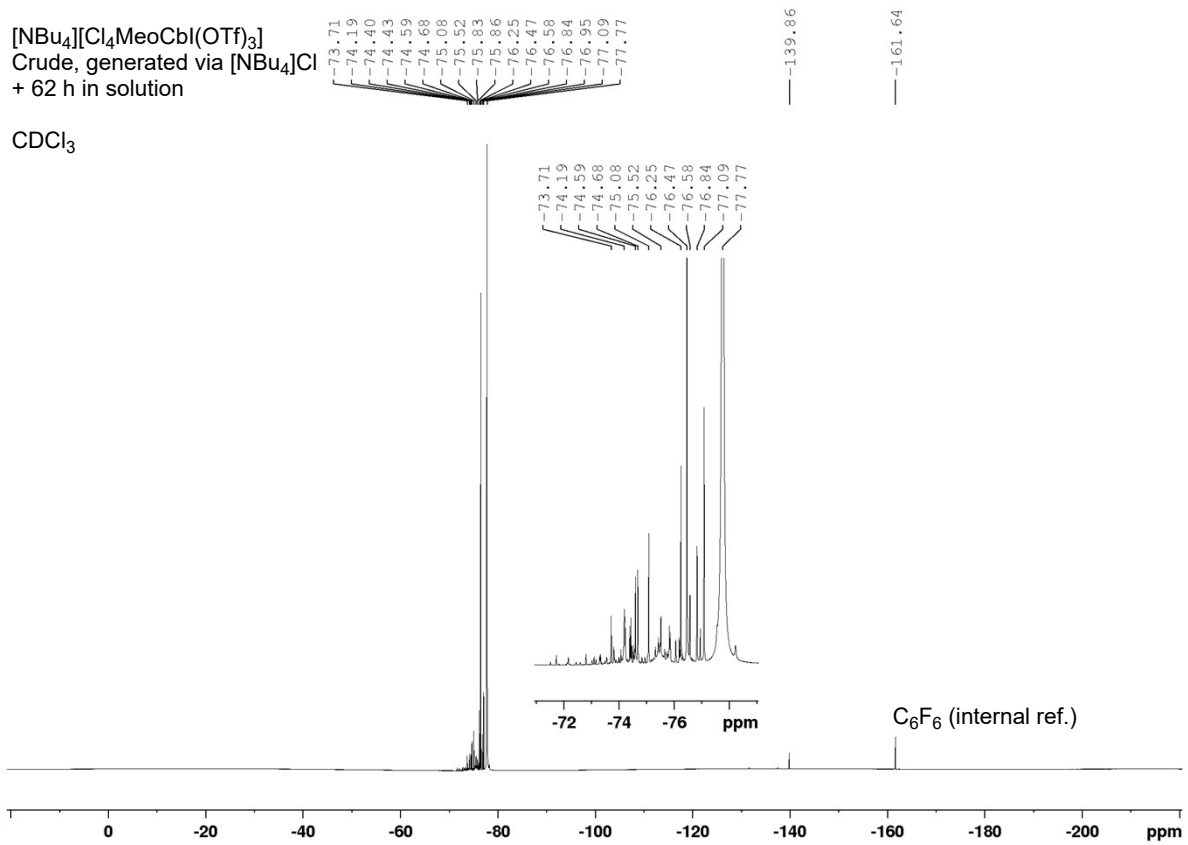

Figure S69. ^{19}F NMR ($CDCl_3$, 470 MHz): $[NBu_4][Cl_4MeoCb\text{-}I(OTf)_3]$ generated *via* $[NBu_4]Cl$ after 62 h in solution.

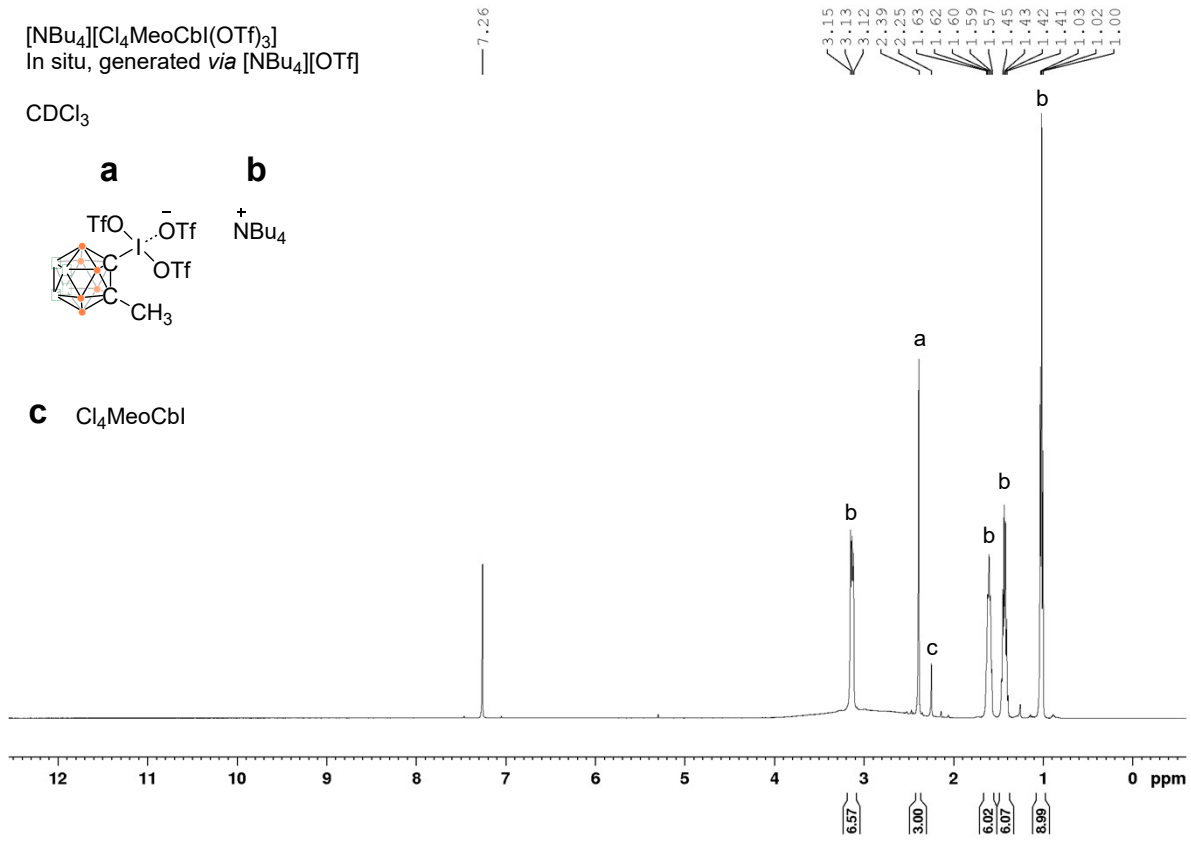

Figure S70. ^{1}H NMR ($CDCl_3$, 500 MHz): [NBu_4][Cl_4MeoCb-I($OTf)_3$] generated *via* [NBu_4][OTf].

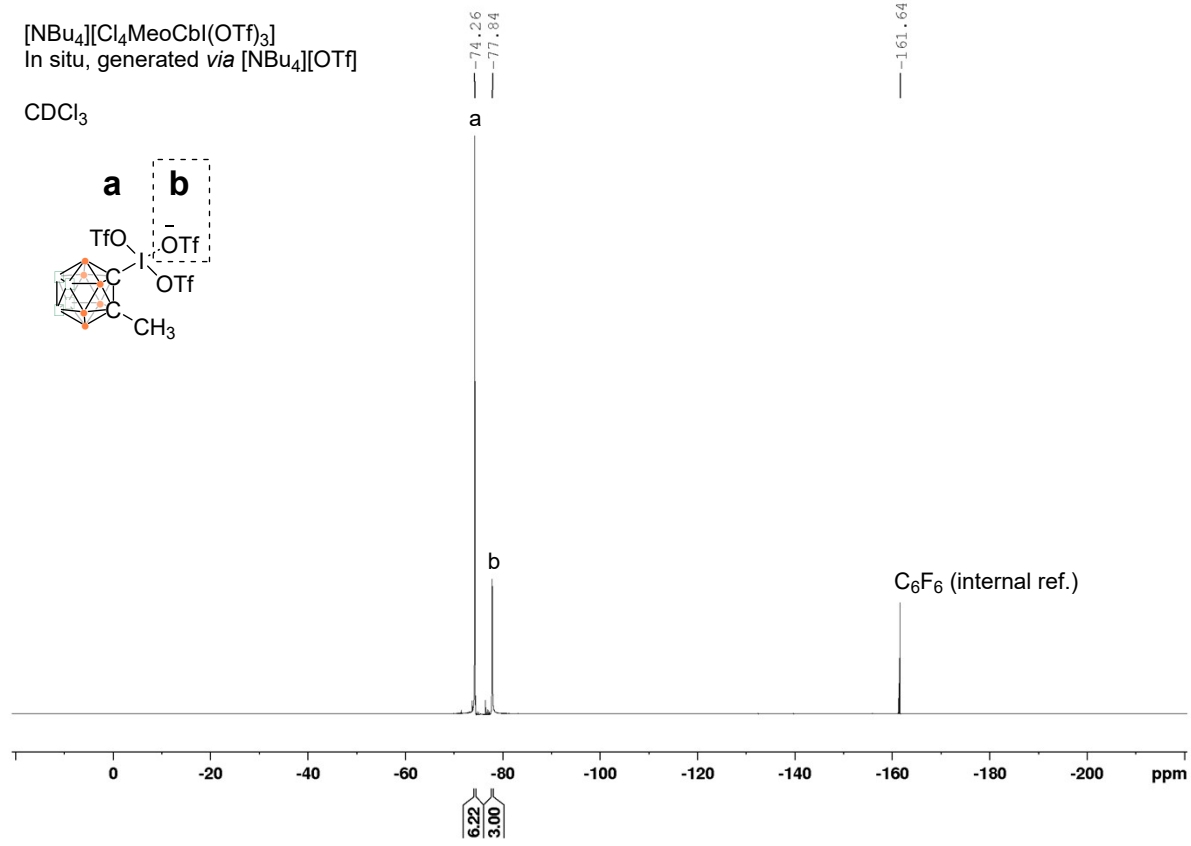

Figure S71. ^{19}F NMR ($CDCl_3$, 470 MHz): [NBu_4][Cl_4MeoCb-I($OTf)_3$] generated *via* [NBu_4][OTf].

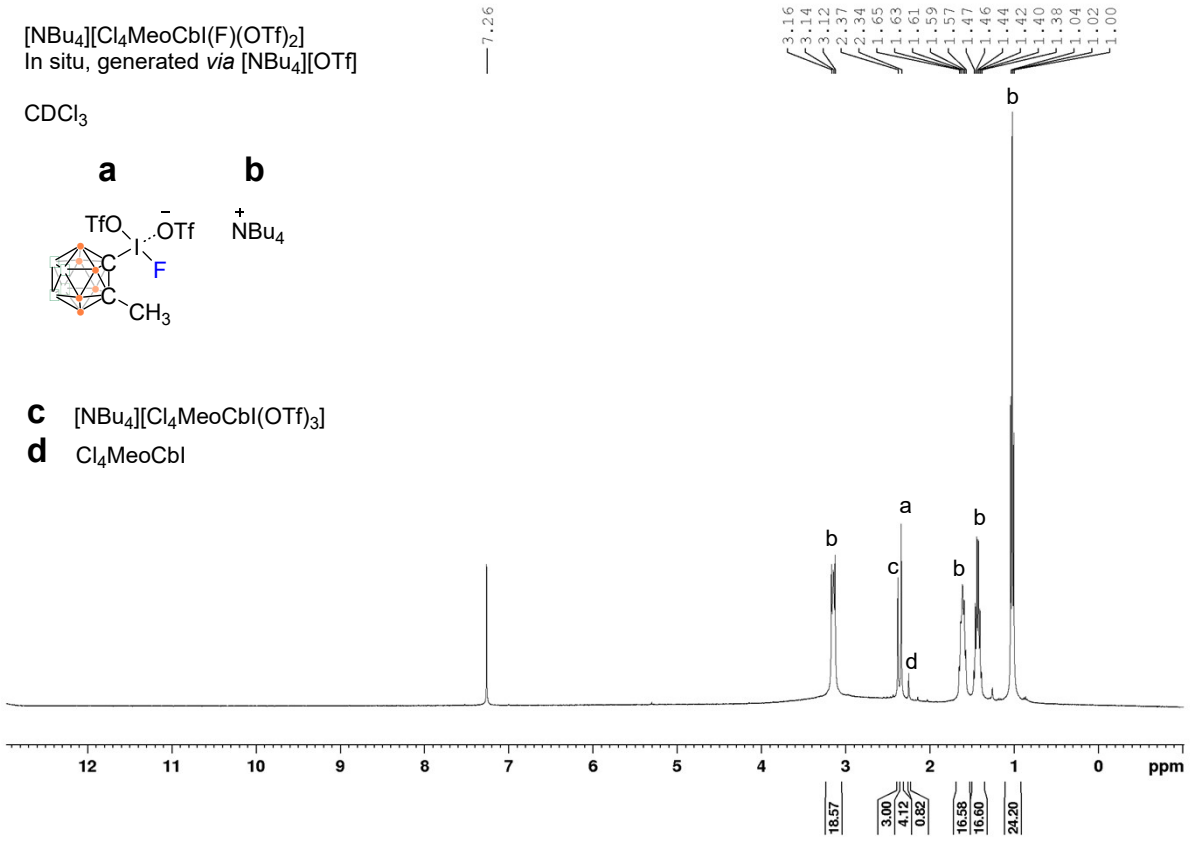

Figure S72. ^{1}H NMR ($CDCl_3$, 400 MHz): [NBu_4][Cl_4MeoCb-I(F)($OTf)_2$] generated *via* [NBu_4][OTf].

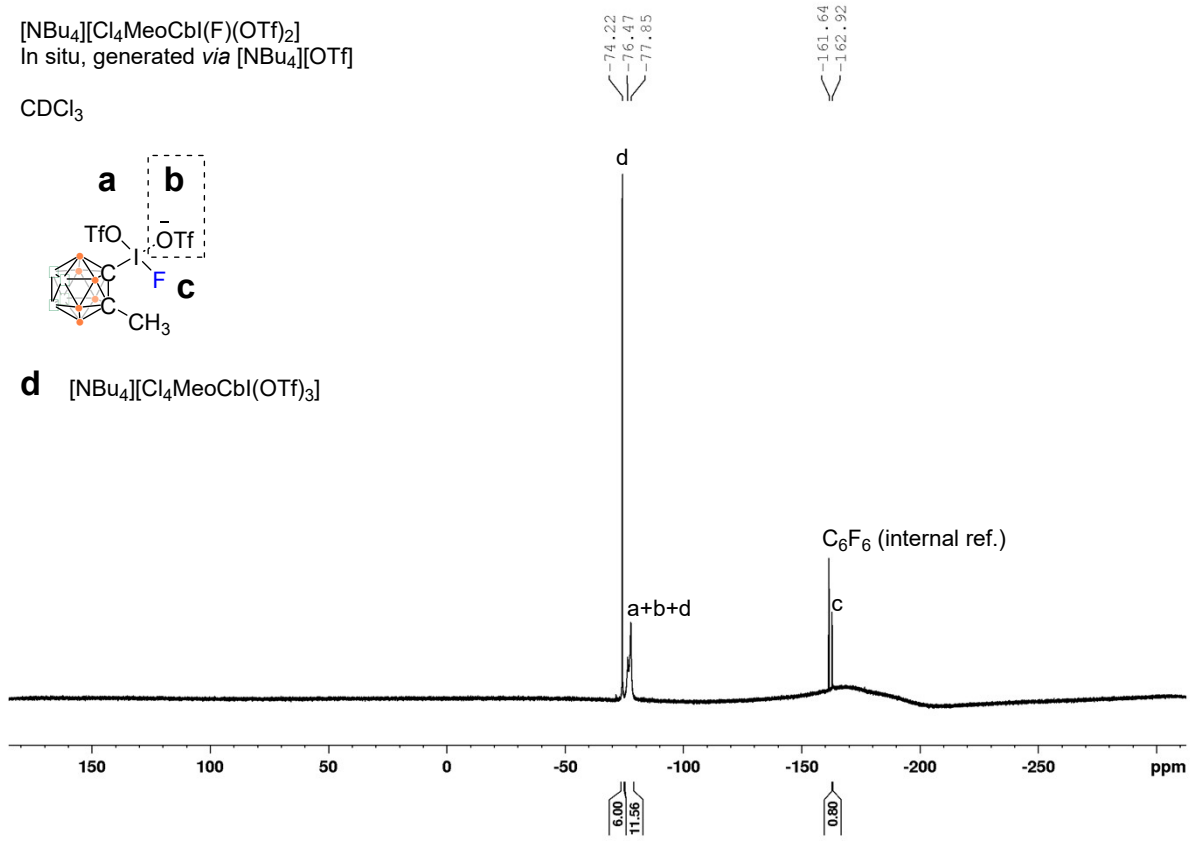

Figure S73. ^{19}F NMR ($CDCl_3$, 376 MHz): [NBu_4][Cl_4MeoCb-I(F)($OTf)_2$] generated *via* [NBu_4][OTf].

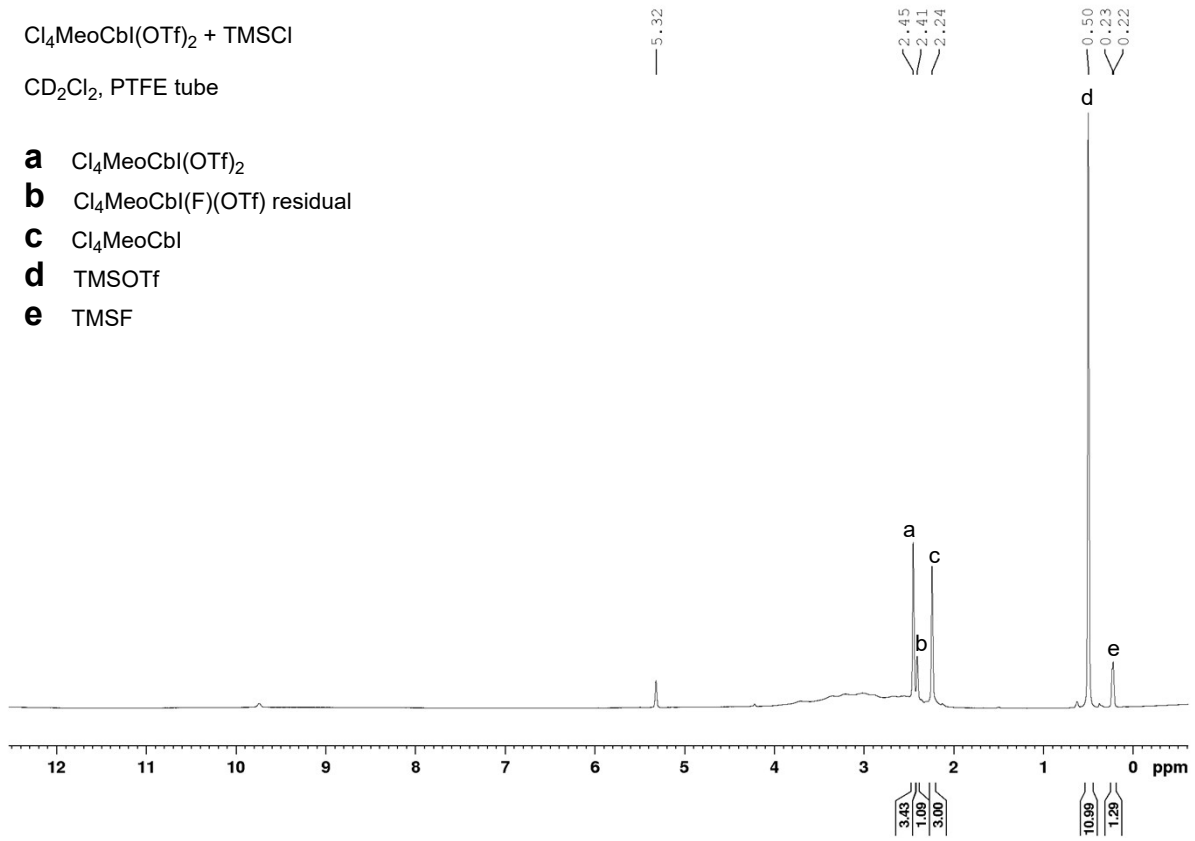

Figure S74. ^{1}H NMR (CD_2Cl_2, PTFE tube, 500 MHz): $Cl_4MeoCb\text{-}I(OTf)_2$ + TMSCl.

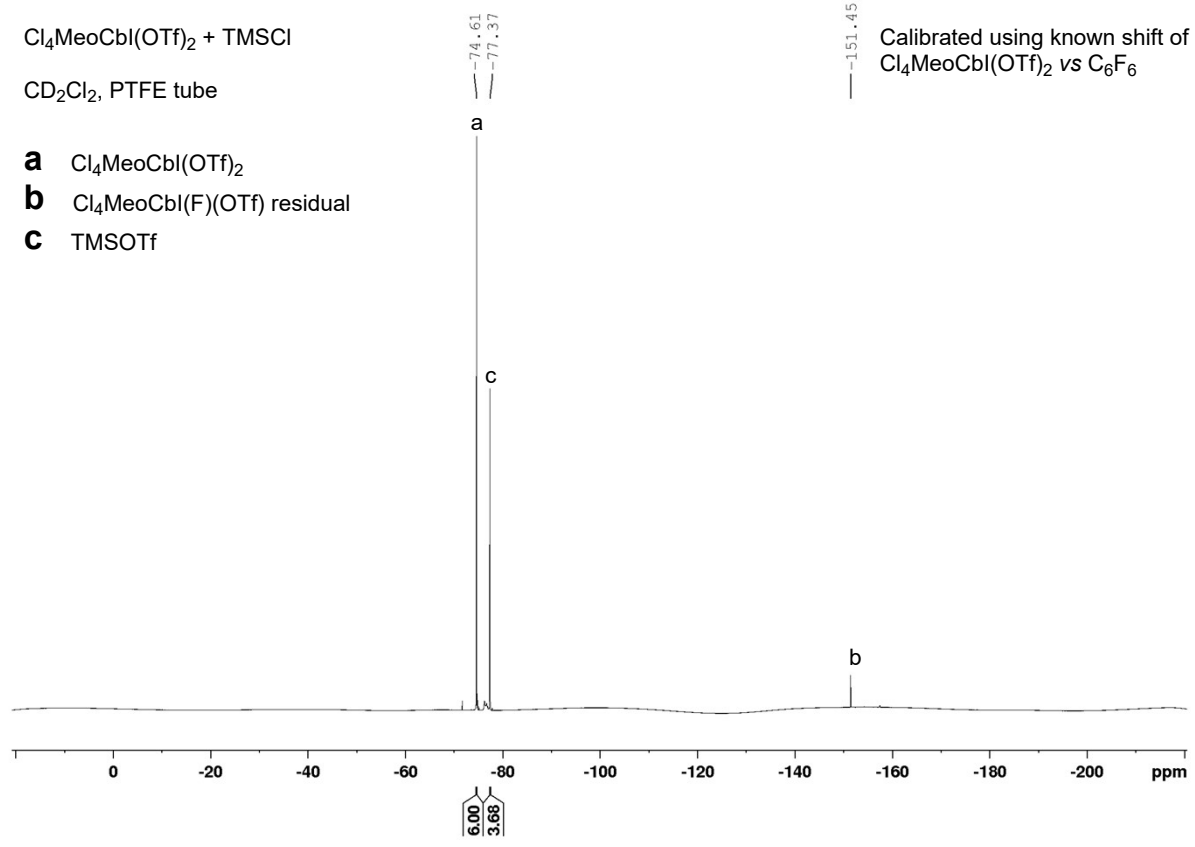

Figure S75. ^{19}F NMR (CD_2Cl_2, PTFE tube, 470 MHz): $Cl_4MeoCb\text{-}I(OTf)_2$ + TMSCl.

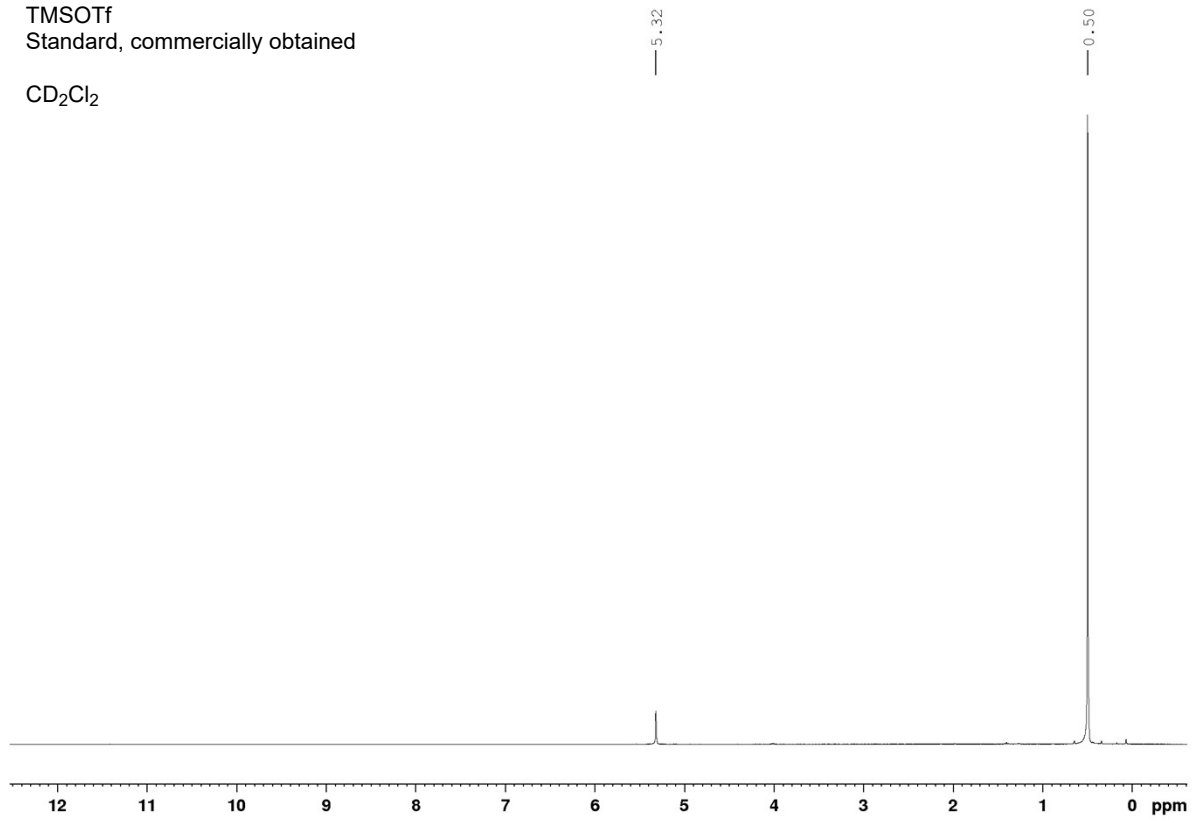

Figure S76. ^{1}H NMR (CD_2Cl_2, 400 MHz): TMSOTf.

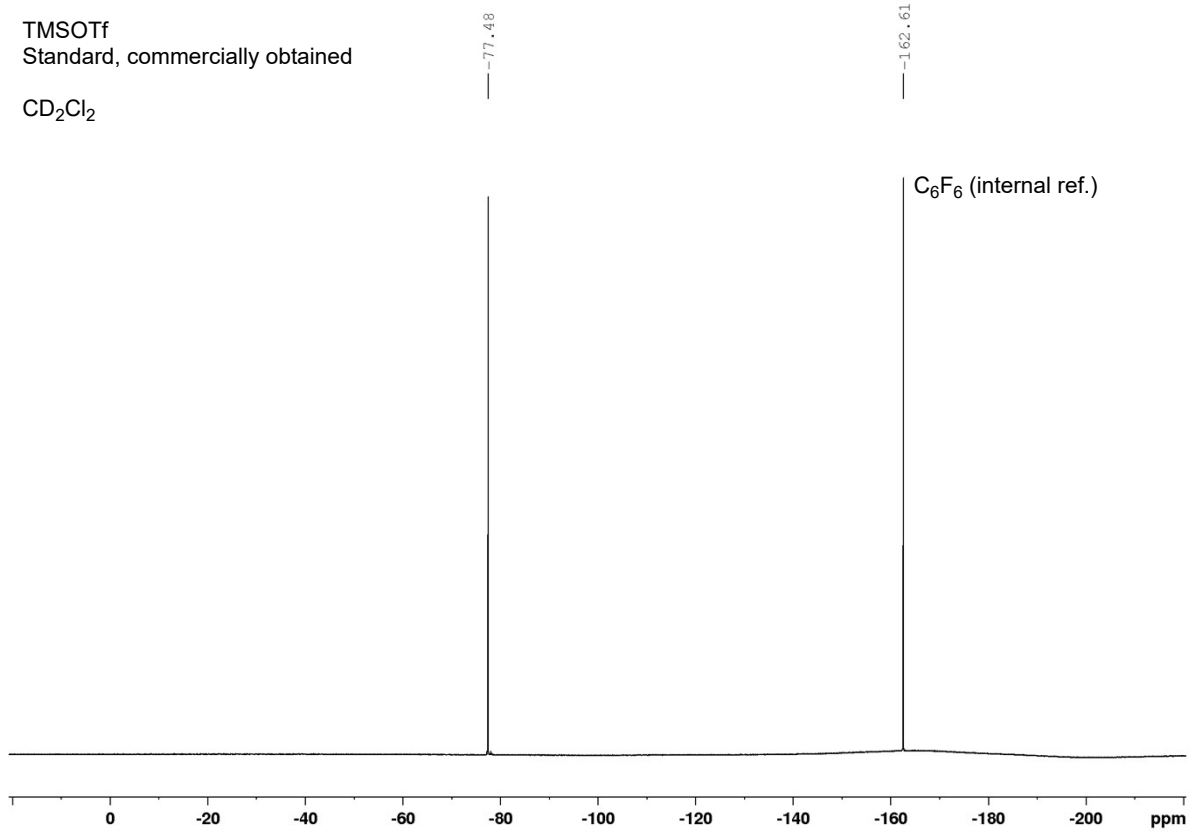

Figure S77. ^{19}F NMR (CD_2Cl_2, 376 MHz): TMSOTf.

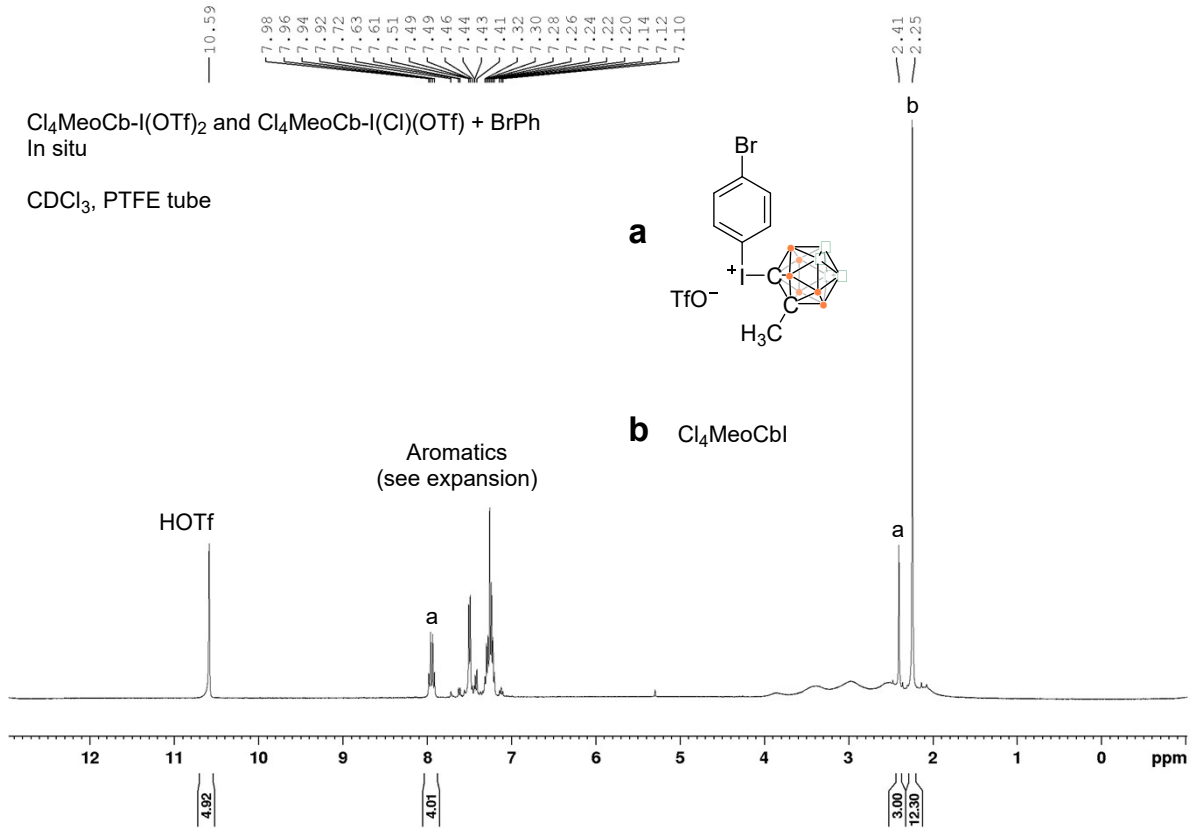

Figure S78. ^{1}H NMR ($CDCl_3$, 400 MHz): Reaction of Cl_4MeoCb-I(OTf)$_2$ and Cl_4MeoCb-I(Cl)(OTf) with BrPh to probe for chlorination (spectrum 1 of 2: full). Baseline correction used for integrals that overlap with BH signals. See Figure S79 for aromatic region expansion.

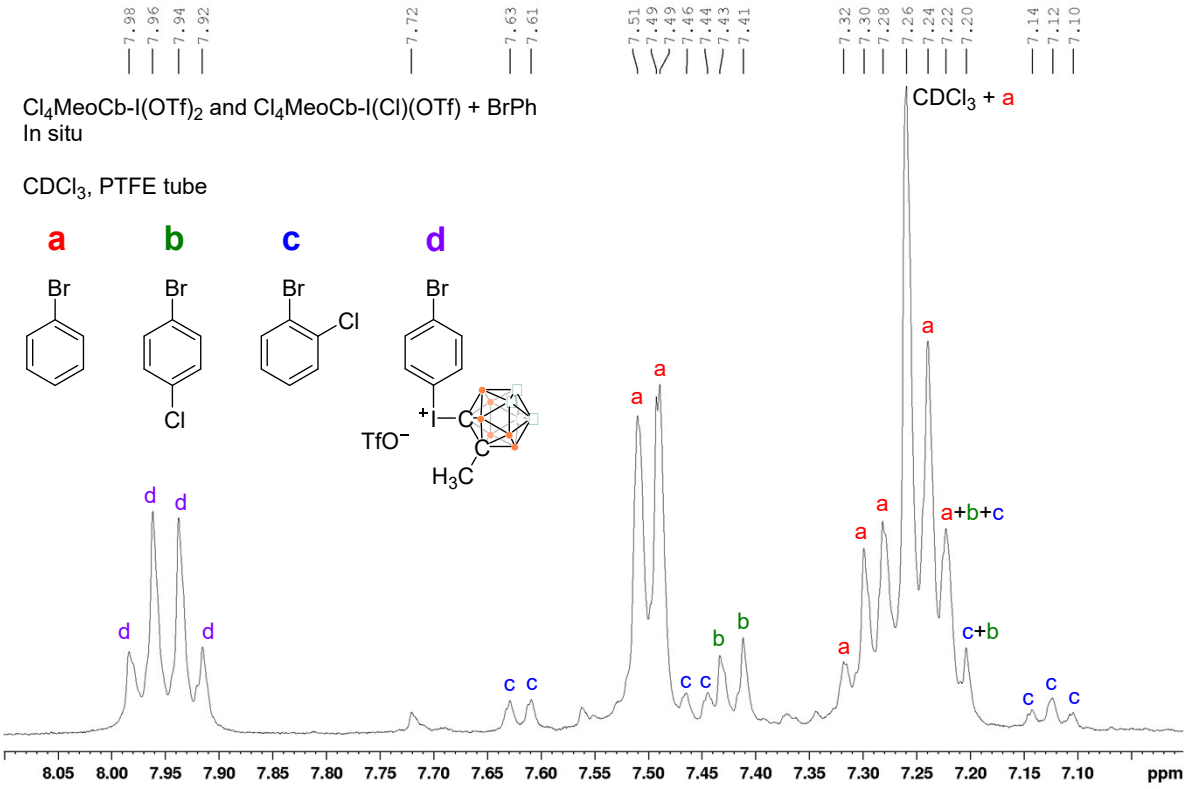

Figure S79. ^{1}H NMR ($CDCl_3$, PTFE tube, 400 MHz): Reaction of Cl_4MeoCb-I(OTf)$_2$ and Cl_4MeoCb-I(Cl)(OTf) with BrPh to probe for chlorination (spectrum 2 of 2: aromatics).

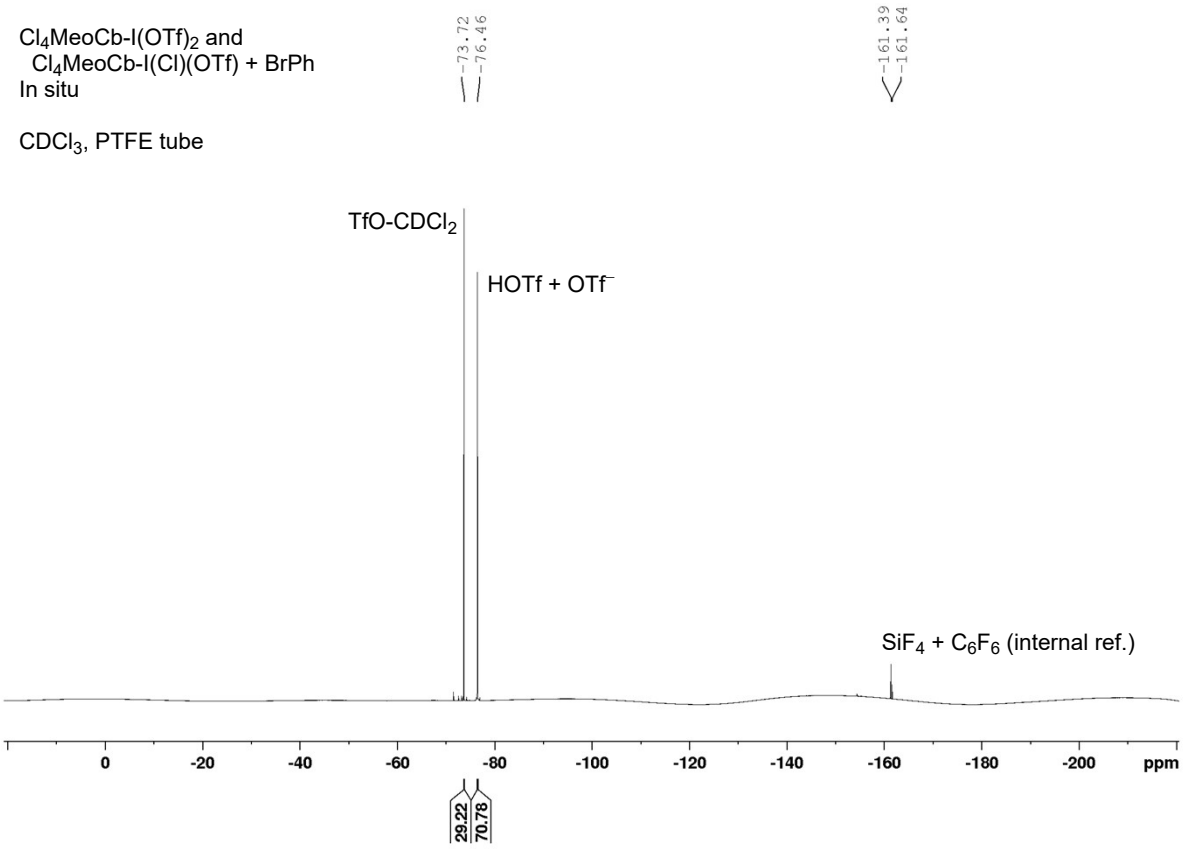

Figure S80. ^{19}F NMR ($CDCl_3$, PTFE tube, 470 MHz): Reaction of $Cl_4MeoCb\text{-}I(OTf)_2$ and $Cl_4MeoCb\text{-}I(Cl)(OTf)$ with BrPh to probe for chlorination.

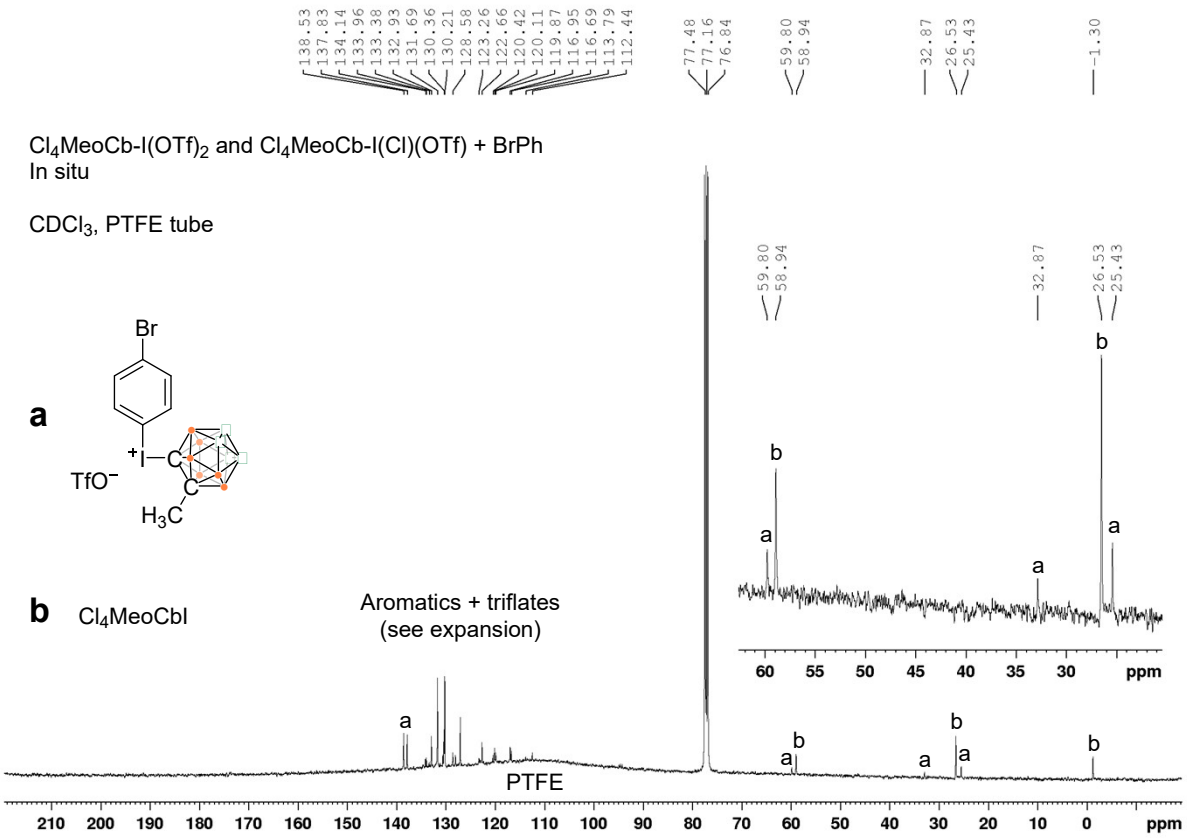

Figure S81. $^{13}C\{^{1}H\}$ NMR ($CDCl_3$, 101 MHz): Reaction of $Cl_4MeoCb\text{-}I(OTf)_2$ and $Cl_4MeoCb\text{-}I(Cl)(OTf)$ with BrPh to probe for chlorination (spectrum 1 of 2: full). 5 Hz line broadening to resolve multiplet oCb signals. See Figure S82 for aromatic and triflate region expansion.

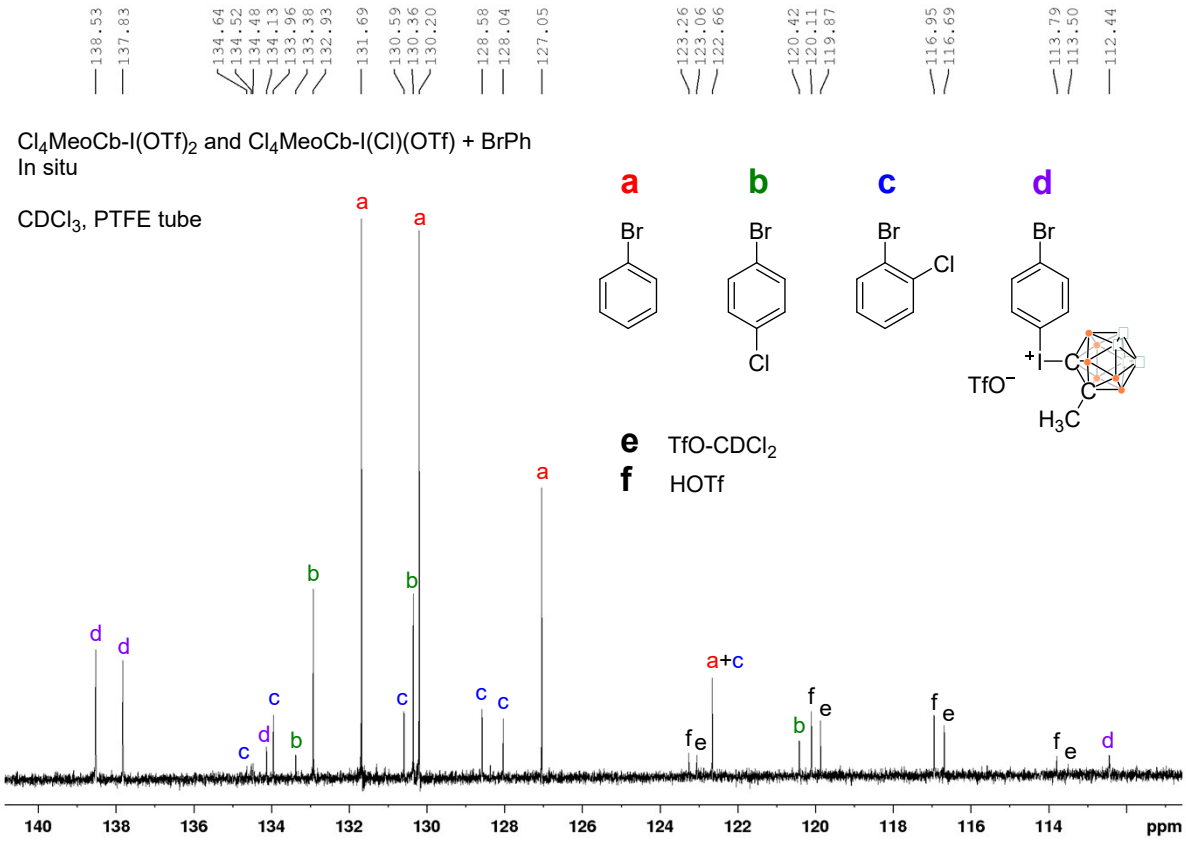

Figure S82. $^{13}C\{^{1}H\}$ NMR ($CDCl_3$, 101 MHz): Reaction of Cl_4MeoCb-I(OTf)$_2$ and Cl_4MeoCb-I(Cl)(OTf) with BrPh to probe for chlorination (spectrum 2 of 2: aromatics + triflates).

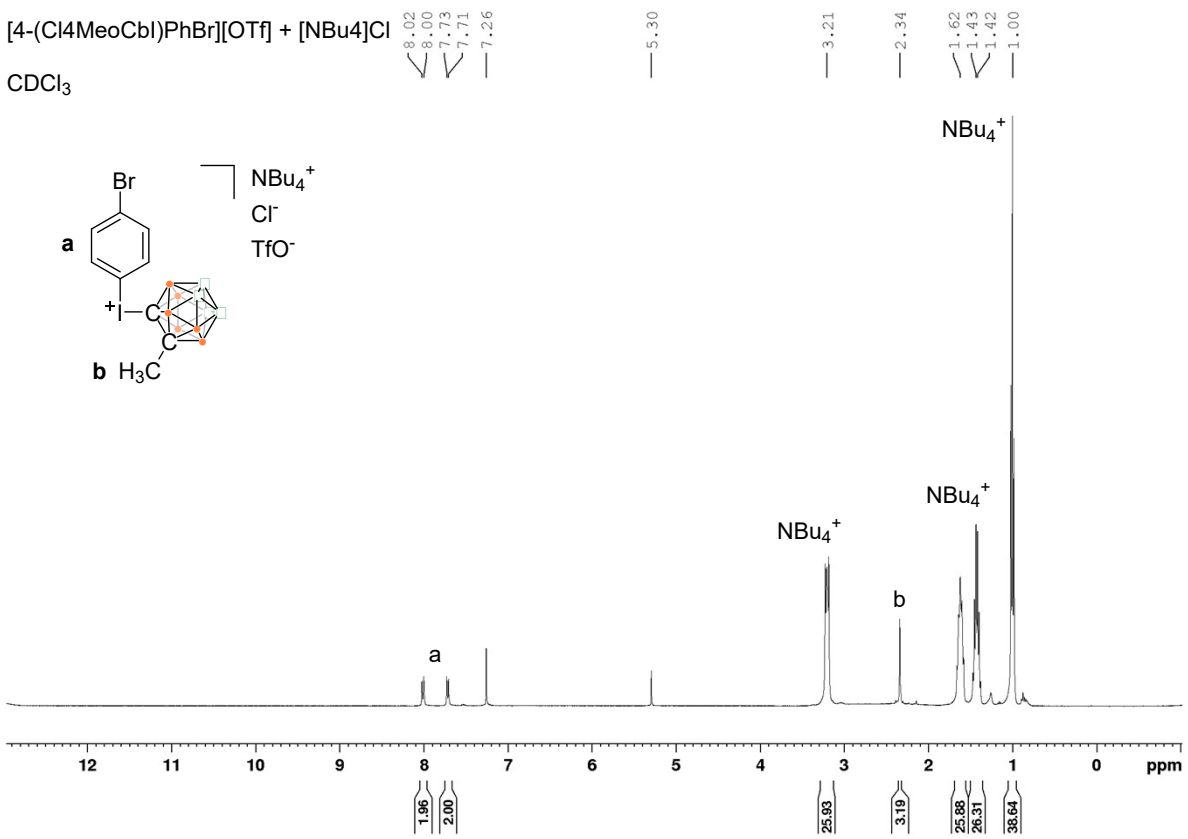

Figure S83. ^{1}H NMR ($CDCl_3$, 400 MHz): [4-(Cl_4MeOCbI)PhBr][OTf] + [NBu_4]Cl.

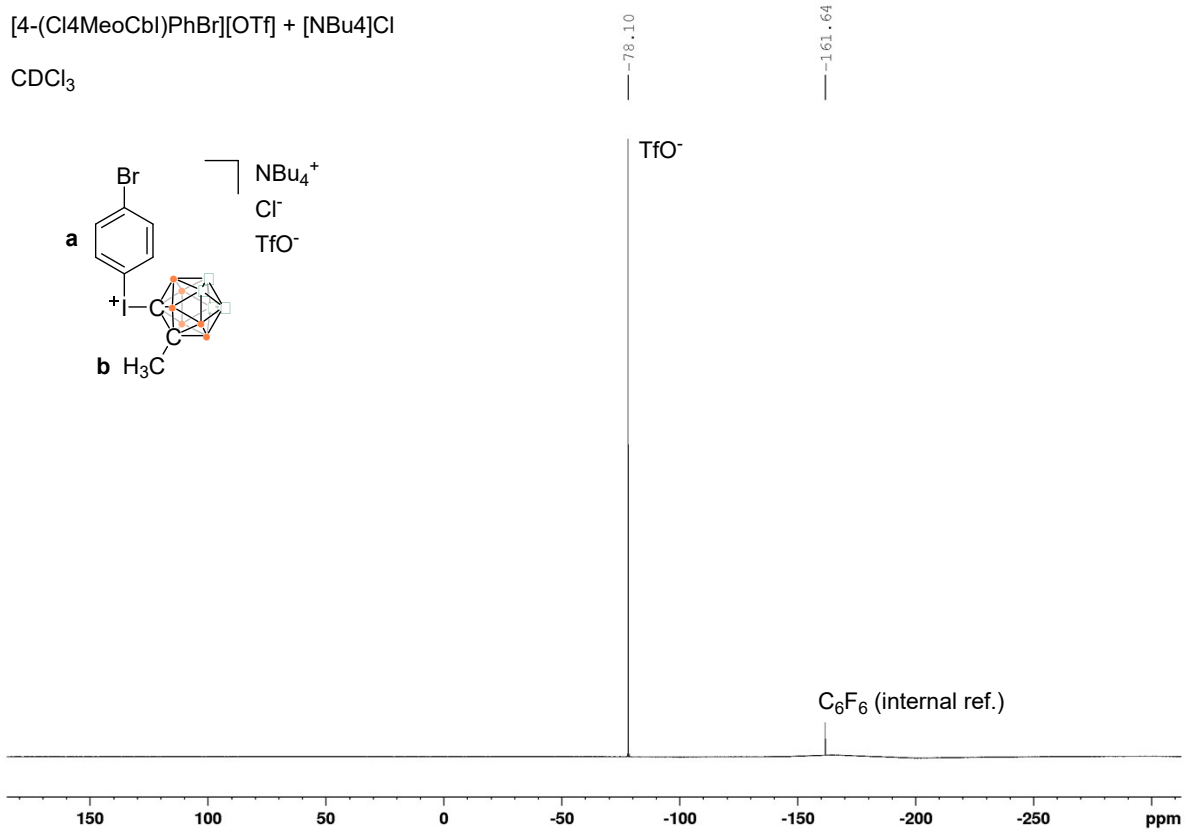

Figure S84. ^{19}F NMR ($CDCl_3$, 376 MHz): [4-(Cl_4MeOCbI)PhBr][OTf] + [NBu_4]Cl.

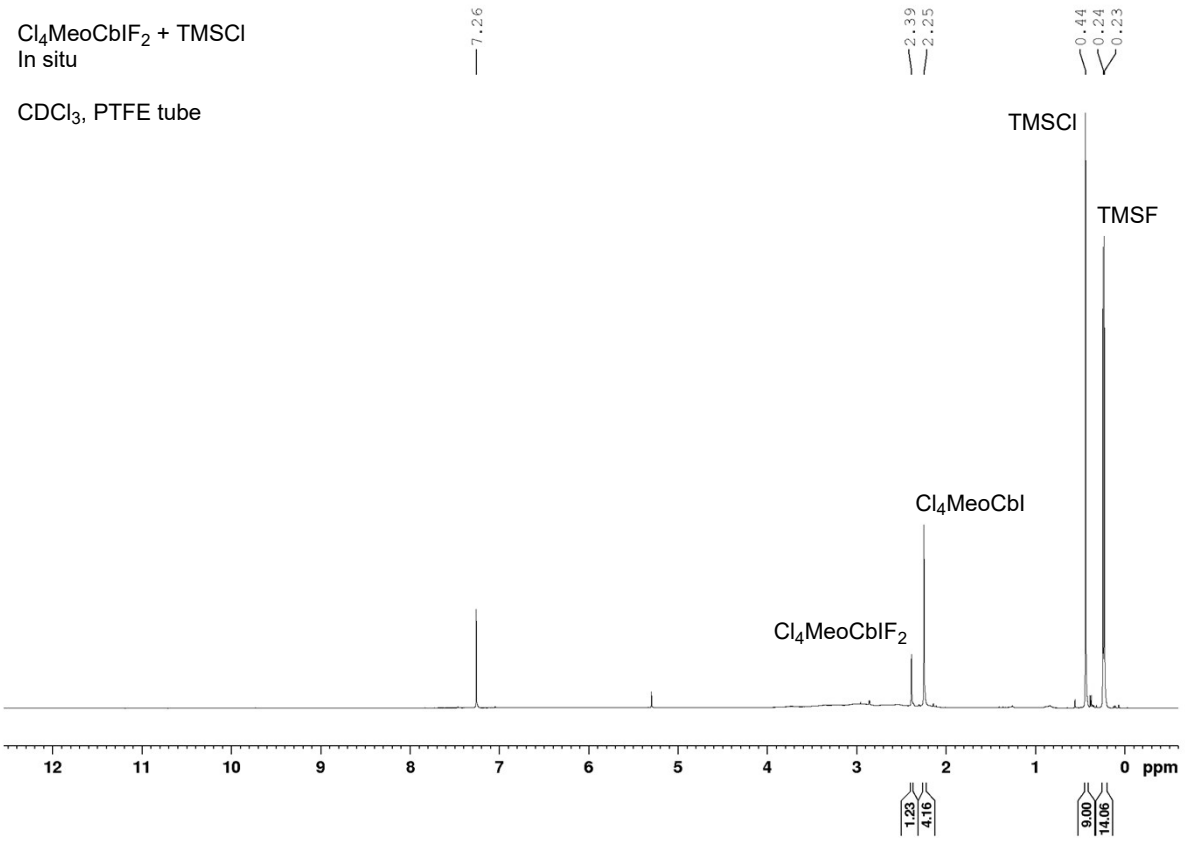

Figure S85. ^{1}H NMR ($CDCl_3$, 500 MHz): Reaction of $Cl_4MeoCb\text{-}IF_2$ with TMSCl.

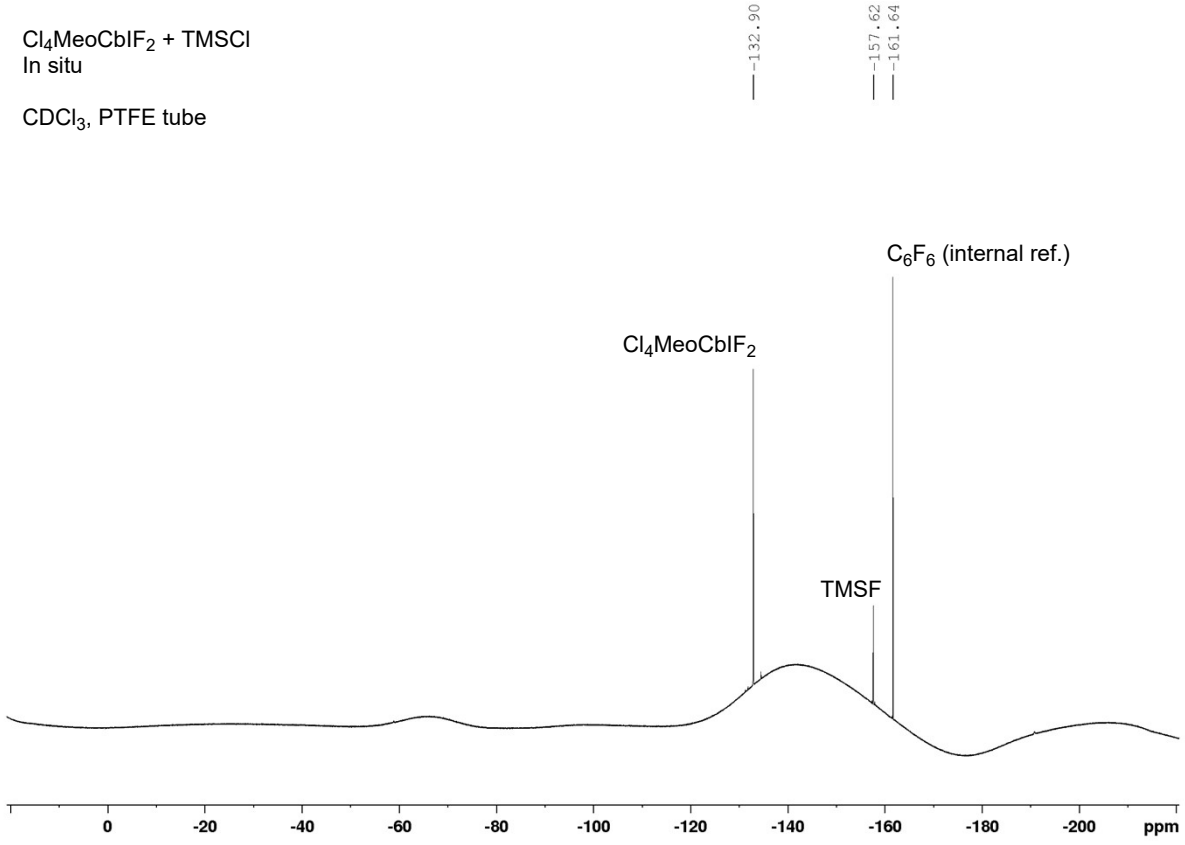

Figure S86. ^{19}F NMR ($CDCl_3$, 470 MHz): Reaction of $Cl_4MeoCb\text{-}IF_2$ with TMSCl.

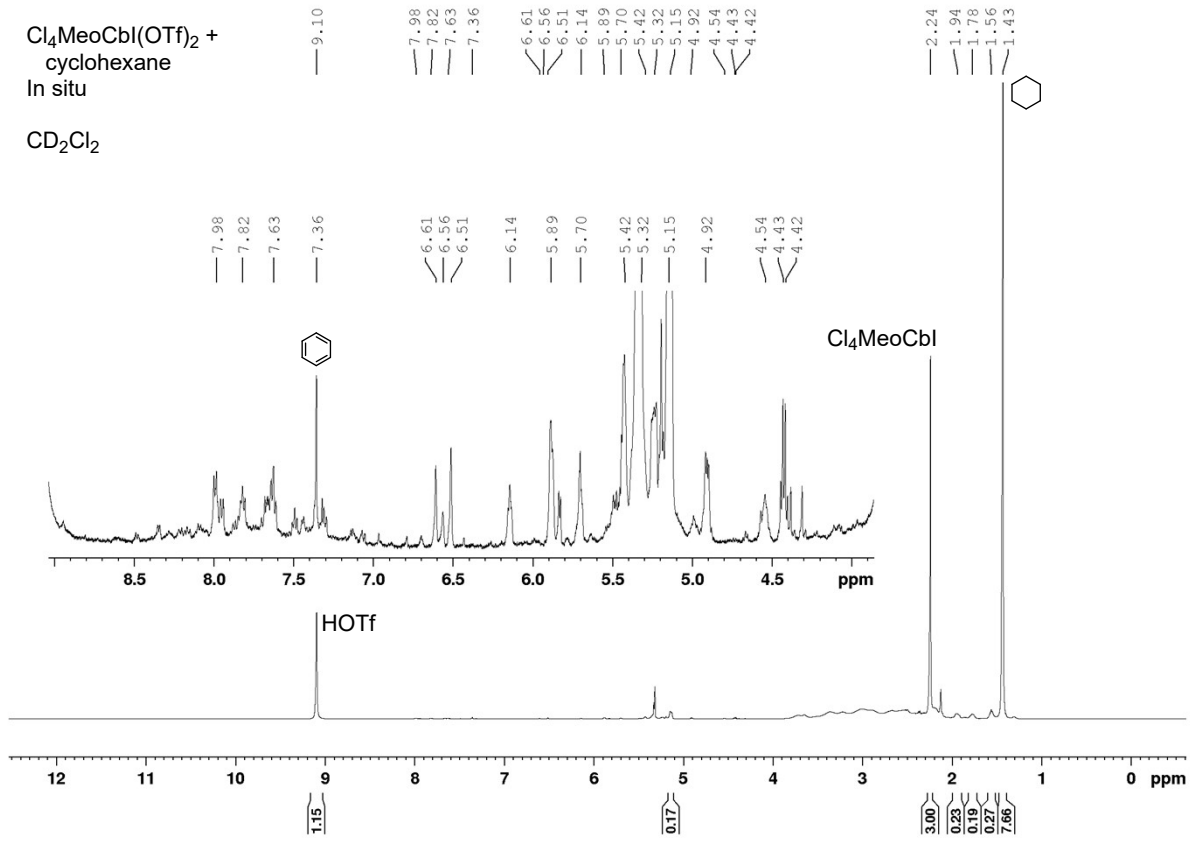

Figure S87. ^{1}H NMR (CD_2Cl_2, 500 MHz): Reaction of $Cl_4MeoCb\text{-}I(OTf)_2$ with cyclohexane.

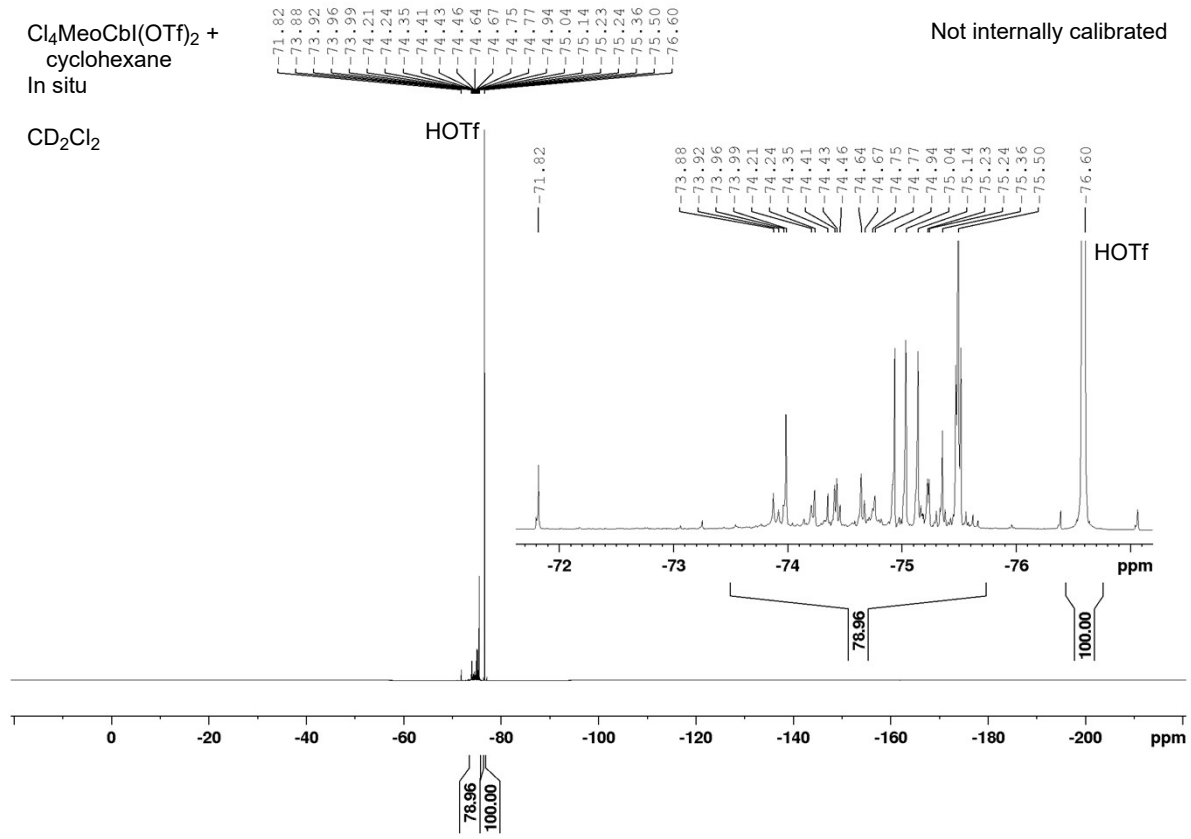

Figure S88. ^{19}F NMR (CD_2Cl_2, 470 MHz): Reaction of $Cl_4MeoCb\text{-}I(OTf)_2$ with cyclohexane.

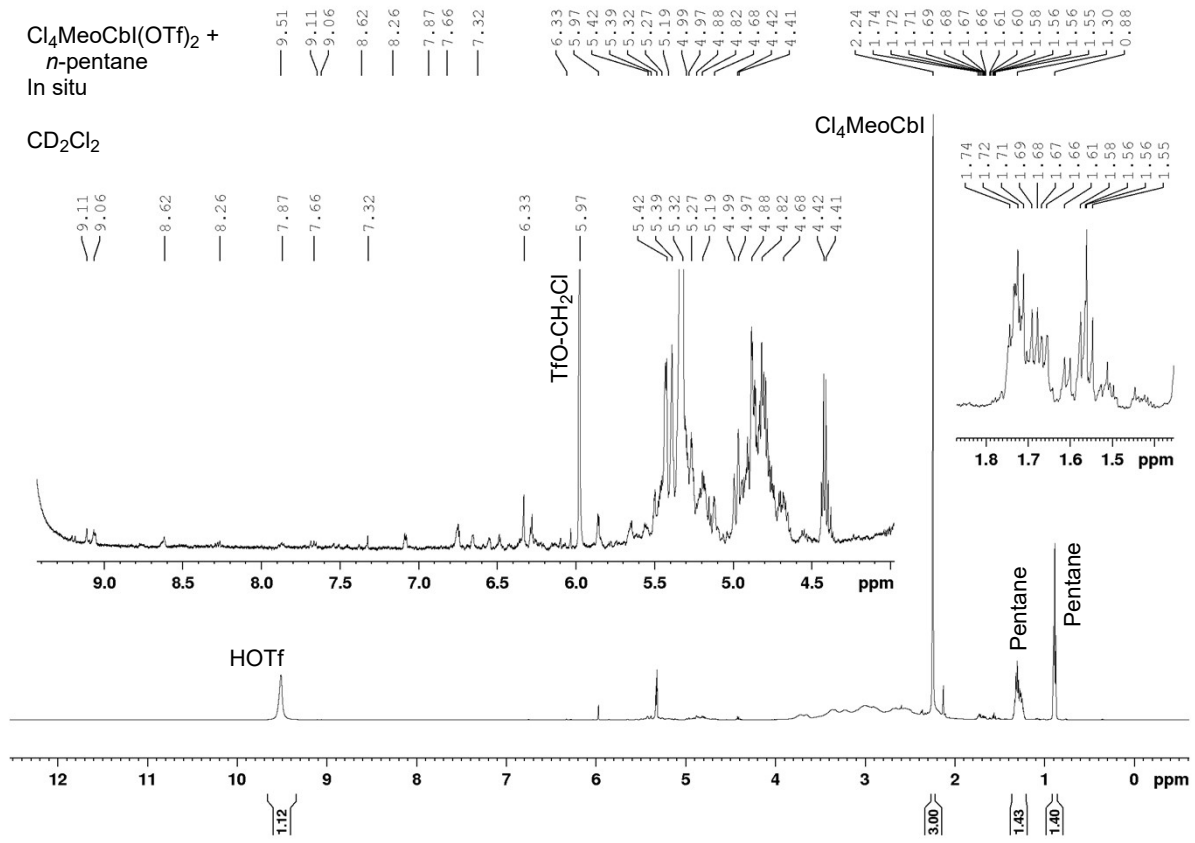

Figure S89. ^{1}H NMR (CD_2Cl_2, 500 MHz): Reaction of $Cl_4MeoCb\text{-}I(OTf)_2$ with *n*-pentane.

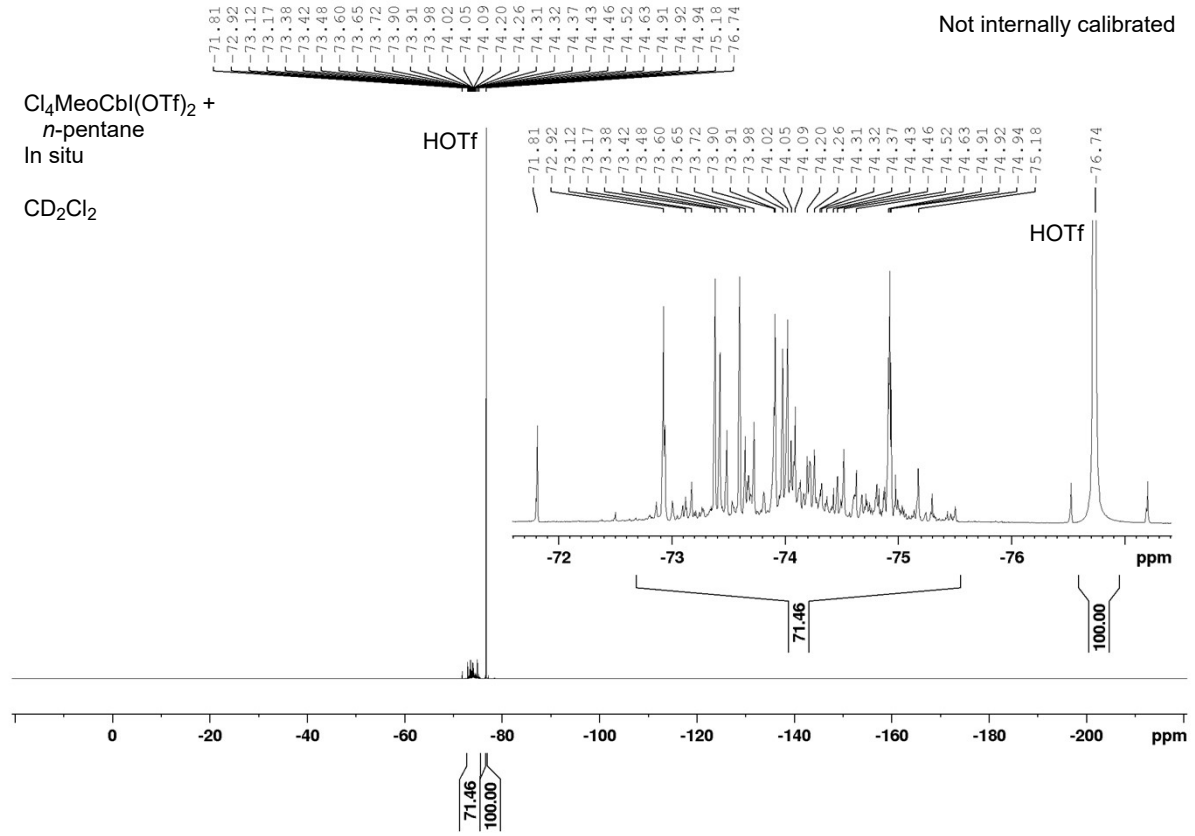

Figure S90. ^{19}F NMR (CD_2Cl_2, 470 MHz): Reaction of $Cl_4MeoCb\text{-}I(OTf)_2$ with *n*-pentane.

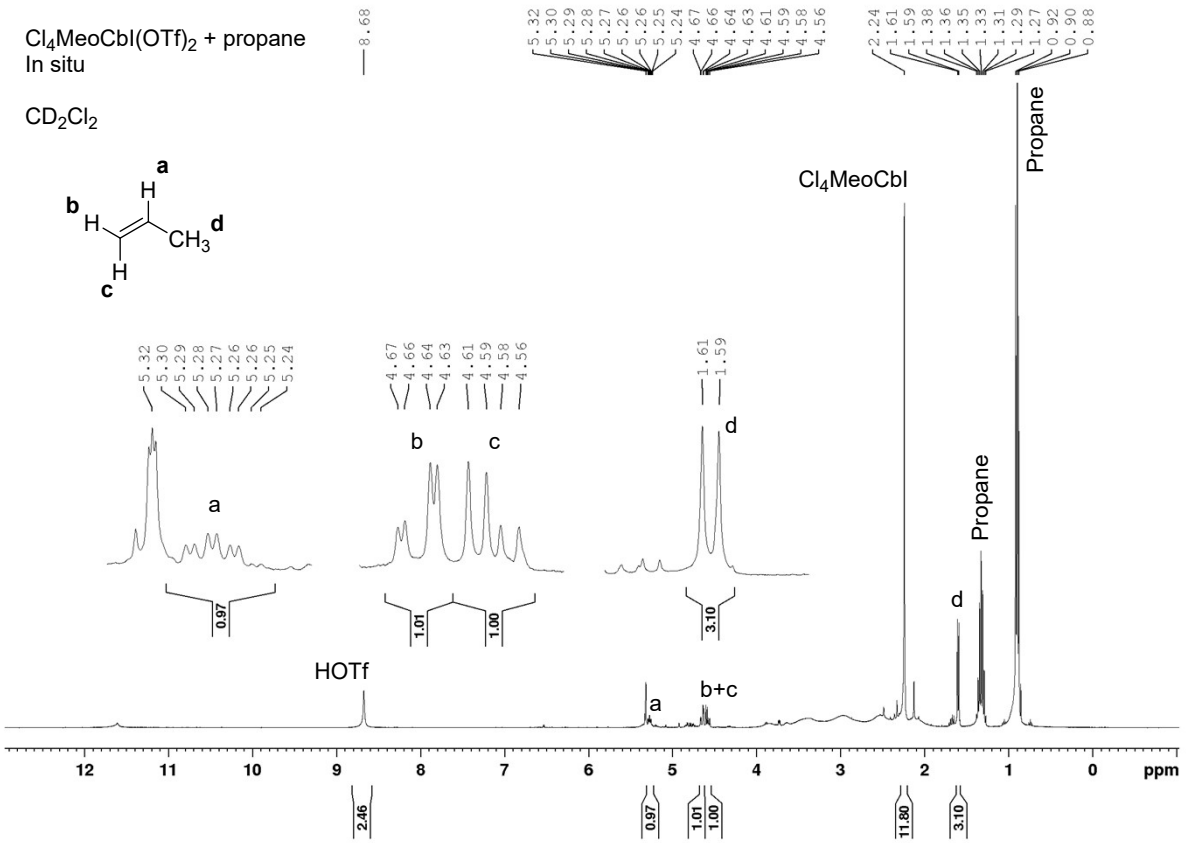

Figure S91. ^{1}H NMR (CD_2Cl_2, 400 MHz): Reaction of $Cl_4MeoCb\text{-}I(OTf)_2$ with propane.

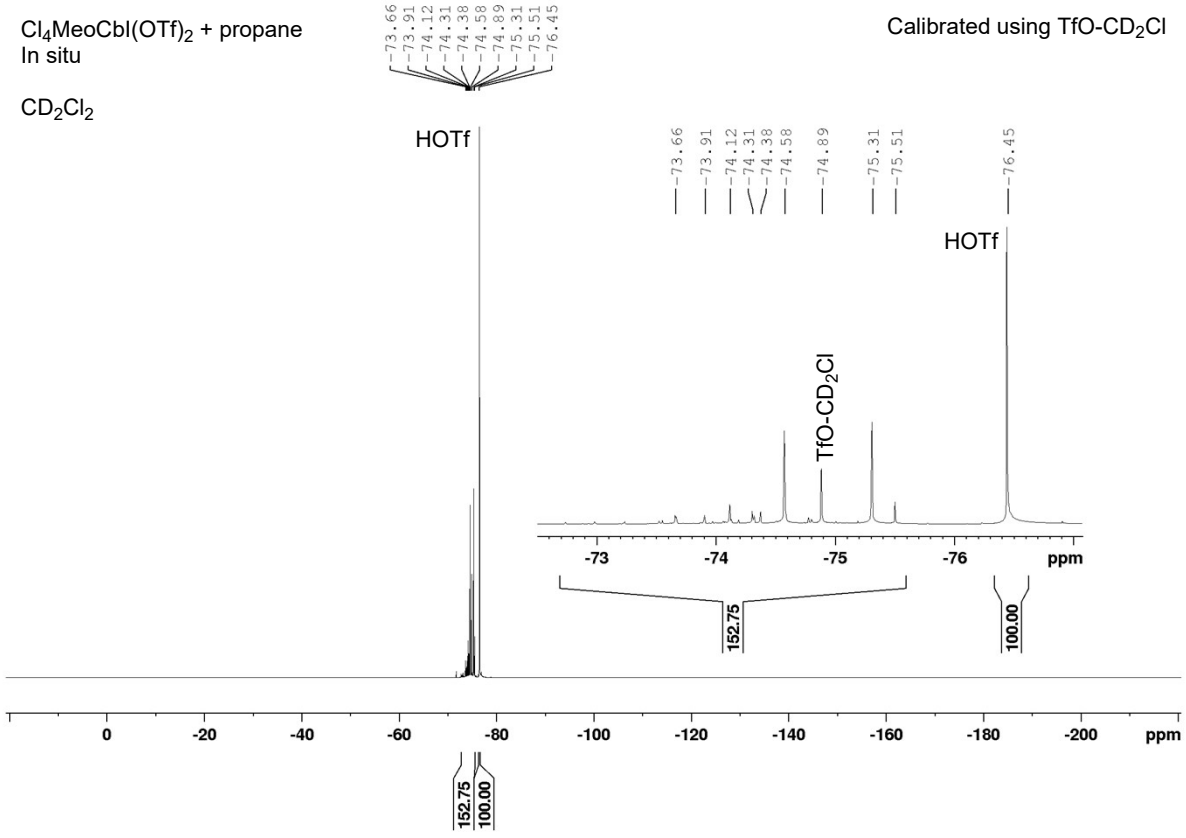

Figure S92. ^{19}F NMR (CD_2Cl_2, 470 MHz): Reaction of $Cl_4MeoCb\text{-}I(OTf)_2$ with propane.

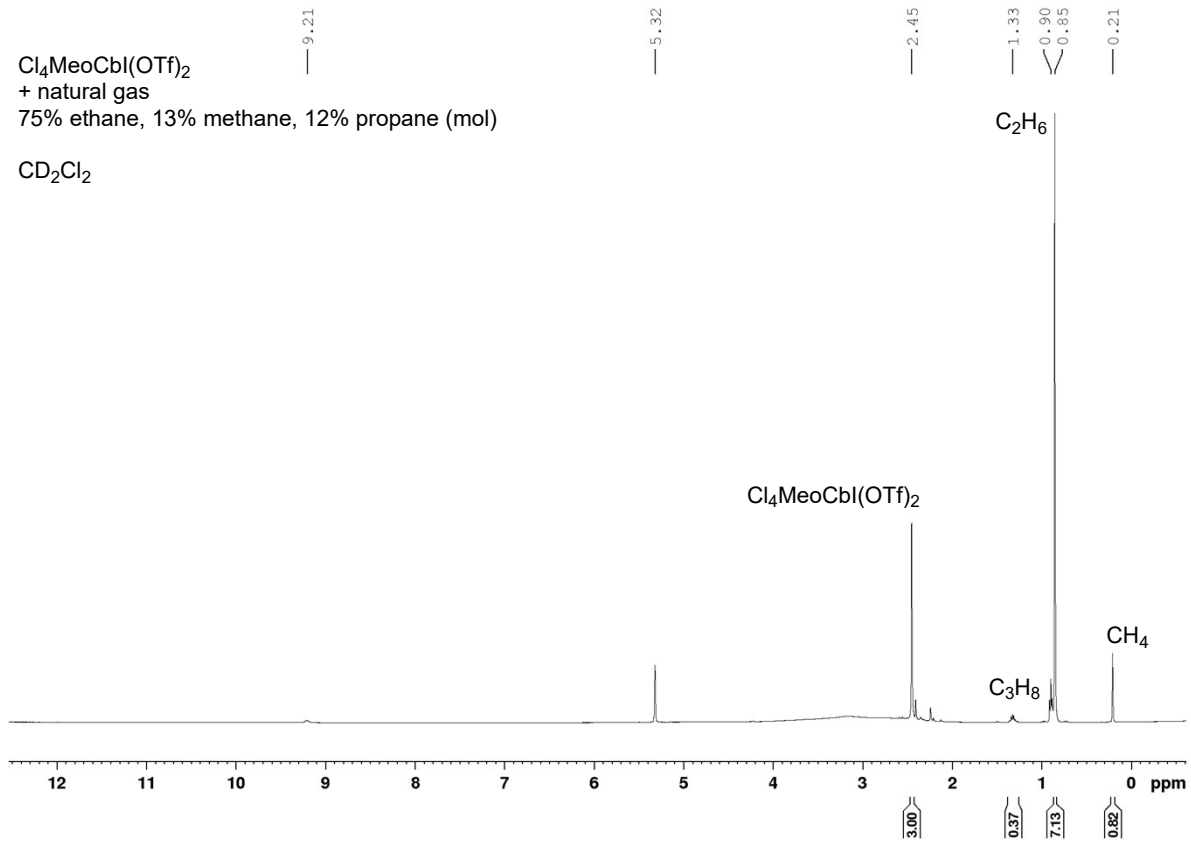

Figure S93. ^{1}H NMR (CD_2Cl_2, 500 MHz): Cl_4MeoCb-I$(OTf)_2$ + natural gas.

Mass Spectra

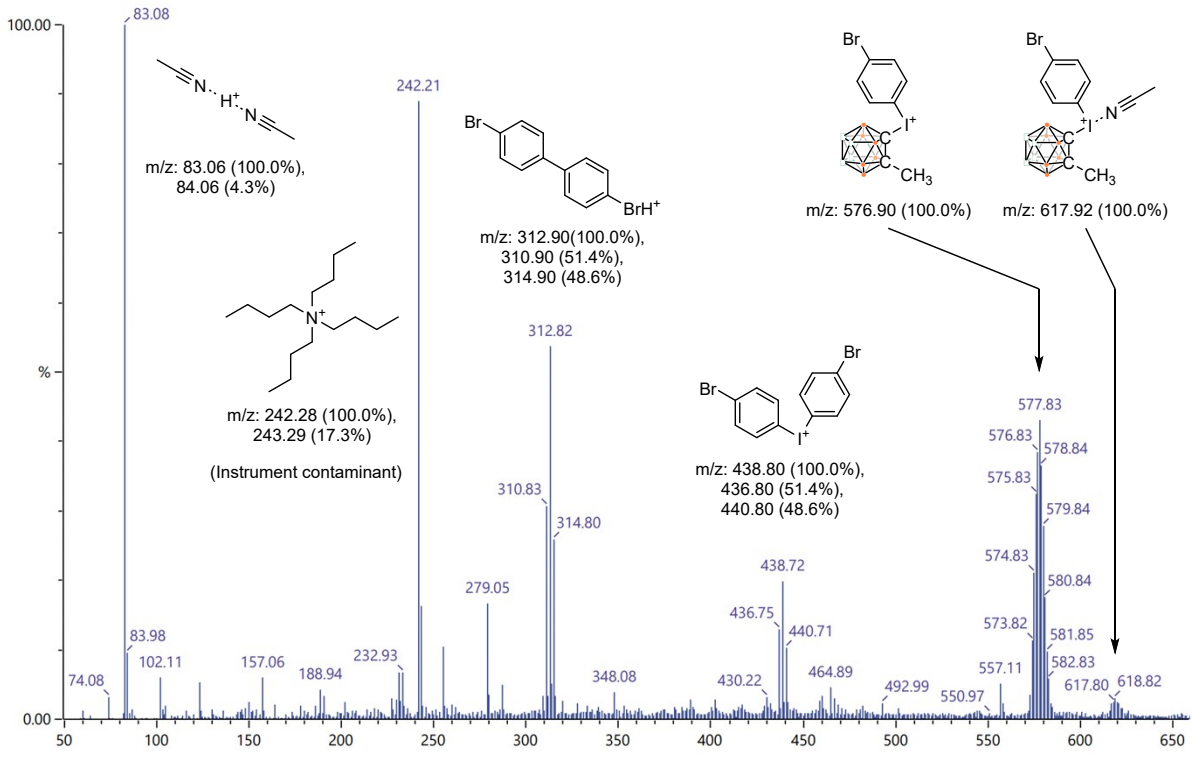

Figure S94. Mass spectrum of Cl_4MeoCb-I(OTf)$_2$ + BrPh reaction mixture. Acetonitrile carrier solvent. Calculated m/z values are displayed beneath each structure.

Computational Details

Geometry optimizations and frequency calculations were performed with Gaussian 16 Rev. C.01[11] at the DFT level using the LC-ωHPBE[12] functional and the def2-TZVP basis set[13] in the gas phase. Default convergence criteria were applied unless stated otherwise. All optimized structures were confirmed as minima by the absence of imaginary frequencies.

Single-point energies were computed on the optimized geometries using ORCA 6.1[14] at the RI-MP2/def2-TZVP[13,15] level of theory. Solvent effects were included via the CPCM[16] model with chloroform parameters. The resolution-of-identity approximation (RIJCOSX) was employed, using the def2/J[17] auxiliary basis set for the Coulomb term and the COSX approximation for Hartree–Fock exchange. MP2 correlation energies were computed using RI-MP2 with the def2-TZVP/C[18] auxiliary basis set. Thermochemical energies were computed at 298 K and 1 atm.

Cartesian coordinates are reported in Å and electronic energies in Hartree.

$CHCl_3$
E (CPCM/RI-MP2/def2-TZVP): -1417.706964
E (LC-ωHPBE/def2-TZVP): -1418.9451610

C	0.000003000	-0.000043000	0.451585000
H	-0.000042000	-0.000198000	1.535864000
Cl	-1.302276000	-1.036783000	-0.083250000
Cl	1.549080000	-0.609334000	-0.083245000
Cl	-0.246802000	1.646143000	-0.083232000

Cl_2
E (CPCM/RI-MP2/def2-TZVP): -919.3563806
E (LC-ωHPBE/def2-TZVP): -920.1369800

Cl	0.000000000	0.000000000	0.982311000
Cl	0.000000000	0.000000000	-0.982311000

HOTf
E (CPCM/RI-MP2/def2-TZVP): -960.9054728
E (LC-ωHPBE/def2-TZVP): -961.9158520

S	-0.848114000	-0.135563000	0.074240000
O	-1.240355000	1.034007000	-0.896057000
H	-1.388914000	1.846408000	-0.390254000
O	-1.228813000	0.209300000	1.395130000

O	-1.196317000	-1.350074000	-0.550749000
C	0.980827000	0.005112000	-0.002769000
F	1.407904000	-0.206692000	-1.235813000
F	1.512586000	-0.890280000	0.812164000
F	1.345917000	1.224312000	0.382808000

Cl_4MeoCbI

E (CPCM/RI-MP2/def2-TZVP): -2503.603256

E (LC-ωHPBE/def2-TZVP): -2506.5070970

B	-1.136881000	-1.445831000	0.063854000
B	0.529671000	-1.425723000	0.615234000
C	1.191341000	0.000022000	-0.020146000
I	3.231262000	-0.000010000	-0.425263000
B	0.148079000	-0.879469000	-1.012223000
B	-1.385302000	-0.000032000	-0.958106000
B	-1.136907000	1.445831000	0.063766000
Cl	-1.982052000	2.974320000	-0.216159000
B	-1.943814000	0.000017000	0.737764000
B	-0.740765000	-0.877284000	1.691370000
C	0.689158000	0.000052000	1.536740000
C	1.711957000	0.000101000	2.643650000
H	2.340904000	-0.886336000	2.593288000
H	1.187642000	-0.000013000	3.596970000
H	2.340708000	0.886682000	2.593392000
B	-0.740755000	0.877381000	1.691320000
H	-0.923534000	1.476786000	2.692273000
B	0.529652000	1.425783000	0.615126000
H	1.253453000	2.324628000	0.854939000
B	0.148063000	0.879437000	-1.012291000
H	0.599570000	1.477760000	-1.923608000
H	-0.923535000	-1.476615000	2.692369000
Cl	-3.652790000	0.000026000	1.178619000
Cl	-2.494637000	-0.000091000	-2.330723000
H	0.599543000	-1.477875000	-1.923506000
H	1.253510000	-2.324536000	0.855050000
Cl	-1.981997000	-2.974346000	-0.216018000

Cl_4MeoCbIF_2

E (CPCM/RI-MP2/def2-TZVP): -2703.000683

E (LC-ωHPBE/def2-TZVP): -2706.1085120

B	-1.421812000	-1.446964000	-0.179338000
B	0.232819000	-1.553506000	0.397569000
C	0.915029000	-0.043608000	0.028709000
I	2.980122000	0.078504000	-0.332582000
F	3.101438000	-1.831765000	0.090835000
F	2.705995000	1.975861000	-0.684988000
B	-0.111279000	-0.729283000	-1.123594000
B	-1.634117000	0.153778000	-0.942740000
B	-1.382818000	1.405187000	0.314680000
Cl	-2.206084000	2.968121000	0.283643000
B	-2.221903000	-0.122592000	0.718348000

B	-1.049708000	-1.167084000	1.530494000
C	0.391900000	-0.301900000	1.556018000
C	1.403454000	-0.512638000	2.654124000
H	2.098907000	-1.308955000	2.393511000
H	0.872884000	-0.802329000	3.558604000
H	1.954402000	0.403613000	2.858202000
B	-1.028432000	0.559220000	1.831512000
H	-1.221473000	0.986247000	2.915267000
B	0.268522000	1.266912000	0.887197000
H	0.998773000	2.096408000	1.292302000
B	-0.090805000	1.007209000	-0.825923000
H	0.374903000	1.743539000	-1.617357000
H	-1.257876000	-1.930546000	2.406550000
Cl	-3.937305000	-0.171965000	1.123137000
Cl	-2.714934000	0.408325000	-2.312365000
H	0.358289000	-1.168556000	-2.113467000
H	0.913923000	-2.503073000	0.502619000
Cl	-2.281132000	-2.892096000	-0.723600000

TfO-$CHCl_2$

E (CPCM/RI-MP2/def2-TZVP): -1918.307504

E (LC-ωHPBE/def2-TZVP): -1920.1616870

C	-1.563085000	0.110247000	0.253775000
H	-1.257395000	0.033646000	1.293309000
C	1.896891000	0.552077000	0.029547000
Cl	-2.907488000	-0.969010000	-0.003563000
Cl	-1.988566000	1.762323000	-0.097918000
O	-0.502998000	-0.265653000	-0.600324000
O	1.314766000	-1.784303000	-1.016775000
O	0.592751000	-1.325109000	1.324255000
S	0.810738000	-0.929597000	-0.018035000
F	2.030566000	1.062951000	-1.180239000
F	1.365656000	1.460598000	0.837765000
F	3.079280000	0.185358000	0.493945000

Cl_4MeoCbICl_2

E (CPCM/RI-MP2/def2-TZVP): -3422.960162

E (LC-ωHPBE/def2-TZVP): -3426.6280310

B	-1.651418000	-1.459458000	-0.206024000
B	-0.015711000	-1.565730000	0.416420000
C	0.675552000	-0.049593000	0.088270000
I	2.773507000	0.094454000	-0.254435000
Cl	3.120629000	-2.303639000	-0.099496000
Cl	2.681281000	2.499429000	-0.446541000
B	-0.317101000	-0.719818000	-1.101299000
B	-1.850725000	0.153618000	-0.945702000
B	-1.639747000	1.381378000	0.341921000
Cl	-2.465063000	2.942738000	0.317541000
B	-2.482447000	-0.155883000	0.693525000
B	-1.328945000	-1.209558000	1.519648000
C	0.110510000	-0.340203000	1.599835000

C	1.097680000	-0.567080000	2.716340000
H	1.793538000	-1.366517000	2.464723000
H	0.547771000	-0.861619000	3.607634000
H	1.650945000	0.343422000	2.939354000
B	-1.323125000	0.508603000	1.852837000
H	-1.545355000	0.918588000	2.937453000
B	-0.004735000	1.236714000	0.958977000
H	0.697029000	2.063705000	1.411972000
B	-0.315565000	1.010012000	-0.769340000
H	0.166077000	1.763093000	-1.535538000
H	-1.554232000	-1.993806000	2.372696000
Cl	-4.207355000	-0.220279000	1.050595000
Cl	-2.893332000	0.429634000	-2.339583000
H	0.182074000	-1.140329000	-2.084872000
H	0.651919000	-2.521674000	0.531917000
Cl	-2.485600000	-2.899005000	-0.799678000

Cl_4MeoCbI(F)(OTf)

E (CPCM/RI-MP2/def2-TZVP): -3563.577619

E (LC-ωHPBE/def2-TZVP): -3567.5796390

B	-3.099679000	-0.989761000	-0.051334000
B	-1.634392000	-1.732414000	0.563433000
C	-0.381376000	-0.698726000	0.061187000
I	1.502419000	-1.576903000	-0.269496000
F	0.769695000	-3.301830000	0.202796000
O	2.131692000	0.415448000	-0.750064000
S	3.640852000	0.548371000	-0.909908000
C	4.082338000	1.328140000	0.691327000
F	3.515305000	2.518800000	0.798740000
F	3.649233000	0.556371000	1.693806000
F	5.394517000	1.451237000	0.779928000
O	4.212733000	-0.765393000	-0.875526000
O	3.983794000	1.476032000	-1.917078000
B	-1.631948000	-0.988144000	-1.037135000
B	-2.631384000	0.470932000	-0.968155000
B	-1.840433000	1.608652000	0.168827000
Cl	-1.920157000	3.361233000	-0.025012000
B	-3.239643000	0.627306000	0.701370000
B	-2.601904000	-0.734835000	1.631628000
C	-0.928390000	-0.565954000	1.600096000
C	-0.072821000	-1.082361000	2.729247000
H	0.164327000	-2.136164000	2.589371000
H	-0.631432000	-0.980274000	3.657177000
H	0.847293000	-0.507428000	2.819270000
B	-1.842872000	0.838038000	1.766311000
H	-1.807020000	1.407141000	2.799975000
B	-0.391176000	0.835905000	0.783872000
H	0.624446000	1.314649000	1.133270000
B	-0.868610000	0.594877000	-0.907057000
H	-0.155938000	0.984256000	-1.758995000
H	-3.090835000	-1.254067000	2.572225000

Cl	-4.801669000	1.349306000	1.078658000
Cl	-3.533805000	1.029470000	-2.374142000
H	-1.415457000	-1.677594000	-1.970651000
H	-1.421584000	-2.866989000	0.773709000
Cl	-4.501337000	-1.978296000	-0.471245000

Cl_4MeoCbI(Cl)(OTf)

E (CPCM/RI-MP2/def2-TZVP): -3923.560198

E (LC-ωHPBE/def2-TZVP): -3927.8416770

B	3.043575000	0.879619000	0.638777000
B	1.392379000	1.195242000	1.136385000
C	0.430979000	0.389113000	-0.004100000
I	-1.440543000	1.310571000	-0.397463000
Cl	-0.596525000	3.482070000	-0.249480000
O	-2.290614000	-0.754949000	-0.505075000
S	-3.772000000	-0.714167000	-0.804774000
C	-4.467132000	-1.109438000	0.845778000
F	-4.069129000	-2.311328000	1.241931000
F	-4.039417000	-0.208660000	1.737536000
F	-5.786926000	-1.075039000	0.801639000
O	-4.152695000	0.647249000	-1.060242000
O	-4.185767000	-1.754465000	-1.667576000
B	1.803802000	1.175980000	-0.585741000
B	2.986130000	-0.106111000	-0.857480000
B	2.191151000	-1.656859000	-0.466488000
Cl	2.575682000	-3.166585000	-1.295540000
B	3.295072000	-0.889476000	0.714848000
B	2.293606000	-0.079833000	1.927266000
C	0.698096000	-0.332838000	1.442773000
C	-0.422780000	-0.400624000	2.448467000
H	-0.726917000	0.594943000	2.767098000
H	-0.067475000	-0.943203000	3.321875000
H	-1.280692000	-0.932150000	2.041168000
B	1.774506000	-1.612179000	1.257230000
H	1.635341000	-2.559245000	1.947756000
B	0.547898000	-1.309912000	0.041421000
H	-0.402833000	-1.984293000	-0.072472000
B	1.278666000	-0.364304000	-1.257619000
H	0.784286000	-0.408884000	-2.328475000
H	2.513094000	0.034764000	3.081485000
Cl	4.853123000	-1.597206000	1.132424000
Cl	4.209204000	0.037218000	-2.116945000
H	1.685471000	2.167602000	-1.209736000
H	0.946155000	2.124307000	1.704874000
Cl	4.325417000	2.049621000	0.963719000

Cl_4MeoCbI$(OTf)_2$

E (CPCM/RI-MP2/def2-TZVP): -4424.150097

E (LC-ωHPBE/def2-TZVP): -4429.0448920

B	-2.946110000	-1.547551000	0.190386000
B	-1.351357000	-1.445386000	0.909993000

C	-0.647047000	-0.058736000	0.211266000
I	1.448896000	0.038387000	-0.038876000
O	1.507716000	-1.906591000	0.759982000
S	2.873615000	-2.603508000	0.634266000
C	2.520187000	-3.771342000	-0.737689000
F	1.572963000	-4.621830000	-0.380184000
F	2.110571000	-3.085013000	-1.802194000
F	3.623071000	-4.431718000	-1.039517000
O	3.143584000	-3.382038000	1.780393000
O	3.806977000	-1.647817000	0.126556000
O	1.107966000	1.969467000	-0.792988000
S	2.381043000	2.814635000	-0.955114000
C	2.236017000	3.909072000	0.511637000
F	1.155860000	4.665979000	0.417809000
F	2.139705000	3.157254000	1.612379000
F	3.309553000	4.670938000	0.600442000
O	3.504089000	1.964739000	-0.710792000
O	2.296733000	3.643991000	-2.092543000
B	-1.564693000	-1.054306000	-0.799004000
B	-3.110635000	-0.206593000	-0.978114000
B	-2.984166000	1.335582000	-0.072505000
Cl	-3.813585000	2.809512000	-0.575130000
B	-3.837654000	-0.064226000	0.644731000
B	-2.727777000	-0.821970000	1.794582000
C	-1.300481000	0.067560000	1.710957000
C	-0.381728000	0.181559000	2.900999000
H	0.294053000	-0.670804000	2.956555000
H	-0.988570000	0.191785000	3.803848000
H	0.193235000	1.105539000	2.866945000
B	-2.753155000	0.920565000	1.636958000
H	-3.040522000	1.609133000	2.551644000
B	-1.389095000	1.404654000	0.652473000
H	-0.721493000	2.339251000	0.901647000
B	-1.594596000	0.700211000	-0.963306000
H	-1.072555000	1.219666000	-1.881691000
H	-2.996527000	-1.343182000	2.818875000
Cl	-5.578530000	-0.065473000	0.908634000
Cl	-4.066785000	-0.351207000	-2.449641000
H	-1.003379000	-1.717128000	-1.598717000
H	-0.690897000	-2.318874000	1.325586000
Cl	-3.732093000	-3.112596000	-0.028462000

TfO-CH_2Cl

E (CPCM/RI-MP2/def2-TZVP): -1459.208031

E (LC-ωHPBE/def2-TZVP): -1460.6849010

C	1.727158000	-0.934180000	-0.023884000
H	1.416747000	-1.104366000	1.003282000
C	-1.732318000	-0.409361000	-0.006934000
Cl	3.261137000	-0.100053000	-0.011806000
H	1.839299000	-1.863790000	-0.573073000
O	0.748305000	-0.180018000	-0.725510000

O	-0.587215000	1.824383000	-0.761979000
O	0.093211000	0.821938000	1.415751000
S	-0.282577000	0.716494000	0.053994000
F	-2.092233000	-0.634423000	-1.258623000
F	-1.415902000	-1.565920000	0.570565000
F	-2.733819000	0.148786000	0.650881000

TMSOTf

E (CPCM/RI-MP2/def2-TZVP): -1368.876235

E (LC-ωHPBE/def2-TZVP): -1370.5325810

S	-0.766115000	0.833965000	0.040864000
O	-0.512279000	1.165724000	-1.318328000
O	-1.263237000	1.793177000	0.953987000
O	0.430293000	0.094163000	0.648816000
C	-1.976067000	-0.544689000	0.027189000
Si	2.018372000	-0.194088000	0.018720000
F	-3.115759000	-0.107163000	-0.486299000
F	-2.190410000	-0.987061000	1.257724000
F	-1.519999000	-1.547365000	-0.717675000
C	2.768633000	1.454504000	-0.347339000
H	2.770800000	2.092654000	0.537383000
H	3.803016000	1.329224000	-0.674403000
H	2.221589000	1.965155000	-1.140296000
C	1.854966000	-1.262704000	-1.479437000
H	1.365535000	-2.208070000	-1.242810000
H	1.279462000	-0.760326000	-2.257002000
H	2.845655000	-1.487743000	-1.880474000
C	2.833371000	-1.060362000	1.433216000
H	2.313616000	-1.987315000	1.678348000
H	3.865419000	-1.309763000	1.178543000
H	2.847433000	-0.430734000	2.323498000

TMSF

E (CPCM/RI-MP2/def2-TZVP): -508.3137316

E (LC-ωHPBE/def2-TZVP): -509.0675320

F	0.000005000	-0.000057000	1.642248000
Si	0.000041000	-0.000103000	0.025367000
C	-1.408279000	-1.076165000	-0.521795000
H	-2.359597000	-0.693229000	-0.149362000
H	-1.465017000	-1.116101000	-1.611531000
H	-1.286895000	-2.096030000	-0.153762000
C	1.636262000	-0.681305000	-0.521800000
H	2.458465000	-0.067297000	-0.151232000
H	1.779818000	-1.697640000	-0.151975000
H	1.700368000	-0.707477000	-1.611545000
C	-0.228018000	1.757581000	-0.521705000
H	0.579160000	2.390239000	-0.149507000
H	-0.234738000	1.826890000	-1.611427000
H	-1.171970000	2.161937000	-0.153221000

TMSCl

E (CPCM/RI-MP2/def2-TZVP): -868.2650381

E (LC-ωHPBE/def2-TZVP): -869.3081380

Cl	-1.738991000	-0.000033000	0.000035000
Si	0.331658000	0.000040000	-0.000019000
C	0.883951000	-1.076413000	-1.407796000
H	0.513165000	-0.693299000	-2.359206000
H	1.974472000	-1.112134000	-1.456352000
H	0.515051000	-2.095510000	-1.286133000
C	0.884031000	-0.681014000	1.636042000
H	0.514259000	-0.066895000	2.457972000
H	0.514189000	-1.696958000	1.779293000
H	1.974557000	-0.704200000	1.691596000
C	0.883912000	1.757450000	-0.228287000
H	0.513168000	2.389723000	0.579313000
H	1.974435000	1.817348000	-0.234957000
H	0.514976000	2.161790000	-1.171601000

ClF

E (CPCM/RI-MP2/def2-TZVP): -559.3419953

E (LC-ωHPBE/def2-TZVP): -559.8359990

Cl	0.000000000	0.000000000	0.558238000
F	0.000000000	0.000000000	-1.054450000

Cl_4MeoCbI(Cl)(F)

E (CPCM/RI-MP2/def2-TZVP): -3062.979518

E (LC-ωHPBE/def2-TZVP): -3066.3679160

B	1.446991000	1.483288000	-0.080585000
B	-0.196119000	1.425871000	0.530461000
C	-0.780263000	-0.094670000	0.065191000
I	-2.837386000	-0.393043000	-0.323517000
Cl	-3.373769000	1.928029000	-0.081026000
F	-2.402312000	-2.304924000	-0.520763000
B	0.171138000	0.737252000	-1.051192000
B	1.757446000	-0.043568000	-0.955101000
B	1.621848000	-1.389936000	0.218549000
Cl	2.552785000	-2.883778000	0.069635000
B	2.358115000	0.163863000	0.711634000
B	1.132758000	1.063167000	1.613211000
C	-0.245002000	0.096360000	1.601432000
C	-1.251792000	0.160242000	2.721554000
H	-2.003775000	0.923837000	2.526462000
H	-0.730313000	0.422287000	3.639678000
H	-1.737682000	-0.803091000	2.864955000
B	1.239450000	-0.674631000	1.795692000
H	1.484146000	-1.160853000	2.843411000
B	-0.022670000	-1.410350000	0.827632000
H	-0.671677000	-2.317745000	1.197079000
B	0.281205000	-1.012770000	-0.871040000
H	-0.153106000	-1.726617000	-1.701094000
H	1.302089000	1.782491000	2.533834000

Cl	4.073281000	0.310237000	1.092471000
Cl	2.825040000	-0.125583000	-2.355536000
H	-0.350247000	1.208738000	-1.999555000
H	-0.932175000	2.318724000	0.720544000
Cl	2.187752000	3.020817000	-0.538333000

C_3H_6

E (CPCM/RI-MP2/def2-TZVP): -117.611286

E (LC-ωHPBE/def2-TZVP): -117.8674020

C	-1.225025000	-0.161400000	0.000002000
C	0.134488000	0.452621000	0.000026000
C	1.269710000	-0.220616000	0.000020000
H	2.227994000	0.284659000	-0.000103000
H	1.283608000	-1.305783000	-0.000045000
H	0.170195000	1.539681000	-0.000043000
H	-1.793989000	0.153990000	0.877396000
H	-1.793878000	0.153839000	-0.877582000
H	-1.168972000	-1.250015000	0.000087000

C_3H_8

E (CPCM/RI-MP2/def2-TZVP): -118.8296337

E (LC-ωHPBE/def2-TZVP): -119.1125200

C	0.000000000	1.262316000	-0.258363000
C	0.000000000	0.000000000	0.584491000
C	0.000000000	-1.262316000	-0.258363000
H	0.880663000	-1.302790000	-0.903025000
H	0.000000000	-2.160241000	0.360875000
H	-0.880663000	-1.302790000	-0.903025000
H	0.873562000	0.000000000	1.241884000
H	-0.873562000	0.000000000	1.241884000
H	0.880663000	1.302790000	-0.903025000
H	-0.880663000	1.302790000	-0.903025000
H	0.000000000	2.160241000	0.360875000

Cl_4MeoCbI(C_3H_7)(OTf)

E (CPCM/RI-MP2/def2-TZVP): -3582.128684

E (LC-ωHPBE/def2-TZVP): -3586.2802040

B	-2.865103000	-1.671645000	0.034124000
B	-1.306802000	-1.364514000	0.792069000
C	-0.828081000	0.157431000	0.233918000
I	1.300845000	0.351494000	0.145543000
O	3.672374000	-1.146600000	1.416823000
S	4.473743000	-0.229117000	0.656438000
C	5.103837000	-1.214824000	-0.754515000
F	5.879261000	-2.197847000	-0.319893000
F	4.079646000	-1.745832000	-1.430552000
F	5.801662000	-0.450472000	-1.588408000
O	5.617019000	0.363570000	1.255144000
O	3.605563000	0.759325000	-0.052036000
C	1.270545000	2.368084000	-0.649756000
C	1.874433000	2.358808000	-2.031288000

H	1.338985000	1.696059000	-2.709837000
H	1.804869000	3.374910000	-2.426046000
H	2.924806000	2.075622000	-2.001772000
C	1.941216000	3.300017000	0.327238000
H	2.993176000	3.052227000	0.453857000
H	1.873319000	4.309242000	-0.085082000
H	1.450470000	3.301127000	1.299824000
H	0.196275000	2.539535000	-0.689350000
B	-1.574204000	-0.876956000	-0.874090000
B	-3.229159000	-0.274448000	-1.023140000
B	-3.357331000	1.182886000	0.010554000
Cl	-4.401471000	2.551879000	-0.390302000
B	-3.987023000	-0.391150000	0.588109000
B	-2.781932000	-1.063503000	1.695949000
C	-1.519331000	0.048414000	1.718466000
C	-0.663333000	0.204013000	2.951608000
H	0.109550000	-0.560989000	2.999732000
H	-1.301394000	0.098346000	3.826487000
H	-0.196119000	1.186178000	2.987035000
B	-3.084609000	0.665609000	1.681966000
H	-3.492994000	1.213669000	2.644760000
B	-1.794439000	1.431994000	0.773734000
H	-1.280909000	2.442908000	1.104410000
B	-1.871146000	0.850237000	-0.886849000
H	-1.434788000	1.526885000	-1.752085000
H	-2.984283000	-1.699976000	2.669414000
Cl	-5.711565000	-0.684541000	0.805313000
Cl	-4.137633000	-0.437805000	-2.525449000
H	-0.910929000	-1.375935000	-1.714231000
H	-0.469201000	-2.125867000	1.130460000
Cl	-3.394464000	-3.315090000	-0.336638000

4-NO_2PhI

E (CPCM/RI-MP2/def2-TZVP): -732.518196

E (LC-ωHPBE/def2-TZVP): -733.753166

I	-2.505387000000	0.000000000000	-0.000001000000
O	4.318845000000	1.070376000000	0.000358000000
N	3.761756000000	0.000000000000	0.000009000000
C	-0.438349000000	0.000000000000	0.000002000000
C	0.245688000000	1.203831000000	-0.000151000000
H	-0.295679000000	2.140855000000	-0.000294000000
C	1.625511000000	1.206207000000	-0.000127000000
H	2.188399000000	2.129375000000	-0.000201000000
C	2.290323000000	0.000000000000	0.000006000000
O	4.318845000000	-1.070376000000	-0.000376000000
C	0.245688000000	-1.203831000000	0.000157000000
H	-0.295679000000	-2.140855000000	0.000298000000
C	1.625511000000	-1.206207000000	0.000138000000
H	2.188399000000	-2.129375000000	0.000212000000

4-NO_2Ph-ICl_2

E (CPCM/RI-MP2/def2-TZVP): -1651.887523

E (LC-ωHPBE/def2-TZVP): -1653.890728

I	-1.952386000000	-0.000002000000	-0.000016000000
Cl	-1.874839000000	-2.392630000000	0.435096000000
O	4.860167000000	-0.808271000000	-0.702535000000
N	4.306741000000	0.000005000000	-0.000003000000
C	0.132610000000	-0.000004000000	-0.000009000000
C	0.791627000000	-0.926419000000	-0.779386000000
H	0.246495000000	-1.653381000000	-1.366277000000
C	2.171923000000	-0.923074000000	-0.780530000000
H	2.736655000000	-1.624727000000	-1.378393000000
C	2.831089000000	0.000001000000	-0.000005000000
Cl	-1.874829000000	2.392641000000	-0.435038000000
O	4.860160000000	0.808263000000	0.702556000000
C	0.791621000000	0.926416000000	0.779369000000
H	0.246485000000	1.653377000000	1.366257000000
C	2.171917000000	0.923075000000	0.780518000000
H	2.736645000000	1.624730000000	1.378382000000

4-NO_2Ph-$I(OTf)_2$

E (CPCM/RI-MP2/def2-TZVP): -2653.083021

E (LC-ωHPBE/def2-TZVP): -2656.310656

I	0.671819000000	-0.834404000000	-0.702887000000
S	3.122847000000	0.942997000000	0.333307000000
S	-1.780753000000	-2.521714000000	0.492852000000
O	2.306817000000	0.457923000000	-0.875280000000
F	4.074660000000	-1.475357000000	0.273170000000
O	3.638569000000	2.235032000000	0.081310000000
F	5.337826000000	-0.029376000000	1.272063000000
O	-1.064174000000	-2.000457000000	-0.762974000000
O	-3.373627000000	4.707520000000	-0.775667000000
F	5.211077000000	-0.047743000000	-0.884951000000
O	-1.338040000000	-1.800952000000	1.639654000000
O	2.436526000000	0.632843000000	1.542777000000
O	-3.060700000000	4.555818000000	1.338814000000
F	-4.277534000000	-2.286886000000	1.122165000000
N	-2.900354000000	4.188527000000	0.203431000000
C	-0.506321000000	0.829083000000	-0.395012000000
O	-1.838499000000	-3.935132000000	0.489197000000
F	-3.922157000000	-2.470997000000	-1.001910000000
C	-2.049822000000	2.997114000000	-0.008645000000
C	-1.495583000000	2.382447000000	1.090804000000
H	-1.685977000000	2.772756000000	2.080791000000
C	-1.851817000000	2.557651000000	-1.299334000000
H	-2.312099000000	3.082762000000	-2.124500000000
C	-0.703041000000	1.267669000000	0.898585000000
H	-0.252831000000	0.757995000000	1.739030000000
F	-3.493398000000	-0.609601000000	0.006853000000
C	-1.060199000000	1.446709000000	-1.500236000000
H	-0.883775000000	1.075527000000	-2.501260000000

C -3.481483000000 -1.935239000000 0.125440000000
C 4.536269000000 -0.223261000000 0.239598000000

4-NO_2Ph-I(Cl)(OTf)

E (CPCM/RI-MP2/def2-TZVP): 2152.489299
E (LC-ωHPBE/def2-TZVP): -2155.105283

I 0.492300000000 1.454801000000 0.012167000000
S 2.693291000000 -0.656784000000 0.860087000000
Cl -0.580317000000 3.392764000000 -0.787106000000
O 1.191806000000 -0.505974000000 0.777579000000
F 2.405144000000 -2.881309000000 -0.484156000000
F 4.306342000000 -1.893939000000 -0.768861000000
F 2.522990000000 -1.102408000000 -1.703719000000
O -5.849639000000 -1.137144000000 0.699306000000
O 3.096435000000 -1.423897000000 1.979360000000
O 3.314526000000 0.601426000000 0.570898000000
N -4.953377000000 -1.611717000000 0.048365000000
O -5.019540000000 -2.625492000000 -0.599283000000
C -1.315698000000 0.434478000000 0.029919000000
C -2.619507000000 -1.412644000000 -0.682676000000
H -2.752903000000 -2.334463000000 -1.231560000000
C -3.665478000000 -0.888610000000 0.043151000000
C -2.362448000000 0.957175000000 0.760119000000
H -2.255924000000 1.881659000000 1.312599000000
C -3.564959000000 0.280011000000 0.764431000000
H -4.416961000000 0.644408000000 1.321259000000
C -1.416108000000 -0.736427000000 -0.692086000000
H -0.573540000000 -1.128620000000 -1.245835000000
C 3.006663000000 -1.705032000000 -0.611647000000

References

[1] C. P. Rosenau, B. J. Jelier, A. D. Gossert, A. Togni, "Exposing the Origins of Irreproducibility in Fluorine NMR Spectroscopy" *Angew. Chemie - Int. Ed.* **2018**, *57*, 9528–9533.

[2] R. D. Chapman, J. L. Andreshak, S. P. Herrlinger, S. A. Shackelford, R. A. Hildreth, J. P. Smith, "Trifluoromethanesulfonate Esters from Dibromoalkane Metatheses with Silver Triflate: Mechanistic and Synthetic Aspects" *J. Org. Chem.* **1986**, *51*, 3792–3798.

[3] V. A. Petrov, "A new route to polyfluorinated trifluoromethanesulfonates. Synthesis of perfluoroallyl and perfluorobenzyl triflates" *J. Fluor. Chem.* **1995**, *73*, 17–19.

[4] A. Hermannsdorfer, M. Driess, "Silicon Tetrakis(trifluoromethanesulfonate): A Simple Neutral Silane Acting as a Soft and Hard Lewis Superacid" *Angew. Chemie - Int. Ed.* **2021**, *60*, 13656–13660.

[5] M. Sceney, K. F. White, J. L. Dutton, "Ortho-Carborane-Supported Hypervalent Iodine(III) Reagents: A Scaffold for Enhanced Oxidative Capability" *J. Am. Chem. Soc.* **2025**, *147*, 32347–32351.

[6] R. Streubel, A. Özbolat-Schön, M. Bode, J. Daniels, G. Schnakenburg, F. Teixidor, C. Vinas, A. Vaca, A. Pepiol, P. Farras, "Investigations on the reactivity of Li/Cl phosphinidenoid tungsten complexes toward various iodine compounds" *Organometallics* **2009**, *28*, 6031–6035.

[7] B. A. Chalmers, M. Bühl, K. S. Athukorala Arachchige, A. M. Z. Slawin, P. Kilian, "Structural, spectroscopic and computational examination of the dative interaction in constrained phosphine-stibines and phosphine-stiboranes" *Chem. - A Eur. J.* **2015**, *21*, 7520–7531.

[8] A. P. M. Robertson, N. Burford, R. McDonald, M. J. Ferguson, "Coordination complexes of Ph3Sb2+ and Ph3Bi2+: Beyond pnictonium cations" *Angew. Chemie - Int. Ed.* **2014**, *53*, 3480–3483.

[9] AIST, "SDBS No.:1494 p-bromochlorobenzene," **1999**.

[10] AIST, "SDBS No.:2011 o-bromochlorobenzene," **1999**.

[11] M. J. Frisch, G. W. Trucks, H. B. Schlegel, G. E. Scuseria, M. A. Robb, J. R. Cheeseman, G. Scalmani, V. Barone, G. A. Petersson, H. Nakatsuji, X. Li, M. Caricato, A. V. Marenich, J. Bloino, B. G. Janesko, R. Gomperts, B. Mennucci, H. P. Hratchian, J. V. Ortiz, A. F. Izmaylov, J. L. Sonnenberg, D. Williams-Young, F. Ding, F. Lipparini, F. Egidi, J. Goings, B. Peng, A. Petrone, T. Henderson, D. Ranasinghe, V. G. Zakrzewski, N. Gao, J.; Rega, G. Zheng, W. Liang, M. Hada, M. Ehara, K. Toyota, R. Fukuda, J. Hasegawa, M. Ishida, T. Nakajima, Y. Honda, O. Kitao, H. Nakai, T. Vreven, K. Throssell, J. A. Montgomery Jr., J. E. Peralta, F. Ogliaro, M. J. Bearpark, J. J. Heyd, E. N. Brothers, K. N. Kudin, V. N. Staroverov, T. A. Keith, R. Kobayashi, J. Normand, K. Raghavachari, A. P. Rendell, J. C. Burant, S. S. Iyengar, J. Tomasi, M. Cossi, J. M. Millam, M. Klene, C. Adamo, R. Cammi, J. W. Ochterski, R. L. Martin, K. Morokuma, O. Farkas, J. B. Foresman, D. J. Fox, **2016**.

[12] O. A. Vydrov, G. E. Scuseria, "Assessment of a long-range corrected hybrid functional" *J. Chem. Phys.* **2006**, *125*, 234109.

[13] F. Weigend, R. Ahlrichs, "Balanced basis sets of split valence, triple zeta valence and quadruple zeta valence quality for H to Rn: Design and assessment of accuracy" *Phys. Chem. Chem. Phys.* **2005**, *7*, 3297–3305.

[14] F. Neese, "The ORCA program system" *WIREs Comput. Mol. Sci.* **2012**, *2*, 73–78.

[15] M. Feyereisen, G. Fitzgerald, A. Komornicki, "Use of approximate integrals in ab initio theory. An application in MP2 energy calculations" *Chem. Phys. Lett.* **1993**, *208*, 359–363.

[16] V. Barone, M. Cossi, "Quantum Calculation of Molecular Energies and Energy Gradients in Solution by a Conductor Solvent Model" *J. Phys. Chem. A* **1998**, *102*, 1995–2001.

[17] F. Weigend, "Accurate Coulomb-fitting basis sets for H to Rn" *Phys. Chem. Chem. Phys.* **2006**, *8*, 1057–1065.

[18] A. Hellweg, C. Hättig, S. Höfener, W. Klopper, "Optimized accurate auxiliary basis sets for RI-MP2 and RI-CC2 calculations for the atoms Rb to Rn" *Theor. Chem. Acc.* **2007**, *117*, 587–597.